INFORMATION TO USERS

This manuscript has been reproduced from the microfilm master. UMI films the text directly from the original or copy submitted. Thus, some thesis and dissertation copies are in typewriter face, while others may be from any type of computer printer.

The quality of this reproduction is dependent upon the quality of the copy submitted. Broken or indistinct print, colored or poor quality illustrations and photographs, print bleedthrough, substandard margins, and improper alignment can adversely affect reproduction.

In the unlikely event that the author did not send UMI a complete manuscript and there are missing pages, these will be noted. Also, if unauthorized copyright material had to be removed, a note will indicate the deletion.

Oversize materials (e.g., maps, drawings, charts) are reproduced by sectioning the original, beginning at the upper left-hand corner and continuing from left to right in equal sections with small overlaps. Each original is also photographed in one exposure and is included in reduced form at the back of the book.

Photographs included in the original manuscript have been reproduced xerographically in this copy. Higher quality 6" x 9" black and white photographic prints are available for any photographs or illustrations appearing in this copy for an additional charge. Contact UMI directly to order.

UMI

A Bell & Howell Information Company
300 North Zeeb Road, Ann Arbor, MI 48106-1346 USA
313/761-4700 800/521-0600

THE EFFECT OF LOADING FREQUENCY AND LOADING LEVEL ON THE FATIGUE BEHAVIOR OF ANGLE-PLY CARBON/PEEK THERMOPLASTIC COMPOSITES.

IMAD A. AL-HMOUZ

A Thesis

in

The Department of Mechanical Engineering.

Presented in Partial fulfilment of the Requirements

for the Degree of Master of Applied Science at

Concordia University

Montreal, Quebec, Canada

April 1997

ABSTRACT

THE EFFECT OF LOADING FREQUENCY AND LOADING LEVEL ON THE FATIGUE BEHAVIOR OF ANGLE-PLY CARBON/PEEK THERMOPLASTIC COMPOSITES.

Imad A. Al-Hmouz

The effect of loading frequency and loading level on the fatigue behavior of $[\pm 45]_{4s}$ carbon/PEEK composite was investigated. Tention-tention load controlled fatigue tests were performed on straight sided samples using a 100-KN MTS machine. Three loading frequencies (1Hz, 5Hz, and 10Hz) and three load levels ($60\%\sigma_{ult.}$, $70\%\sigma_{ult.}$, and $80\%\sigma_{ult.}$) were used, with a load ratio of R=0.13. During each fatigue test, the cyclic load, axial strain, and the sample's surface temperature were recorded through a data acquisition system.

It was found that the fatigue life of this material decreases as loading frequency increases. At the same frequency, the fatigue life decreases as the loading level increases, with more decline at higher frequencies. High levels of temperature rise were obtained during fatigue tests at high frequencies, which increase as loading level increases. Consequently, it can be said that the major effect of loading frequency on the fatigue life is the temperature rise and the consequent thermal degradation. High levels of creep deformation were observed throughout the tests. At high frequencies, the high levels of temperature rise accelerate the creep deformation rates.

A model for the effect of loading frequency on the fatigue life was suggested, based on the general degradation of the material's strength under fatigue loading. Also, the variation in viscoelastic properties during fatigue were investigated, and the thermal behavior was anlyzed.

AKNOWLEDGEMENT

The author wishes to express his gratitude and deep appreciation to his supervisor Dr. X.R. Xiao who provided guidance and encouragement throughout this research project. Special thanks to the Natural Science and Engineering Research Council (NSERC) for providing the funds in making this research project possible. The author gratefully acknowledges the cooperation and help from Mr. Paul Ouellette from Concordia Center for Composites. He also deeply expresses his appreciation to Mr. Jacques Dufault from the National Research Center (NRC) for his help and cooperation in manufacturing the composite plates.

The author also wishes to express his acknowledgment to Mr. Motaz El-Karmalawi, a Ph.D. student from Concordia University for his assistance.

TABLE OF CONTENTS

CHAPTER 3

Description of the material and experimental procedure

CHAPTER 4

Experimental results

LIST OF FIGURES

Figure

LIST OF TABLES

Table

CHAPTER 1

INTRODUCTION

1.1 General

The use of today's advanced composite materials in modern applications has increased as a result of the need for improved performance. Those applications range from aerospace industries to medical implant devices. For instance, the interests in achieving aircraft fuel conservation have resulted in a growing need for energy-efficient aircrafts in both commercial and military fields. This need calls for the use of advanced composites in both primary aircraft structures, such as wings, fuselages, and fins, and in energy-efficient components such as fan blades, nacelles, and engine frames.

The structural integrity of mechanical components is normally insured by designing them to be damage tolerant under static and cyclic loads they would encounter in service; that is, they must retain a residual strength sufficient to withstand specified damage and load levels. Composite materials are known to show significant damage tolerance under dynamic loading. This is attributed in part to the high strength and high modulus of fibers, and in part to the unique structure of composites. The interface provides additional energy dissipation sites which are not available in conventional single

phase materials. Those sites increase the composite's capability to withstand high levels of damage and applied loads.

1.2 The Fatigue Problem in Composites

Fatigue is one of the main forms of loading in structural elements, which can (if not understood properly) lead to catastrophic failure in certain situations. Fatigue can be defined as the ultimate failure of a component when subjected to a cyclic load whose maximum amplitude, when continuously applied in a static situation, would be insufficient to cause failure [7]. Almost all engineering components are subjected to varying loads through their working life, and fatigue is often one of the causes of failure in service. Designing against fatigue failure is difficult and complex since fatigue life can be influenced by a number of variables such as maximum and minimum stress levels, temperature, loading frequency, component size and geometry, and environment.

Unlike metals, where fracture under cyclic loading is known to result from the initiation and subsequent growth of a single dominant flaw [7,31], the failure of long fiber-reinforced composites is characterized by the development and accumulation of several kinds of defects. These include matrix cracking along the fibers, delamination between adjacent plies, debonding between matrix and fibers, and fracture of fibers. Damages are not isolated in composite systems, but rather interconnected, making the

identification of crack paths highly complex. Also, much of this damage occurs long before the ultimate failure, and hence, there can be many types of subcritical failures [7,16,21,23].

For matrix dominated composites, the fatigue behavior is controlled to a large extent by the behavior of the polymeric matrix. Polymers do not have an equivalent to stage I crystallographic crack propagation as in the case of metals, and thus, crack initiation is the most important stage in the fatigue life of polymers [16]. Polymers also suffer from two other types of failure which are not found in metals. These are cyclic creep and thermal failure, which arise under certain combinations of loading conditions. Cyclic creep occurs under conditions of sufficiently high loads and low frequencies. Thermal failure occurs at high frequencies where the energy loss due to the inherent high damping in the polymer cannot be dissipated. This results in significant temperature rises, causing thermal softening and loss of properties [1-4,16,20].

Many attempts have been made to study and quantify the nature and rate of heat generation and temperature rise during cyclic loading. Most of these studies have agreed that loading frequency and the material's damping capacity are the most important factors affecting the heat generation process and the associated temperature rise.

The present study aims to investigate the effect of loading frequency on the fatigue life and the associated viscoelastic and thermal behavior of a composite material.

The material used in this study is carbon/PEEK; an advanced thermoplastic composite system. The following section gives an overview of this material and its most important features.

1.3 Carbon Fiber PEEK Composites (APC2/AS-4)

For the last three decades, the greater part of organic matrix composites in service were based on crosslinked thermosetting resins. Epoxy resins were the most used ones, especially in advanced composite systems employed in critical applications such as aircraft and aerospace industries. However, three problems have become evident with epoxy composite materials; their brittleness, their sensitivity to water and humidity, and the slow manufacturing processes [24]. Even with the possibility of solving some of these problems, it was found that any improvement in one property usually leads to a falling off in the other. These problems gave rise to more efforts to develop new (advanced) composite systems to overcome (fully or partially) the drawbacks in epoxy-based materials. Thermoplastic based materials have been the most successful candidates for this objective.

Several attempts have been made, after carbon fibers were first introduced, to develop composite materials based on thermoplastic resins which are inherently tougher than thermosets. Many difficulties have appeared, such as the relatively poor capability of

thermoplastics to wet carbon fibers, the poor resistance of amorphous thermoplastic resins to solvents, and the special fabrication requirements.

The introduction of carbon fiber reinforced polyetherether ketone (PEEK), a high temperature semi-crystalline polymeric composite in continuous tape form, offered reasonable solutions for these problems [24,34,36]. PEEK was introduced by ICI in 1981 under the trade name Victrex PEEK. The maximum achievable degree of crystallinity in PEEK is about 48%. The high crystallinity of PEEK resin offers high prevention against solvent and environmental factors (unlike the early generations of amorphous thermoplastics), and enhances the high temperature performance and the creep resistance of the polymer. The excellent adhesion between fibers and matrix is also another promising feature of this material.

Thermosetting resins offer low viscosity during processing, which is an important requirement in the wetting of fibers. Such low viscosities are not available in many thermoplastic polymers due to their high molecular weights, and hence special impregnation techniques are usually required. Nevertheless, PEEK has a moderate viscosity when melted, and hence, it offers good processing capabilities: too low viscosity leads to excess resin flow, while too high viscosity imposes difficulties in the impregnation of fibers, consolidation of the laminate, and the relative movement of fibers. The melting and processing temperature of PEEK resins are reasonable for the

technology available at the present time. The thermal stability of PEEK is very good in the range of processing temperatures, which is another requirement in the manufacturing of very large structures, which may require a relatively long processing time.

In contrast to thermosetting resins, the long chain thermoplastic materials can be shaped easily upon melting in a purely physical process. The absence of chemistry means that thermoplastic polymers can be fabricated rapidly. This also increases the possibility for recycling, remolding, and repairing thermoplastic components.

Two important factors influence the morphology and mechanical properties of semicrystalline thermoplastic polymers. First is the processing conditions (such as their melting temperature and the time to be held at that temperature, and cooling rate). Second is the foreign surfaces, which in the case of composites, are the fibers. It has been found that PEEK crystallizes with high nucleation densities as the content of carbon fibers increases, where the fiber surfaces act as nucleation sites [35]. It has also been found that, as the degree of crystallinity of PEEK resin increases, its modulus and strength increases, while its fracture toughness decreases. In general, a lower level of crystallinity will produce a higher elongation, better toughness, but a lower strength and thermal stability. Even though the achievable degree of crystallinity in PEEK can be about 48%, a value of about 35% is found to provide optimal mechanical properties. In other studies it has been

found that the effect of thermal history is more significant than crystallinity in determining the room temperature properties [34-36].

In terms of solvent resistance, the only common material that dissolves PEEK is concentrated sulfuric acid. Concentrated nitric acid does not dissolve PEEK, but significantly degrades its tensile strength. Also, PEEK has exceptional resistance to radiation and burning [26, 34-36].

The counter part composite material (APC-2) contains about 62% carbon fibers by volume. Due to the high strength of carbon fibers and excellent fiber-matrix interfacial adhesion, CF/PEEK composites exhibit high tensile and flexural strengths at room temperature. Nevertheless, like other thermoplastic composites, CF/PEEK composites are relatively weak in compression. The high strength of PEEK composites prevents its high intra-ply cracking and provides good transverse properties.

1.4 Problem definition

Carbon/PEEK thermoplastic composites offer a number of promising features such as high specific strength and stiffness, high fracture toughness, excellent thermal and geometrical stability, excellent resistance to solvents and environmental factors, and

efficient processing. These features make this type of composites increasingly attractive for advanced applications.

The fatigue behavior of carbon/PEEK composites is of great concern in characterizing the overall performance of the composite. A number of studies have been conducted to characterize the fatigue behavior of such thermoplastic composites. Most of these works have focused on the general fatigue behavior and the statistical analysis of this behavior.

In general, thermoset matrix composites have a tendency to interply cracking as a stress release mechanism, whereas in thermoplastic composites that energy is dissipated internally within the structure. The energy dissipation in thermoplastic composites appears as heat generation during fatigue, and leads to loss of properties and fatigue failure as a result of significant temperature rise. On the other hand, while thermoset matrix composites begin to loose their strength and stiffness as soon as they start to microcrack during fatigue, no such reduction is seen in thermoplastic composites as a result of their inherently high toughness.

The effect of loading frequency on the fatigue behavior of advanced thermoplastic matrix composites requires more investigation. The pronounced viscoelastic nature of the matrix material, and the accompanied thermal effect during fatigue loading play an

important role in the reliability and mechanical performance of such composite materials. As the role of the matrix becomes more dominant, the viscoelastic effect increases for the whole composite, and in turn, its effect on the time-dependent properties increases. Due to this effect, and because of the nature of fatigue loading, loading frequency is assumed to be one of the most important factors that characterizes the material's fatigue behavior. Yet, the effect of loading frequency is not fully clear, especially for advanced thermoplastic matrix composites.

Different effects of loading frequency on the fatigue life of composites have been reported. Fatigue failure associated with large-scale hysteretic heating have been observed in polymers [34, 35] and in glass reinforced epoxy [1] where fatigue life decreased as load frequency increased. The effect of hysteretic heating was less substantial in graphite/epoxy composites, and consequently fatigue life increased as load frequency increased [5]. Similar trend was observed in Boron/epoxy composites [3]. Several studies on fatigue of AS4/PEEK composite have shown that hysteretic heating is much more pronounced as compared to that in thermoset composites [2-4] and that the fatigue life decreases remarkably as loading frequency increases.

1.5 Scope of the study

In this study, the tension-tension fatigue behavior of the matrix-dominated angle-ply carbon/PEEK (APC2/AS-4) composite is investigated under a variety of loading

conditions (loading levels and frequencies). The purpose of carrying out those fatigue tests is to develop an understanding of how the material will behave when fabricated into components to be subjected to dynamic loading. In turn, this understanding can be used to develop new models for the material's fatigue behavior that can be used for design purposes.

The objective of this study is to investigate the following:

1-The effect of loading frequency on the fatigue life of this composite material under different loading levels.

2-The temperature behavior during fatigue at different loading conditions.

3-The stress-strain and hysteresis behavior during fatigue at different loading conditions.

4-The variation of the material's dynamic mechanical properties as a function of temperature and frequency.

1.6 Selection of study parameters

A thermoplastic matrix composite carbon/PEEK (APC2/AS-4) is selected for the present investigation.

The angle-ply lay-up $[\pm 45]_{4s}$ is selected because it represents a typical matrix-dominated composite that shows a significant viscoelastic behavior. In addition, the

angle-ply lay-ups are found in many practical applications, especially in applications that require high shear strength and geometrical stability such as pipes and pressure vessels.

The (tension-tension) fatigue test is selected because it is considered the most appropriate type for testing thermoplastic material. The tension-tension fatigue test also represents the most uniform and severe form of fatigue loading. The selected loading wave form (sinusoidal) represents the most practical wave form in actual fatigue cases, since it does not imply long holding periods.

As proper fatigue data is of main concern for developing a better understanding of fatigue behavior, real time data of the applied fatigue stress, fatigue strain, and temperature were collected throughout the tests.

1.7 Study outline

A review of relevant works of the effect of loading frequency on the fatigue behavior of composite materials is presented in chapter 2 of this study. The role of fiber type and matrix type are investigated in this review.

In chapter 3, the material used is described, followed by a description of the manufacturing process of the composite plates and the preparation of the static and

fatigue samples from the manufactured composite plates. The experimental set-ups for both static and fatigue samples are also described.

The experimental results for static and fatigue tests are displayed in chapter 4. On-line observations of fatigue damage during fatigue tests are presented, along with explanations for the different results obtained. In chapter 5, experimental data are analyzed, and a model for the thermal effect is proposed. Finally, a discussion of the results is presented in chapter 6, and a number of concluding comments are outlined.

CHAPTER 2

Effect of loading frequency on the fatigue behavior of composite laminates: A review

2.1 General

Because of the nature of the fatigue problem, loading frequency is considered as one of the most important factors in characterizing the material fatigue behavior. This importance becomes more pronounced for materials that exhibit time-dependent behavior during the course of loading, such as plastics and polymeric matrix composites.

A number of studies on metallic materials [8,9] have shown that loading frequency does not have a significant effect on the fatigue behavior of these materials over a wide range of frequencies. The hysteresis was observed to be extremely small in the elastic stress range for such isotropic materials.

However, the situation is quite different for composite materials. The pronounced viscoelastic behavior of the matrix material implies that composite systems are, in general, highly frequency dependent in their fatigue behavior. In some cases, increasing loading frequency results in a proportional decrease in fatigue life or material properties, while in other cases high loading frequencies result in increased fatigue life. In other

studies[14,20] nonlinear fatigue behavior and inelastic deformation have been reported as a function of frequency.

Therefore, understanding the effect of loading frequency on the fatigue behavior of a certain composite material requires a good understanding of the viscoelastic behavior of that material. Also, other related features such as the material toughness, damage propagation and fracture modes, matrix type, fiber type, and interface strength, are of the same importance.

2.2 Viscoelasticity and hysteretic heating

When a homogeneous isotropic material (such as a metal or an alloy) is loaded, a certain amount of strain energy is given to the material, which is supposed to be released upon unloading. Since such materials behave elastically up to yielding, the stored energy is released during unloading without a significant loss.

The loss of strain energy in any material can be defined as the area between the consecutive paths of loading and unloading in a stress-strain curve, which is known as the hysteresis loop. For isotropic materials, the two paths of loading and unloading almost coincide, indicating an extremely small hysteresis or a very insignificant amount of energy loss.

Different behavior is usually observed in composites, especially in those employing polymeric matrix materials. The chemical structure of the matrix materials and the nonhomogeneous nature of the composite systems result in a quite different behavior of the composite, which is known as "viscoelasticity". Due to this behavior, the composite material looses a certain amount of its strain energy; this amount depends on the material's nature and the significance of its viscoelastic behavior.

Basically, the viscoelastic behavior of a composite material can be clearly observed if the material exhibits a time-dependent behavior during its loading course, such as rate dependence creep or stress relaxation. Fatigue loading is another case in which the viscoelastic behavior becomes more feasible. Due to this behavior, the cyclic loading leads to energy losses (hysteresis) for each cycle of the applied stress. This energy loss results in the generation of internal heat (hysteresis heating) which is supposed to be transferred to the surface by conduction and then to be dissipated to the surrounding by convection and radiation.

The amount of energy loss and hysteresis heat generated depend on a number of factors. Among those are; the loading conditions (loading level and frequency), the viscoelastic properties of the material (such as its damping characteristics, its response to creep and recovery and stress-relaxation), the heat transfer characteristics (such as the material's thickness, geometry, and thermal conductivity), and the material damage

characteristics as manifested by the rate of damage development and growth under fatigue loading.

As fatigue proceeds, a number of damage types start to develop and progress within the material. The damage influences the heat generation by increasing the effective stress acting on the undamaged regions of the material and by increasing the hysteretic losses[1]. Moreover, the cracks between plies increase friction and alter the heat transfer characteristics of the material[1,2,7].

Depending on the amount of the energy loss, the heat generated in the material will be manifested as a temperature rise. Since the thermal conductivity of composites is generally low, not all the heat generated will be dissipated through the surface as expected. This may lead to a temperature gradient within the material, with a maximum value at the center[1].

2.3 Effect of loading frequency

Because of the pronounced viscoelastic nature of polymeric matrix materials, polymeric composites are highly sensitive to loading conditions, that is, the load level and loading frequency. However, because of the complexity of frequency effect, and because the behavior patterns are not yet fully elucidated, the number of works that deals with this effect is still very limited.

In general, two major types of failure modes can be identified in fiber-reinforced composites[6], that is, fiber-dominated failure and matrix-dominated failure. Most studies tend to consider that the material behavior under fatigue as mostly a matrix-related criterion, even though in some specific cases the effect of fiber can be clearly identified.

The following sections discuss some of the recent findings about the role of the constituents (that is, the fibers and matrix) on the fatigue behavior of composites under a variety of loading frequencies.

2.3.1 Effect of fiber

The effect of the fiber on the fatigue behavior of polymeric composites can be recognized in two major situations. The first involves the fiber type, while the second involves fiber-dominance in the mechanical behavior and failure modes of the composite.

The type or nature of the fiber has an important effect on the composite's behavior under fatigue. It can be said that carbon and boron fibers are more effective than glass fibers in terms of fatigue resistance. This superiority can be attributed in part to the higher thermal conductivities which will tend to reduce the hysteric heating by dissipating the generated heat in a faster and more effective way, and in part to the lower matrix strain at a given applied stress[7]. The latter effect is a consequence of the exceptionally high

Young's modulus. For this reason, the number of works that investigate high modulus high strength fibers as a major cause of fatigue failure is relatively small since the nature of the problem is fairly explained.

Glass-fiber reinforced composites are generally more sensitive to fatigue loading than composites based on high modulus fibers[1,6,7,13,17]. The relatively low elastic modulus of glass fibers results in higher strain levels in such laminates than with other fibers[13]. This exercises the matrix and the interface so that matrix cracking and debonding occurs at lower stresses than with other systems.

The effect of the fiber type can also be recognized according to its sensitivity to time-dependent phenomena such as creep and relaxation. In general, glass and organic fibers such as for kevlar-49 do not exhibit particularly good creep resistance especially at high stress levels[66]. Also, because of their silica-based structure, glass fibers are known to suffer from static fatigue (or creep rupture) due to a stress-corrosion mechanism acting in the presence of even a small amount of moisture. On the other hand, the creep rates of other fibers such as graphite and boron are much lower.

These aspects affect the overall fatigue performance of the composite. A number of studies has shown the special sensitivity of glass fiber composites to fatigue loading. The results of Kujawski and Ellyin[6]and James et al.[17]have shown the significant

effect of stress rate and frequency on the creep and relaxation behavior of glass reinforced composites during fatigue. At low stress levels, an increase in cyclic creep rate results as frequency decreases. Hence, the fatigue lives were found to decrease as frequency decreases, with more decline at higher load levels. Longer fatigue lives were reported when frequency increased at low stress levels. On the other hand, fatigue lives were found to decrease at high load levels and frequencies as local heating took place[6,13]. Also, cyclic creep rates were found to increase at higher load levels and lower frequencies. Therefore, it would appear that at high loads an increase in frequency will result in an (accelerated) increase in cyclic creep and properties deterioration due to local heating and stress heterogeneity. At low loads more cyclic creep can develop as frequency decreases because there will be more time under load for this to occur. The higher damage rates at lower frequencies[13] implies the sensitivity of glass fibers to static fatigue phenomenon.

However, in the above mentioned works, only low to moderately high frequencies were employed (0.01Hz-3.6Hz) so that thermal effects were not significant. At fairly high frequencies (10Hz-40Hz), Dally and Broutman[1] have found that the fatigue lives of glass reinforced composites decrease as loading frequency increases, with more decrease at higher stress levels. As a result, the material properties are reduced because the effect of temperature rise becomes more significant, with more elongation at higher frequencies. Miner et al.[18] have shown similar load-rate sensitivity of kevlar-49 composites. The

fatigue life of unidirectional kevler/epoxy at 30Hz was much less than that at 10Hz. However, the fatigue life of kevler/epoxy was found advantageous to that of glass/epoxy under similar loading conditions, even though they have similar creep behavior. This can be attributed to the higher modulus and higher resistance to static fatigue of the kevler fibers.

The effect of fiber on the fatigue behavior can also be recognized in fiber dominated composites. It has been customary to consider composites having a sufficient number of layers in the loading direction(25% or more 0°-plies) as fiber dominated composites. A number of studies have investigated the fatigue behavior of fiber dominated composites.

Saff [12] has found that graphite/epoxy fiber-dominated composites are less sensitive to tension-tension fatigue loading than matrix dominated ones. Also, the results of Dally and Broutman [1] have indicated that under similar fatigue conditions, cross-plied glass/epoxy laminates exhibit less hysteresis effects and longer lives than isotropic ones. Similarly, graphite/PEEK isotropic laminates have shown less temperature rises and longer fatigue lives than angle-plied ones [4].

On the other hand, the results of Jumbo et al. [2] have shown the high sensitivity of fiber-dominated composites when loaded under tension-compression fatigue. As

frequency decreases, a small variation in load level results in very different fatigue life, with extremely low lives at low frequencies. When fibers are loaded near to their buckling load for longer times, they exhibit buckling failure more easily. At higher frequencies, the effect of fibers becomes less significant since the decrease in fatigue life results mainly from the significant temperature rises as frequency increases.

2.3.2 Effect of matrix

In general, matrix materials are considered the strength limiting factor in composite systems. Moreover, because of the pronounced viscoelastic nature of polymeric materials, the fatigue performance of polymeric composites is usually considered a matrix-related phenomenon. Therefore in most fatigue studies, the materials, lay-ups, and frequencies are selected to examine the effect of the matrix material on the fatigue behavior of the composite.

Although both thermoplastic and thermosetting resins are used, thermosetting resins are usually used for composites subjected to the most severe service conditions because of their higher modulus and dimensional stability, especially at elevated temperatures. Unlike thermoplastics, the properties of thermosetting resins are coupled with a generally brittle, low fracture toughness and lower fatigue resistance characteristics.

Nevertheless, both thermosetting and thermoplastic composites show a high viscoelastic behavior (although in different levels), and thus, their fatigue behavior is highly frequency-dependent as shown by a number of works.

Recent works[1,6,13,17,18] have indicated the high susceptibility of glass/epoxy composites to loading frequency, related to both the special nature of glass fibers and the viscoelastic nature of the epoxy matrix. Results of Mandell and Meier[13] have shown that the sensitivity of glass/epoxy composites to cyclic stresses is generally much greater than their sensitivity to static fatigue. Shorter fatigue lives and more damage rates have been reported[6,13,17] as frequency decreased, especially at low load levels, even though the temperature rises were not significant under these conditions. Also, higher values of failure strain have been reported[17] as frequency decreased. These features show the effect of the matrix creep behavior that epoxy composites exhibit when exposed to longer times under load, since at low load levels, more cyclic creep can develop as frequency decreases. It appears that more cyclic creep can develop in epoxy-based composites at low frequencies and load levels as there will be more time under load for this to occur.

The viscoelastic nature of the epoxy matrix is more pronounced at higher frequencies. Longer fatigue lives have been reported[13] as frequency increases. On the other hand, the values of strain to failure decrease as frequency increases, with immediate

failure as the strain exceeds a certain critical value. This may explain the reason for longer fatigue life at moderately high frequencies.

At fairly higher frequencies, a significant accumulation of cyclic creep and a decrease in stiffness were found[6] with a significant temperature rise[1] which results in more elongation and shorter fatigue lives. It would appear that at high load levels, the increase in loading frequency will result in an increase and accumulation of cyclic deformation due to local heating and stress heterogeneity, as evidenced by the increase in damage rates[21].

Reifsnider et al.[3] and Stinchomb et al.[14] have investigated the fatigue behavior of boron/epoxy and boron/aluminum composites as a function of loading frequency. Their results have shown similar fatigue trends of both composites at high frequencies in terms of both stress sensitivity and surface temperatures. The rate of temperature increase in the Boron/epoxy composites follows the rate of load increase due to the matrix damage development and viscoelasticity that results in significant temperature rise. Also, an increase in cyclic strain were found as frequency increases, with nonlinear changes in the material's stiffness and specific damping. On the other hand, the B/Al composites have shown a decrease in cyclic strain as frequency increased, with similar nonlinear effects for the stiffness changes as a function of fatigue life. The matrix damage caused by the low frequency loading was found greater than that caused

by higher frequencies (as reflected by the decrease in stiffness) at the same number of cycles. This indicates that the low frequency fatigue loading produces more concentrated local damage in the matrix accompanied with higher stiffness reduction, whilst the high frequency loading produces more dispersed damage and less stiffness reduction. In general, the fatigue performance of B/Epoxy composites was found to be much better than that of B/Al composites at all frequencies, evidenced by less reduction in fatigue strength and stiffness.

For graphite/epoxy composites, the high modulus of the graphite fibers results in composites with excellent fatigue resistance and low strength degradation rates. However, because of the viscoelastic properties of epoxy, the fatigue behavior of graphite/epoxy is considered highly frequency-dependent. Sun and Chan[5] have found that at low frequencies, the fatigue life of notched angle-plied graphite/epoxy increases as frequency increases, provided that the temperature rise is not significant. On the other hand, a decrease in fatigue life was noticed as frequency increased. Also, peak lives were noticed at different frequencies for different load levels, with the peaks shifting towards the higher frequencies as load level decreases when temperature rises took place . However, at high load levels and frequencies, significant temperature rises were reported, which clearly indicates that the decline in fatigue life might be a result of the significant temperature rise. The results of Saff [12] may provide an evidence for this behavior: when similar specimens were cycled under cooled fatigue tests, it was found that the fatigue life increased as frequency increased, even though the rate of fatigue life increase

started to decline at higher frequencies. At low frequencies, the increase in fatigue life as frequency increases can be related to the common creep behavior that most epoxy composites exhibit as time under load decreases.

In contrast to thermosetting matrix composites, thermoplastic-based composites such as graphite/PEEK are known for their ductility and high fracture toughness, which is attributed mainly to the matrix material. The high values of interlaminar fracture toughness enables thermoplastic composites to sustain more loading deformation before their final failure.

However, the fatigue behavior of thermoplastic composites seems to be different from their behavior under static loading. The results of Curtis et al.[4] have shown that the fatigue strength of graphite/PEEK decreases as loading frequency increases. Significant temperature rises were recorded as frequency increased[4,15], which appeared to be a function of frequency, stress level and specimen thickness. At high frequencies, it was noticed that the temperature increases as load level and thickness increase, while at lower frequencies the temperature increases as load level and thickness decrease. The temperature rise was more significant at higher frequencies, especially in laminates with more matrix influence. It can be concluded that the thermal effects are more pronounced in this type of composites at all frequencies and load levels, and therefore they might be responsible for the decline in fatigue lives and properties.

Two important features have been observed during the fatigue life of angle-plied laminates[4]. Firstly, a significant temperature rise was reported as frequency increases (170°C at 5Hz, 60°C at 0.5Hz)which is quite high for a composite with a glass transition temperature of 143°C. Secondly, a peak in temperature was observed at a certain number of cycles during the specimen's life. Moreover, higher levels of temperature rise were observed at higher load levels and frequencies, which resulted in shorter fatigue lives. The X-ray photography has shown that a significant fatigue damage occurred well before the temperature peak.

2.4 Summary

From the previous review, it is clear that the fatigue behavior of polymeric composites is generally frequency-dependent. This dependency varies from one composite to another, depending on the nature of the fiber, matrix, and interface. Other factors such as the composite's geometry (thickness and lay-up), loading level, and loading form (tension, compression, etc.) also have a significant influence on the frequency effect.

The effect of the fiber type can be seen in two cases. The first is when the fiber itself shows a significant time-dependent behavior, such as in glass reinforced and Kevlar-49 reinforced composites. In such cases, the fibers exhibit significant

accumulation of creep rates which result in lower fatigue lives as frequency increases. As frequency reaches higher values, the fatigue life starts to decline sharply as a result of temperature rise which deteriorates the composite's stiffness and strength. The exceptional sensitivity of glass fibers to "static fatigue" increases the influence of the fiber on the fatigue behavior of the composite, and in turn the sensitivity of such composites to loading frequency.

The second case can be seen in composites that exhibit fiber-dominated behavior during both static and fatigue loading. Composites with more percentage of fibers in the load direction show special sensitivity under fatigue, since the fatigue loading may result in fiber deformation, breakage, and buckling. These features can be seen essentially if the fatigue loading contains a compression component. In this case, even composites with high modulus fibers may show extensive fiber buckling as a major cause for fatigue failure.

Except in the cases mentioned above, the matrix material can be considered the major factor that affects the fatigue behavior of the composite system. The pronounced plasticity and viscoelasticity of polymeric matrices result in the frequency-dependency of their composites, even in those reinforced with relatively high modulus fibers such as graphite/epoxy and graphite/PEEK composites.

These matrix properties of plasticity and viscoelasticity, in addition to others such as the material toughness and ductility, contribute to the fatigue behavior of the composite in a relative manner according to their evolution in the virgin matrix material. The relatively low plasticity and the brittle behavior of epoxy assists in an early initiation of transverse cracking in graphite/epoxy composites, which progresses throughout the fatigue life until the final failure when the damage reaches a certain level of saturation[21]. On the other hand, because of the higher plasticity and toughness of thermoplastic PEEK, very late damage occurs shortly before the final failure[23-25].

A general behavior of graphite/epoxy composites can be concluded [2,3,5,12]. At low frequencies, fatigue life increases as frequency increases if the temperature rise is not significant. On the other hand, the temperature rise becomes more significant at higher frequencies, and fatigue life decreases accordingly.

In contrast, the fatigue life of graphite/PEEK decreases in general as loading frequency increases. Significant temperature rises are obtained at all frequencies, increasing as frequency increases. In general, the temperature rises were found to be more significant in graphite/PEEK than in graphite/Epoxy composites at all frequencies for the same number of cycles, resulting in shorter fatigue lives of PEEK composites at higher frequencies. This behavior of graphite/PEEK is unexpected from such a thermoplastic, high toughness composite. It appears that the high fracture toughness of such materials

becomes ineffective or even disadvantageous during fatigue loading. O'Brien [22] has found that, although the static interlaminar fracture toughness of CF/PEEK composites is much higher than that of CF/epoxy, the delamination fatigue interlaminar fracture toughness threshold was only slightly greater, which means that the delamination resistance of CF/PEEK composites in fatigue is significantly less than its resistance to delamination under static loading.

In general, it can be concluded that the fatigue behavior of CF/PEEK is superior to that of CF/Epoxy at low frequencies, while at high frequencies the significant temperature rise in CF/PEEK results in a poor fatigue behavior when compared to CF/epoxy. On the other hand, catastrophic failure is a common feature for CF/Epoxy composite, while in CF/PEEK composites the higher rates of plasticity and toughness result in nonlinear deformation and delayed failure.

From the damage propagation and failure modes in both materials, it seems that the brittle nature of the epoxy resins results in a fatigue behavior that is dependent on both damage propagation and the viscoelastic nature of the epoxy. In PEEK-based composites the ability of this high toughness material to sustain more cyclic deformation and to delay damages indicate that the fatigue behavior of these composites is purely viscoelastic-dependent.

CHAPTER 3

DESCRIPTION OF THE MATERIAL AND EXPERIMENTAL PROCEDURE

3.1 Material Description

The material used in the present investigation was Carbon/PEEK (APC-2/AS-4). The material was supplied by ICI Fiberite Inc. (U.S.A.) in the form of continuous unidirectional prepreg tape of 12-inch width. The fiber content in this material is 62% by volume and 68% by weight[26].

3.2 Manufacturing of composite laminates

The composite plates were manufactured by hot press molding, in a 100-ton Wabash press. The press used is a computer program-operated so that all processes and parameters can be controlled by pre-setting values. Temperatures, pressures, and time required for each step were all set in advance, so that the required heating (or cooling) level is achieved in a certain time, and the desired pressure is applied at a certain time and for a certain period. Also, it was possible to achieve maximum cooling rates using both air and water simultaneously.

An aluminum picture frame mold was used to mold the composite plates. The mold was made of three main components as shown in Fig.3.1; the base, the picture frame, and the upper matching plate. For easier stacking of the prepreg and removal of the plates after molding, the picture frame part was made of four equal pieces at right angles to one another, and the inner dimensions of the frame were about 3mm larger than those desired for the composite plates.

The prepreg tape was cut into 8″×8″ sheets inclining at 45° to the fibers direction. The sheets were layed-up into stacks of sixteen plies at ±45° directions, balanced and symmetric with respect to the midplane to avoid any bowing due to differential thermal contraction on cooling. Also, to avoid the effect of the curvature caused by supplying the material on reels, the individual plies were stacked in opposite curvatures with respect to the midplane. The angle-plied stack was placed in the mold with the upper matching plate covering the stack.

The mold was placed between the plates of the press which was preheated to 400°C. Fig.3.2 shows manufacturing set-up of the composite plates. A contact pressure of 0.5MPa (70 psi) was applied to ensure good heat transfer to the material without stressing the fibers before the PEEK matrix is soft enough to be compliant. Heating was continued at this stage for about 10 minutes which was sufficient to achieve thermal equilibrium at 380°C. When the temperature was stabilized at 380°C, consolidation pressure of 1.4MPa

(200 psi) was applied for 10 minutes. After that, post-consolidation cooling was applied at maximum rate to achieve optimum crystallization. Both air and water cooling were used in maximum rate so that it was possible to achieve an average cooling rate of about 22°C/minute.

To provide accurate control and monitoring of the temperature history during molding, temperature was measured by a thermocouple passing through a tiny hole in the frame's wall, with the tips touching the edge of the stacked laminate. The temperature variation was recorded by an X-Y plotter. Fig.3.3 shows a typical temperature record for the composite plates.

3.3 Preparation of Samples

The samples for both static and fatigue tests were cut from the composite plates using a diamond-impregnated cutting saw. High speeds and low feeding rates were used during cutting, in accordance with the manufacturer's recommendations.

Subsequently, each sample was finished by smooth filing to achieve near final dimensions and to avoid any stress concentration along the samples edges. Aluminum tabs of 1.5mm thickness and 38mm long were bonded to the end of the samples using high shear strength epoxy based adhesive.

The final dimensions of the samples were in accordance with ASTM D3039[27], ASTM D3479[28], and other references as follows:

Total length : 196mm±3%

Gage length : 122mm±1%

Sample's width : 18mm±1%

Sample's thickness : 2mm±5%.

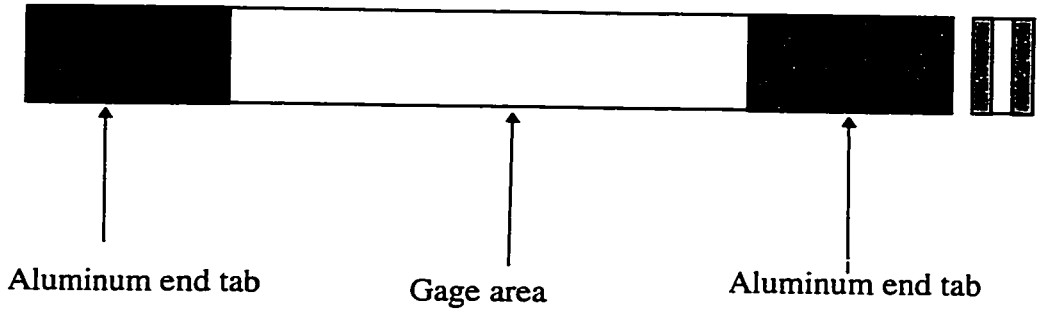

Fig. 3.1(a) Straight-sided samples used for the static and fatigue tests.

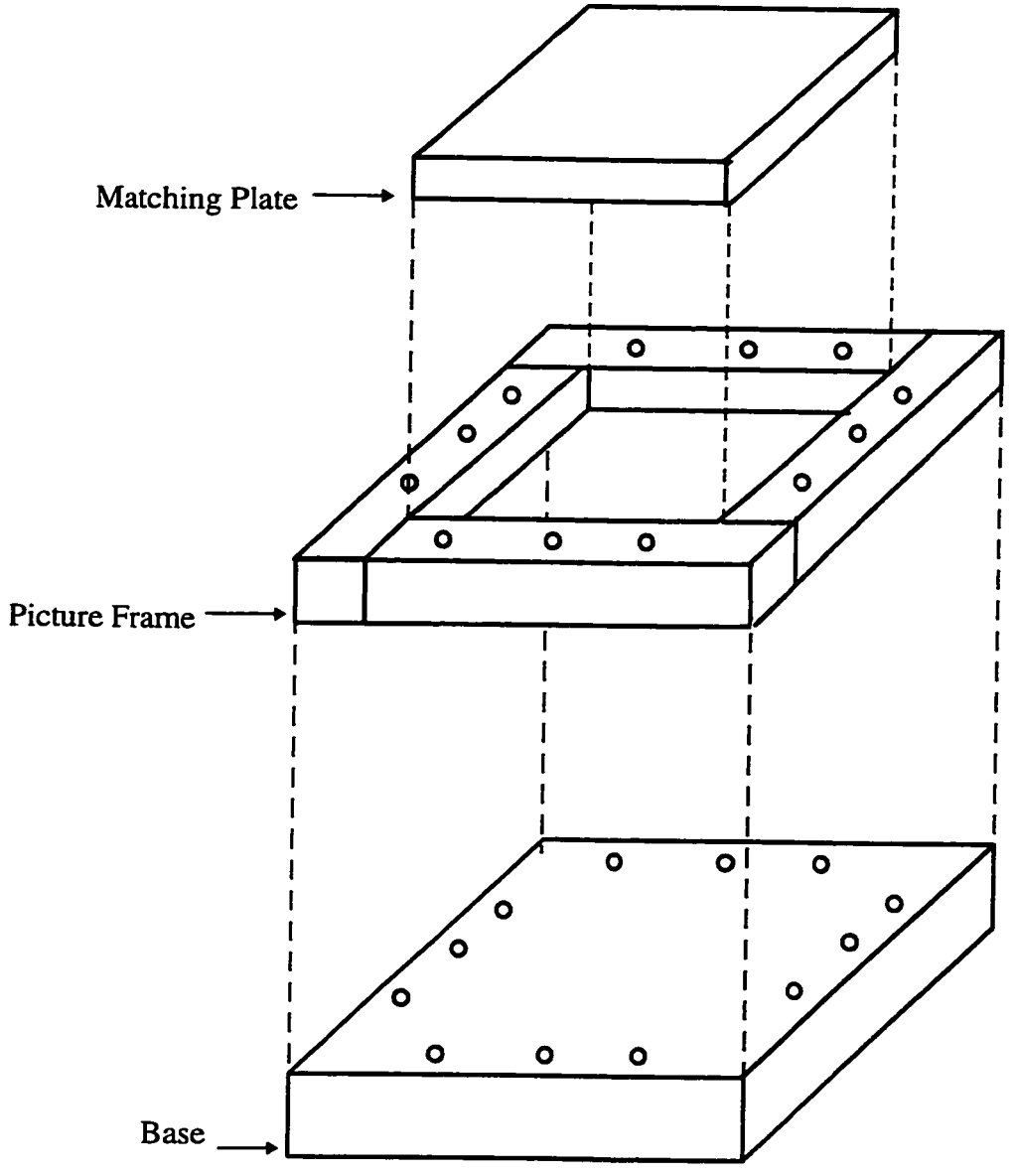

Fig. 3.1(b) A schematic drawing for the picture frame mold used in manufacturing the (APC-2/AS4) composite plates.

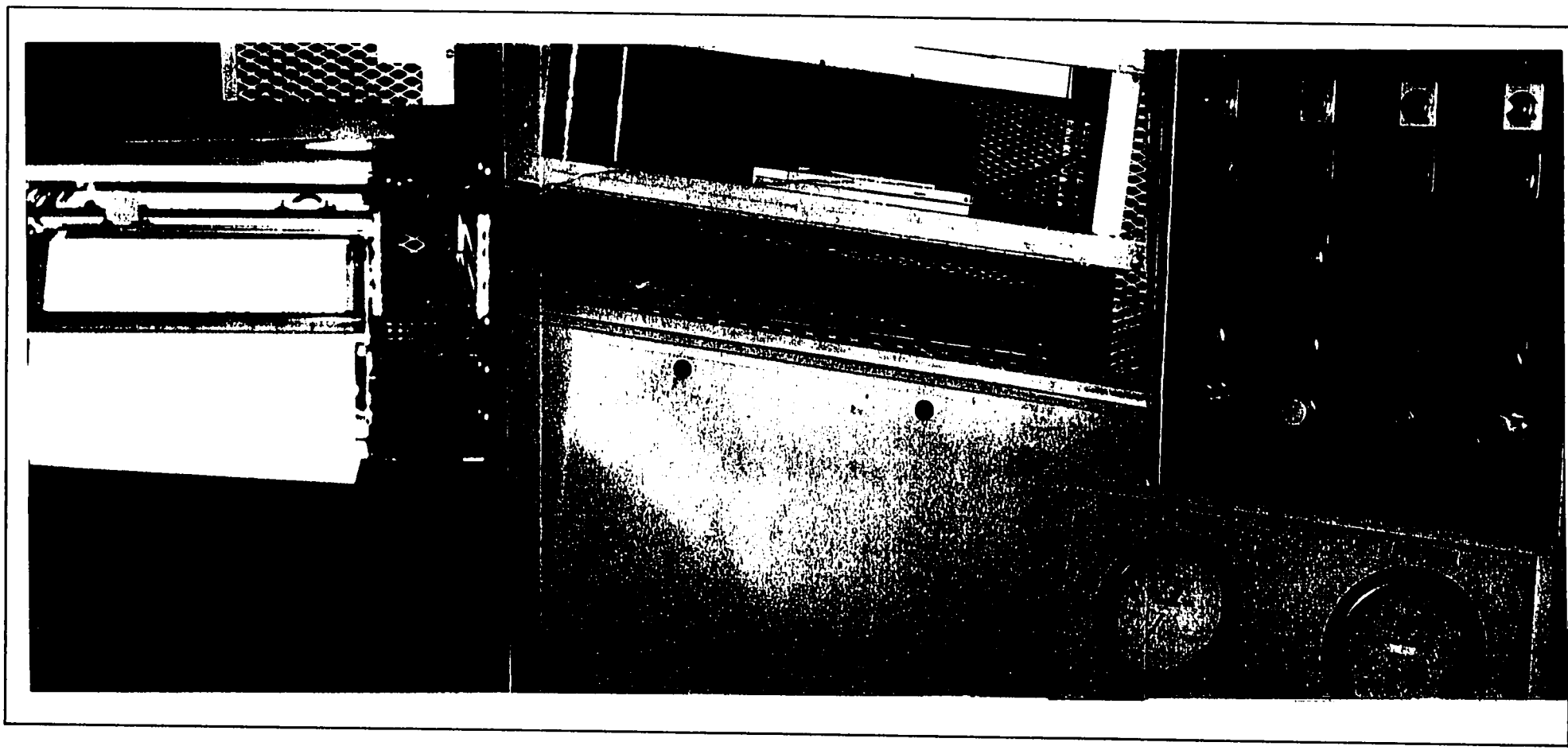

Fig. 3.2 Manufacturing set-up for composite plates by hot-press molding.
Shown; control panel (left), press and mold (center), and temperature recording X-Y plotter.

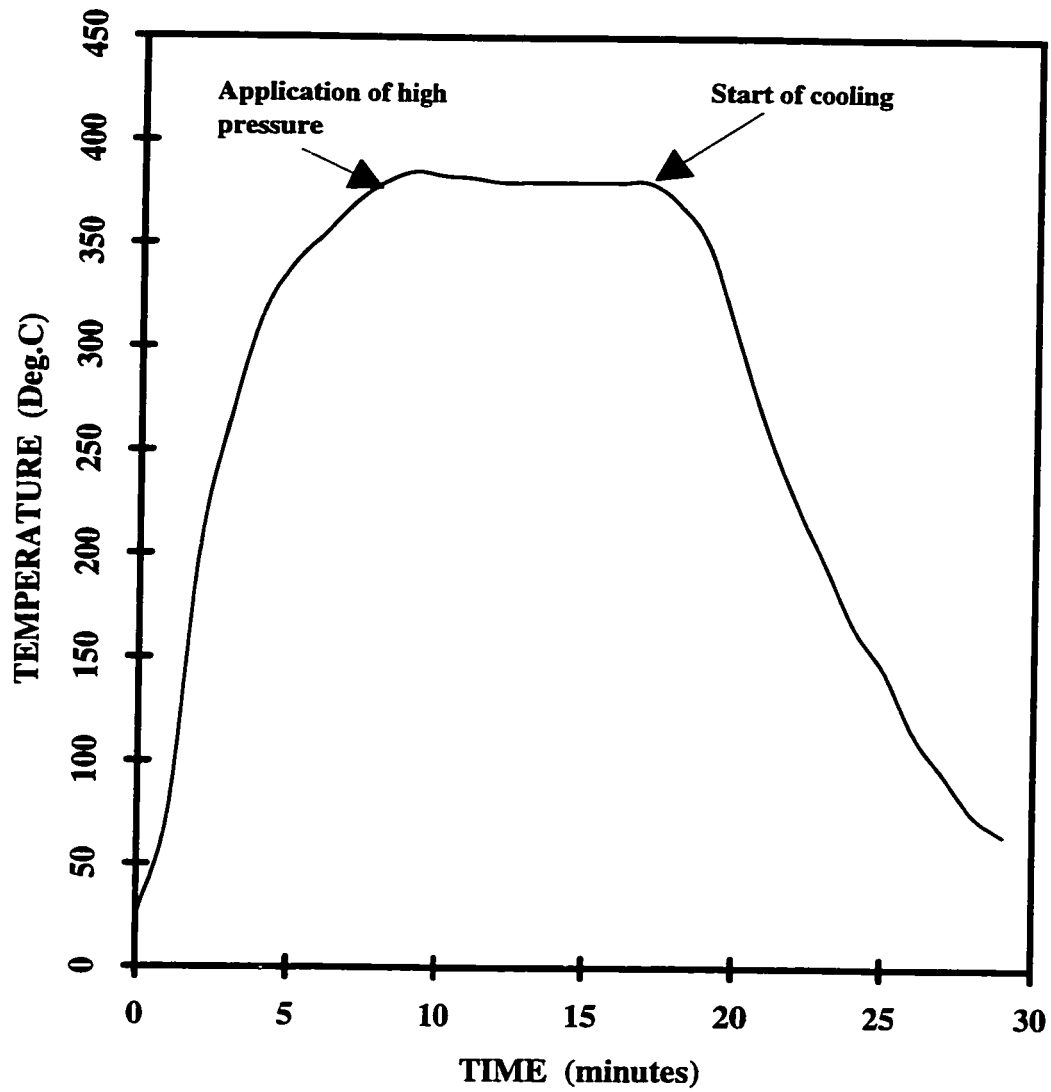

Fig.3.3 A typical manufacturing cycle for APC2/AS-4 composite plates by hot-press molding (produced from the original chart)

3.4 Experimental Set-up

A 100-kN MTS machine and testing system was used for both static and fatigue tests. The machine was operated through a computer program (provided by MTS) which allows a wide range of control features such as the application of different load forms, the rate of loading and unloading, the use of different loading wave forms and frequencies, in addition to the calibration option which allows pre-calibrating and presetting any control signal out or into the testing system. Samples were aligned and clamped between hydraulic grips which provided strong and stable holding of the sample during testing without slipping by applying a pre-selected hydraulic pressure in a transverse direction to the end of the sample. The aluminum end tabs provided better gripping and protected the samples from crushing under the grips transverse pressure.

Axial strain was measured by using a ±15% extensometer. However, to account for strains over the extensometer's range, the displacement of the cross head was recorded as well. Because the values of axial strain were of main concern, a number of measures were taken to insure that the extensometer's and displacement readings are real and accurate:

1-On-line calibration was performed before each test, including shunt calibration of the extensometer's circuitry.

2-Electronic drifting test was performed for a period of 24 hours, which revealed an

extremely insignificant drifting.

3-Some samples (at different frequencies and load levels) were marked at measured points before loading in fatigue. The changes in the location of these marks were measured using a high precision vernier, either at different stages during cycling or after failure, and compared to the strain values from the extensometer at that specific stage.

4-In addition to the strain values from the extensometer, cross head displacements were also recorded and the apparent strain values were then compared.

As a result, it was found that the strain values measured by the extensometer were quite reasonable and accurate, and that the strain values calculated from the displacement's readings were in good agreement with those measured by the extensometer.

K-type thermocouples were used to record the temperature variation during fatigue tests. The thermocouple was mounted at the center of the sample's surface. In fatigue tests at 5Hz and 10Hz, another two thermocouples were used for recording the temperature variation at points near the upper and lower ends of the sample's surface, and were mounted at equal distances from the center. Fig.3.4 shows a schematic diagram for the experimental set-up of the fatigue tests. A data acquisition system (System 200 from Scimetric) was used in acquiring and saving the experimental data. The system consists mainly of three parts; an analog/digital (A/D) converter which converts the incoming data

signals from analog differential voltages into digital ones, a data acquisition card which collects the digital data signals and converts them into readable data points according to a preselected format, and a personal computer which controls all the acquisition process through a data acquisition software called WINGEN. Data were collected through signals from the load cell (for applied load), extensometer (for axial strain), cross head displacement (for axial displacement), and from thermocouples (for temperature). For static tests and fatigue tests at high stress levels and frequencies, data acquisition was continuous. For fatigue tests at low frequencies, data were collected periodically to limit the size of the data file.

In the first stages of fatigue tests, it was noticed that some samples were twisted at different levels (depending on the loading frequency) indicating that the samples were under torsion. It was found later that this problem was neither related to the symmetry of the samples nor to the experimental set-up or machine alignment, but rather to the testing machine itself. The restrictions of weight and length of the hydraulic pressure hoses, the fluctuation in pressure during cycling, and the floating actuator of the machine's lower cross head, all led to rotation in the actuator, and therefore induced a twisting moment on the sample (even after self-aligning the machine). To avoid this problem, a mechanical guide was made and installed on the machine so that it kept the machine in place during cycling without affecting the test's parameters or the machine's hardware.

3.5 DMA TESTS:

To provide more information about the material's viscoelastic dynamic properties and their variation as a function of frequency and temperature, a number of dynamic mechanical analysis (DMA) tests were performed on virgin samples of the same material.

DMA 983 (By TA Instruments) was used for the tests, along with a (TA Thermal Analyst 2100) data acquisition and analysis system for saving and analyzing the tests results. Tests were conducted at different frequencies (which are necessarily the same frequencies used in fatigue tests, i.e., 1Hz, 5Hz, and 10Hz) and a temperature range between room temperature and 150°C.

The samples used in the DMA tests were of the following dimensions;

Sample's total length	100mm ±2%
Sample's gage length	48.5mm ±1%
Sample's width	10mm ±2%
Sample's thickness	2mm ±5%

3.6 Measurement of fibers reorientation

An electronic optical imaging instrument was used to measure the fibers orientation after fatigue failure. The instrument provides accurate results for measuring

the angle between two solid edges of an object, provided that the object reflects a dark image for its surface on the optical display of the instrument. Angle measurements can be achieved to within ±5 seconds of a degree depending on the straightness of the edges enclosing the angle. In our case, it was possible to measure the angle between fibers in fatigue failed samples to within ±0.1 degree. In fatigue samples that did not fail, the angle between the fibers in the surface layer was measured using a high precision digital protractor.

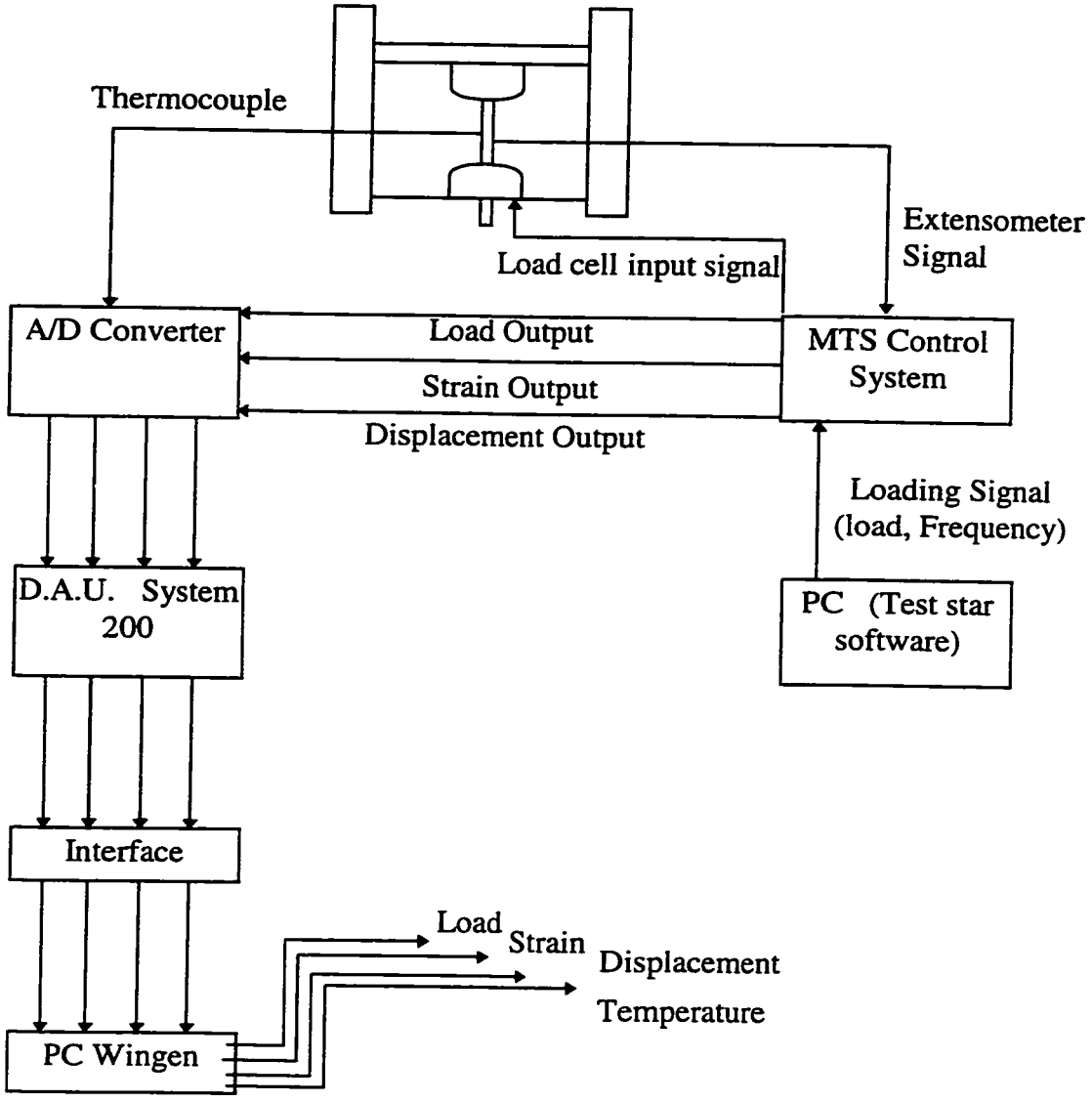

Fig. 3.4 A schematic diagram of the experimental set-up for fatigue tests.

CHAPTER 4

EXPERIMENTAL RESULTS

4.1 Static Tests

Five samples were selected randomly and tested to failure under displacement-controlled quasi-static tensile loading. The test speed was 2mm/min in accordance with a number of references [25,27,29,30]. During each tests, load and strain were recorded continuously up to failure. The results of static tests are shown in Table 4.1. The stress-strain diagram for a typical sample under static test is shown in Fig.4.1.

It can be noticed that the scatter in the results of static tests is very small, and hence, the static tensile mechanical properties can be considered as the average values of the different samples tested. That is:

Ultimate tensile strength σ_{ult}=338 MPa

Ultimate tensile strain ε_{ult}= 17.23%

Those values are very close to the ones mentioned in a number of references including the manufacturer's data sheet (σ_{ult}=300-365MPa).

Table 4.1 Results of static tensile tests of $[\pm 45]_{4s}$ APC2/AS-4 laminates.

Sample No.	Dimensions (mm)		Failure Load	Ultimate Strength	Failure Strain
	Width	Thickness	(KN)	(MPa)	%
ST-1	18.12	2.08	12.80	339.60	16.80
ST-2	17.98	1.94	11.95	342.60	17.50
ST-3	17.92	2.03	12.50	343.60	17.40
ST-4	18.06	2.08	12.30	327.45	16.95
ST-5	18.12	1.96	12.00	338.00	17.35
Average	**18.04**	**2.02**	**12.51**	**338.25±4**	**17.23±0.5%**
S.D.				**5.76 MPa**	**0.274%**

S.D. : Standard deviation.

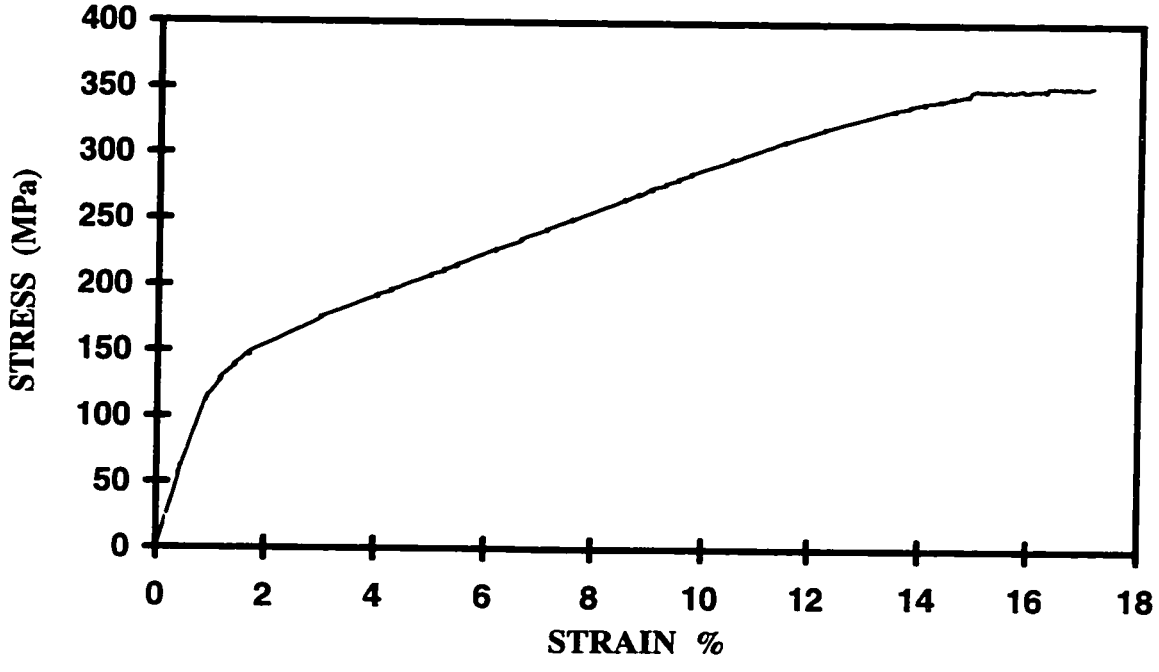

Fig.4.1 STRESS-STRAIN BEHAVIOR OF ANGLE-PLY APC2/AS-4 UNDER STATIC LOADING

4.2 Fatigue Tests

All fatigue tests were performed under tension-tension, load-controlled cycling at room temperature. Three load levels were used (60%, 70%, and 80% of the ultimate tensile strength), with a fatigue ratio of R=0.13. Due to technical difficulties in the MTS machine, especially at high frequencies and load levels, it was found that the most affordable fatigue ratio that can be performed is $R=\sigma_{min}/\sigma_{max}=0.13$. Below this ratio, the dynamic response of the machine, especially at high frequencies and load levels was not uniform. Samples were tested at three loading frequencies (1Hz, 5Hz,and 10Hz).

In order to achieve a uniform cycling amplitude at the required fatigue ratio, samples were first loaded in a quasi-static ramp up to the minimum load level. This load value was in the elastic range for all samples, and therefore, the strain induced in this stage was recoverable and small in value (~0.7%).

The stability of fatigue cycling was found to be dependent on the loading frequency. At 1Hz, the cycling was found to stabilize at the required load amplitude after only few cycles (~ 20 cycles). At 5Hz and 10Hz, stability was achieved at higher number of cycles (~50 cycles). This feature was more pronounced at 10Hz where more samples were discarded because of the instability and overshooting in load amplitude. In some cases, it was necessary to use higher minimum load levels and/or lower maximum load

levels (as inputs to the computer program which controls the machine parameters) in order to reach the required fatigue ratio and amplitude. The only way to reach this level of experience was by trial and error. Many samples were lost or discarded until reaching high levels of accuracy at each loading condition. Also, more samples were tested at loading conditions where these problems appeared, in order to achieve more confidence in the results at those loading conditions. Table 4.2 shows a summary of the fatigue tests results, while Fig 4.2 shows the results in the form of S-N curves (stress-number of the cycles to failure) at the three frequencies used.

In general, it is clear that the fatigue life (in terms of number of cycles to failure) decreases as the load level increases. At the same load level, the fatigue life decreased drastically as the loading frequency increases. Furthermore, it can be seen that the decline in fatigue life at high frequencies is much faster than that at lower frequencies.

4.3 Fibers reorientation after fatigue

The variation in fibers orientation after fatigue was measured using an electronic optical imaging device in the case of fractured samples and a high precision digital protractor for samples that did not fracture under fatigue. The new fibers orientations are shown in Table 4.3 for the three frequencies and load levels.

It can be noticed that fibers reorientation occurred in all samples at the different loading frequencies and load levels. The variation in fibers direction increases as the load level increases at the same frequency. Also, the variation increases as the loading frequency increases for the same load level.

Table 4.2 Results of fatigue tests for $[\pm 45]_{4s}$ carbon/PEEK samples at different loading conditions.

Load Level % (MPa)	1Hz		5Hz		10Hz	
	Sample	N	Sample	N	Sample	N
60% (203MPa)	1	1,400,000*	1	100,000	1	540
	2	1,200,000*	2	186,000	2	575
					3	1040
					4	580
70% (236.7MPa)	1	20650	1	1500	1	450
	2	16000	2	2200	2	260
	3	21000	3	1100	3	280
	4	18800	4	2600	4	470
80% (270.4MPa)	1	2900	1	350	1	200
	2	3000	2	200	2	180
	3	3350	3	220	3	315
	4	3570	4	200	4	120
					5	100

*: denotes that the sample did not fail at this number of cycles.

- N: number of cycles to failure.

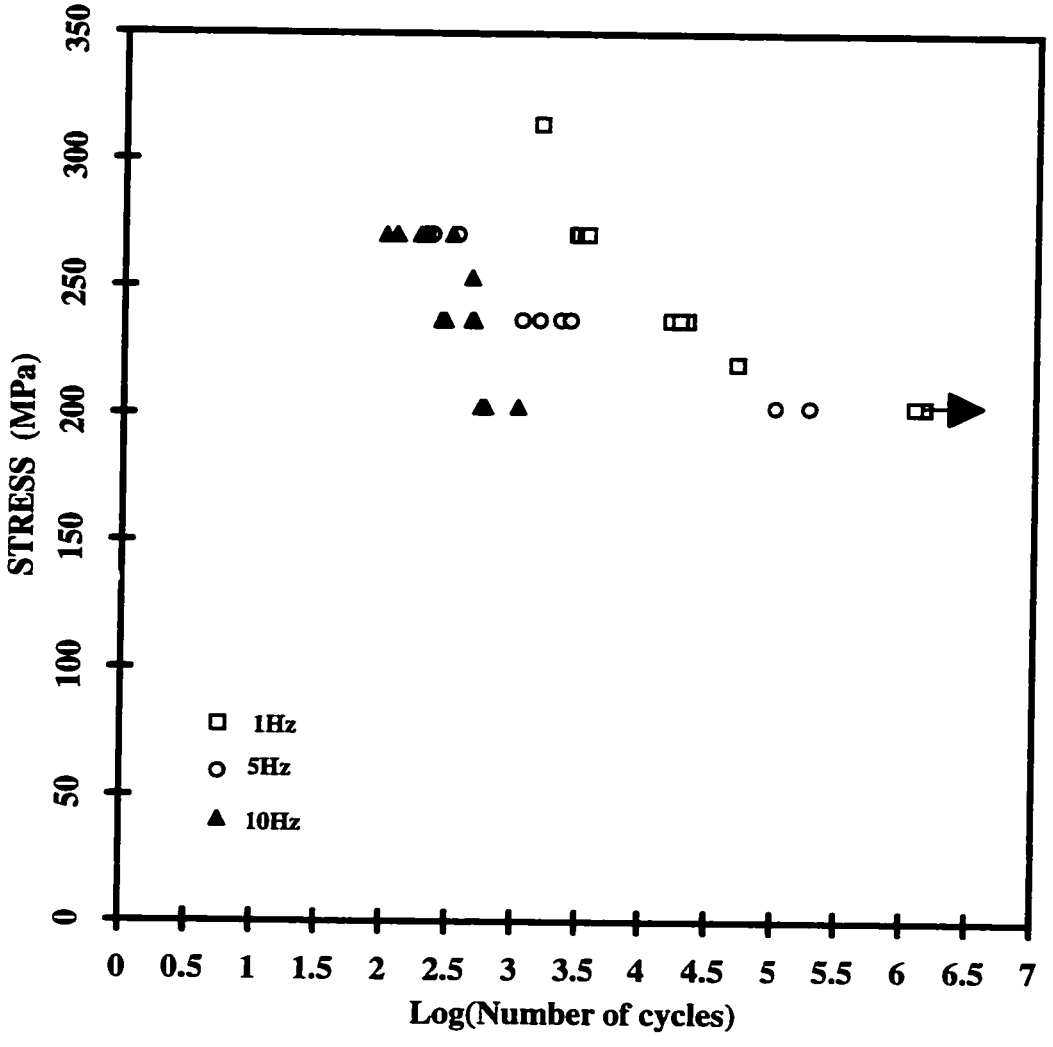

Fig.4.2 Stress-number of cycles (S-N diagram) for angle-ply APC2/AS-4 samples after tension-tension load-controlled fatigue (R=0.13)

Table 4.3 Fibers orientation* after fatigue at the three loading frequencies and load levels.

	1Hz	5Hz	10Hz
60%σ	86	78.28	74.06
	86	75.31	74.56
70%σ	84.25	73.41	71.30
	83.50	72.55	69.90
80%σ	81.00	71.06	69.12
	82.31	71.04	67.56

*For a ±45 fiber orientation, the original angle between fibers is 90° .

4.4 Results and observation of fatigue tests

The following sections show the most noticeable observations collected during fatigue tests. Even though damage monitoring and analysis were beyond the scope of this thesis, some damage observations were made and documented during the course of testing of most samples. Other observations of concern were collected and documented at certain events, and are reported here too.

Because of the variations in the material's behavior during each loading condition, the results are displayed in the following section according to each loading condition.

4.4.1 Fatigue tests at 1Hz

4.4.1.1 60%$\sigma_{ult.}$

The fatigue tests at this loading condition were characterized by the smoothness of cycling, with no signs of visible damage until about half of the fatigue life when some visible surface cracks started to appear. These surface cracks were very small in size and density. As fatigue progressed, surface splitting along the fiber direction in the surface layer started to appear in small quantities at different locations along the surface, even though no signs of damage were observed through the thickness. Fig.4.3 (top) shows

a sample fatigued to 1.4 million cycle at this loading conditions.

Fig.4.4 shows the stress-strain behavior in terms of hysteresis loops at different number of cycles at this loading condition, while Fig.4.5 shows the strain variation behavior during fatigue life for the same sample. The stress-strain behavior shows some hysteresis losses in the early stages of fatigue, which was accompanied by a slow and an almost constant increase in strain until a certain stage (number of cycles). Also in this stage, the strain rate started to decrease but in a smaller rate, which can be noticed from the slight decrease in the slope of the curve (notice that a logarithmic scale is used in Fig.4.5). At high numbers of cycles, the size of the hysteresis loops decreased, and the strain reached an almost constant value as the strain rate in the earlier stage continued to decrease . A number of features can be observed from the experimental data at this loading condition: first is the continuous shifting in hysteresis loops during the early stages of fatigue, which indicates that the material experiences a continuous creep under the applied cyclic loading. This behavior can be related to the nature of the thermoplastic matrix (PEEK). Under low loading frequencies, the material is almost under a constant load a period of time. During this stage, the strain increased in the beginning, followed by a decrease in strain rate around the end of the stage.

Second is the decrease in the rate of shifting in hysteresis loops and strain variation (and consequently the decrease in creep rate) during later stages of fatigue. For example, the strain variation between loops 6 and 7 in (Fig.4.4) was about 1% for 426,000 difference in cycles (2.37×10^{-8}/cycle), while for loops 1and 2 variation of about 0.5% in strain for 33550 difference in cycles (1.49×10^{-7}/cycle). This feature can be attributed to a state of secondary creep following cyclic hardening that took place in the earlier stage due to the continuous creep. Another possible reason for this behavior is the fibers rotation during cycling which may result in increasing the material's stiffness.

Third is the relative decrease in the energy dissipation (as reflected by the size of hysteresis loops) as the number of cycles increased. This observation is probably related to the state of secondary creep and the associated cyclic hardening that occurred previously.

Fig.4.6 shows the temperature variation during fatigue at this loading condition. In general, it is clear that the temperature rise was not severe throughout the loading course. Also, it can be observed that the temperature stabilized at a certain value (~34°C) after a certain number of cycles, which can be related to the low damage levels and insignificant hysteresis losses during fatigue at this loading condition

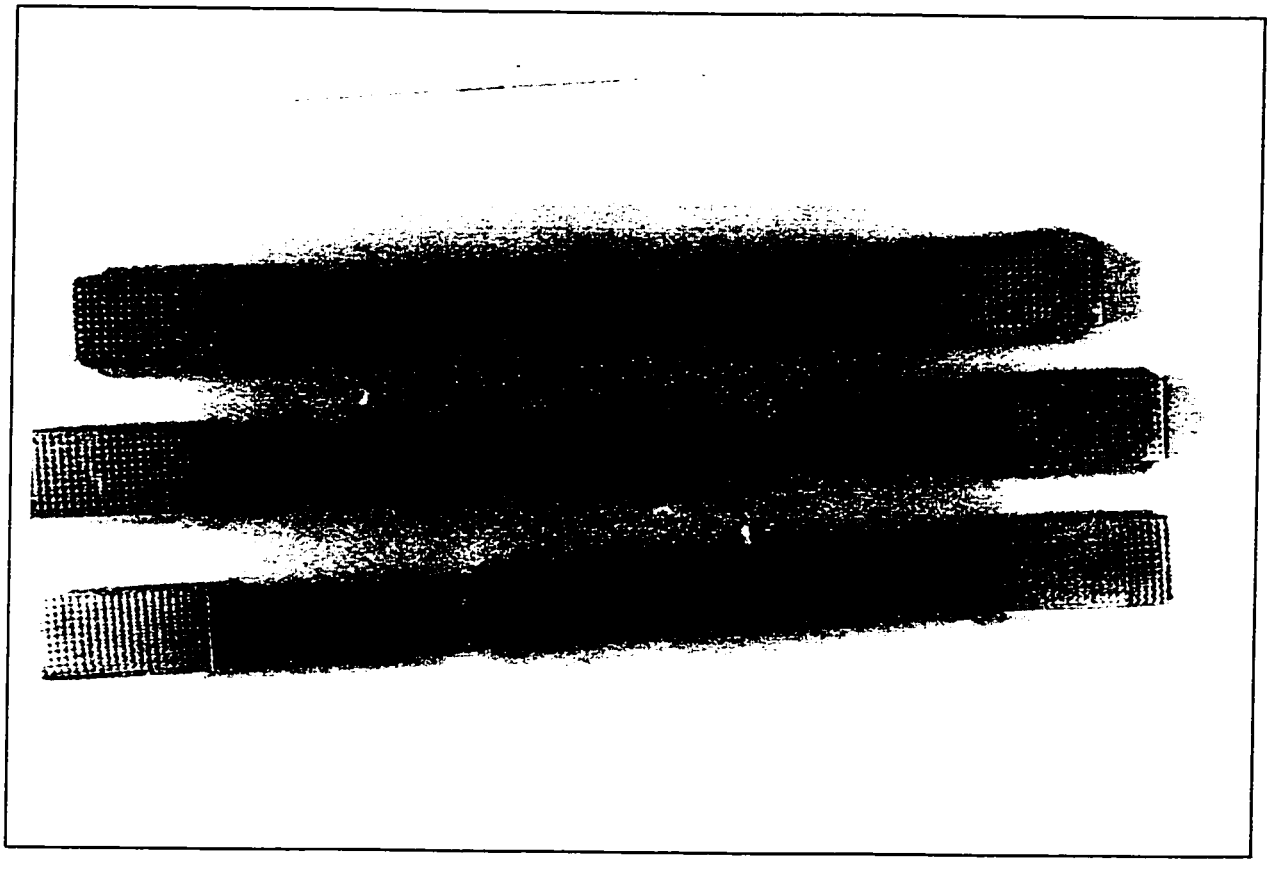

Fig. 4.3 Typical fatigue samples cycled at 1Hz and the three load levels, where: (top) at 60%$\sigma_{ult.}$, (center) at 70%$\sigma_{ult.}$, and (bottom) at 80%$\sigma_{ult.}$.

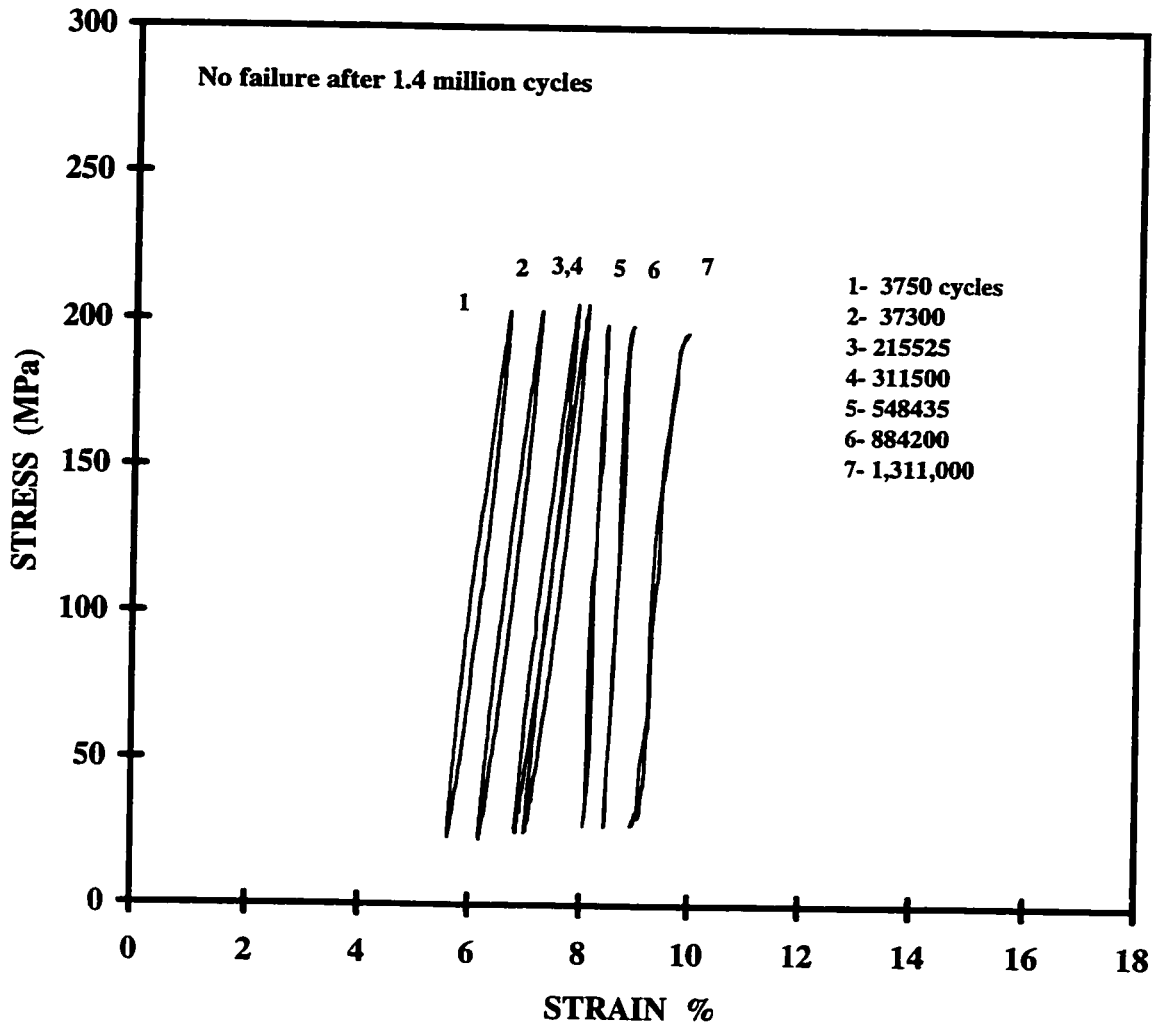

Fig.4.4 Variation in hysteresis loops during fatigue at 1Hz and 60% of the ultimate strength.

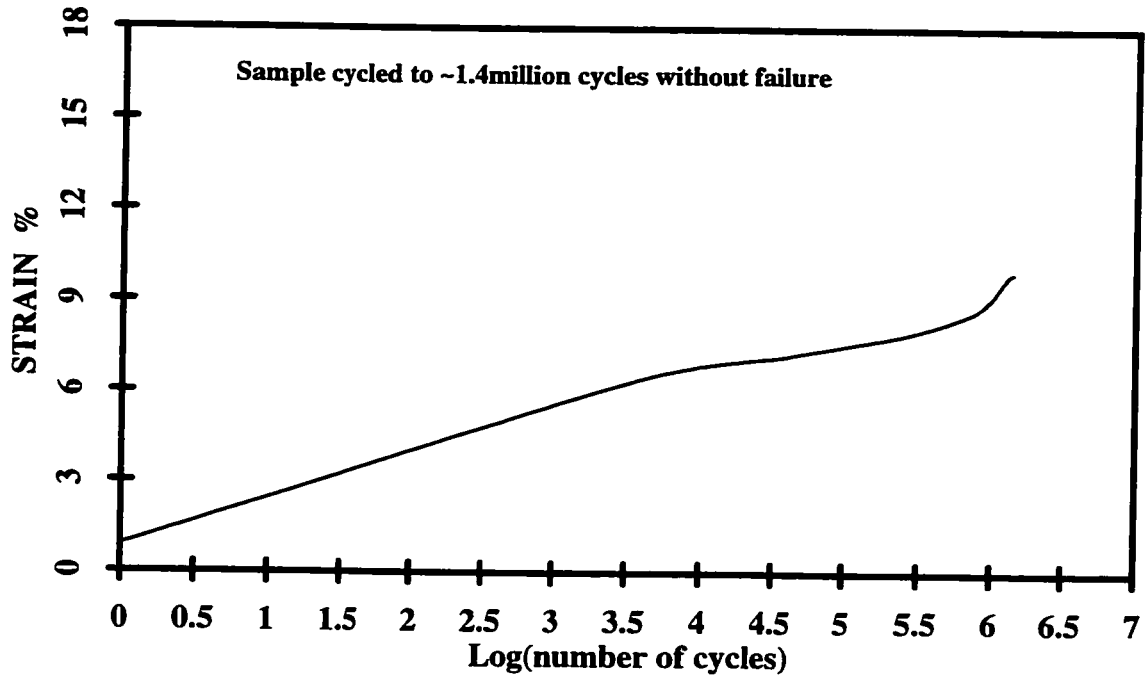

Fig.4.5 Variation of maximum strain during fatigue at 1Hz and 60% o the ultimate strength

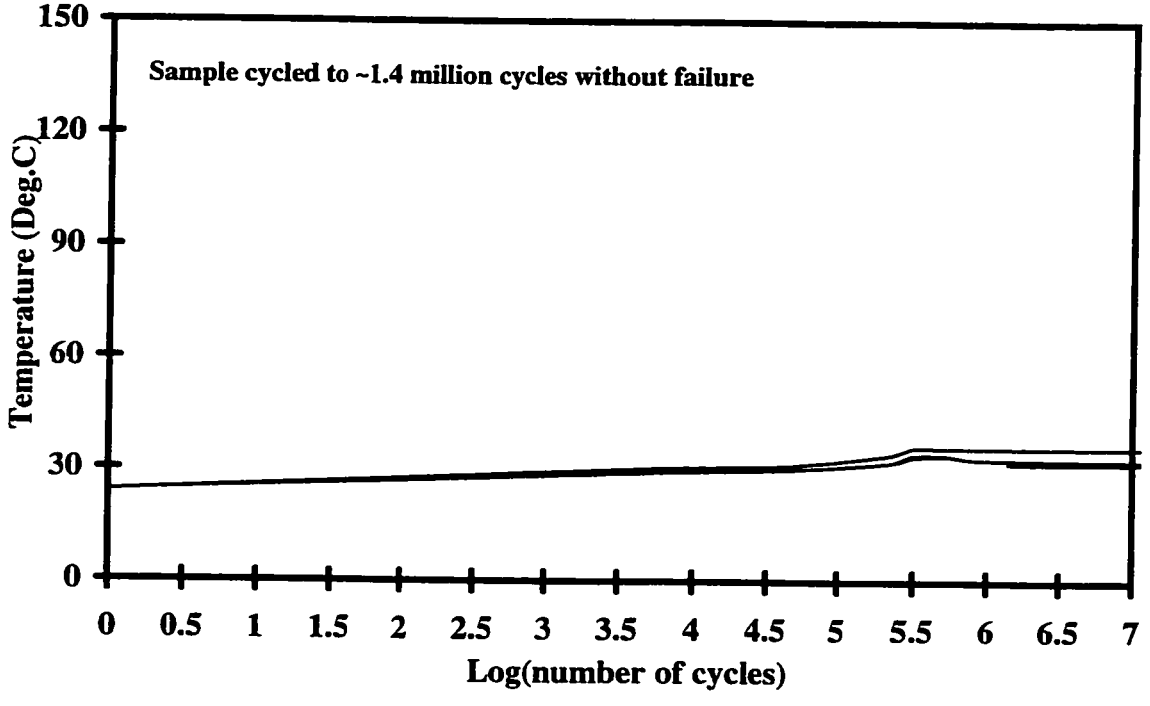

Fig.4.6 Temperature variation during fatigue at 1Hz and 60% of the ultimate strength.

4.4.1.2 70%$\sigma_{ult.}$

Shorter fatigue lives were obtained at this loading condition. The visible damage appeared at earlier stages relative to the previous loading condition. After only few hundred cycles, very small cracks were observed in small densities in a nonuniform distribution across the surface. The number of cracks increased slowly until about half of the fatigue life when they became more visible, grew faster, and oriented along one of the fibers (+45) direction in the surface. Shortly after, more cracks were noticed which initiated at points along the earlier cracks and moving perpendicular to them. The visible damage was generally small in size and density at this loading condition but greater than that in the previous (1Hz, 60%$\sigma_{ult.}$) loading condition, with more surface splitting that appeared shortly before the final failure (Fig.4.3 center).

Variation in the hysteresis loops at this loading condition is shown in Fig.4.7 at different number of fatigue cycles. At early stages, the material shows a considerable amount of hysteresis losses, as well as strain deformation (Fig.4.8) and temperature rise (Fig.4.9). The rate of deformation started to decrease after a certain number of cycles, as the strain rate and temperature started to stabilize to certain values, with some decrease in hysteresis losses. A third stage can be noticed as the material shows a slight increase in strain shortly before the final failure, with no significant temperature rise, and rather further decrease in hysteresis losses.

It can be noticed that the material's behavior at this loading condition was similar to that at the previous loading condition, where three distinct zones can be noticed in the temperature and strain variation. In the first zone, the material experienced continuous creep deformation accompanied with high levels of damage, followed by a decrease in strain rate, and some temperature increase. In the second stage, the creep rate stabilized to a certain value, and the temperature stabilized to a certain level; since the temperature rise at this loading condition was not that severe (with a maximum of around 50°C), it is evident that the material experienced a state of secondary creep characterized by cyclic hardening during the early stages and continued most of its fatigue life which led to loss in the material's resistance for further plastic deformation. As fatigue proceeded, the rate of damage accumulation increased, and the material failed at shorter fatigue life due to high levels of damage. This behavior can also be related to the rotation of fibers during cycling (as can be noticed in Table 4.3) which resulted in an increase in the material's stiffness.

4.4.1.3 80%$\sigma_{ult.}$

A drastic decrease in fatigue life was obtained at this loading condition, and more visible damage appeared earlier with greater size and density as compared with that at previous condition (Fig.4.3 bottom). The damage in this case was distributed throughout

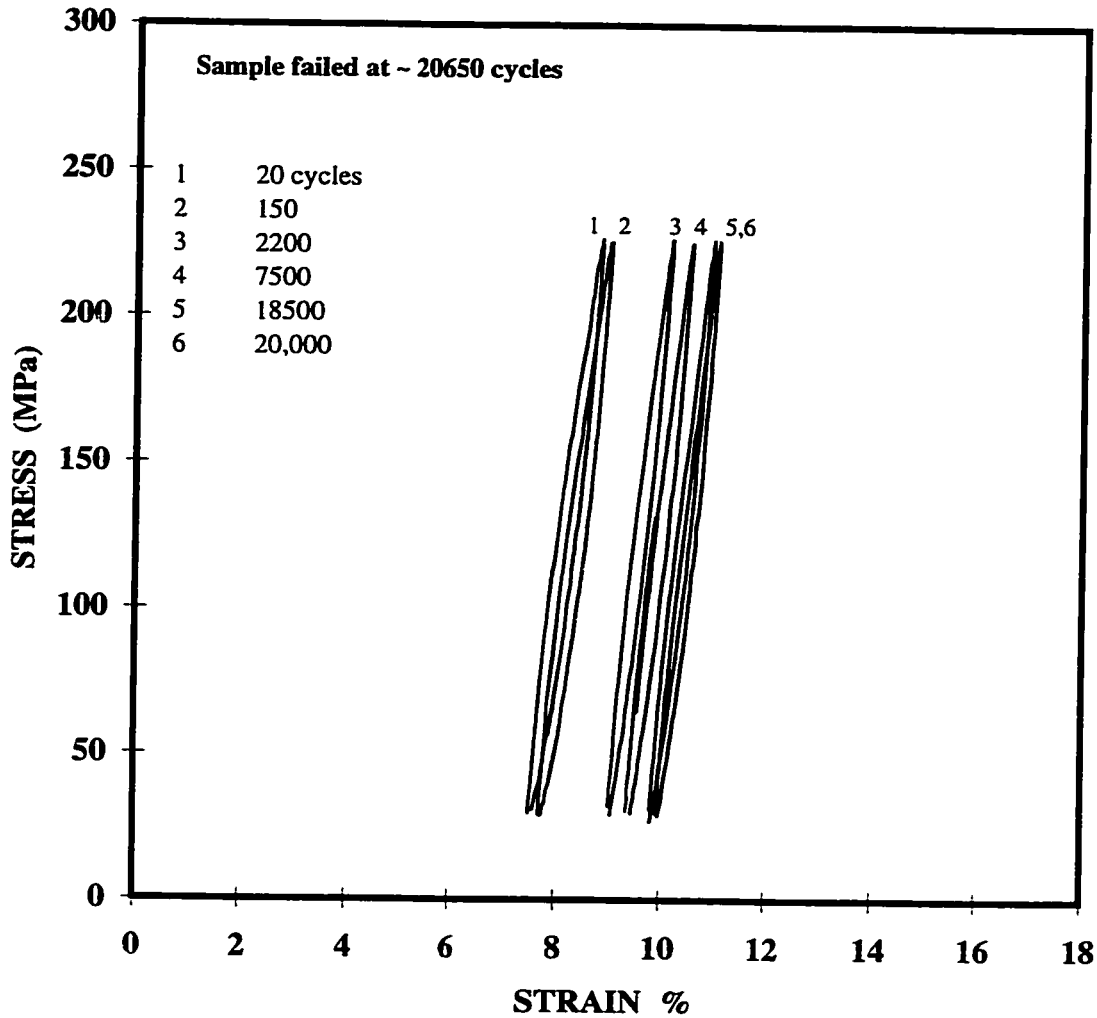

Fig.4.7 Variation in hysteresis loops during fatigue at 1Hz and 70% of the ultimate strength

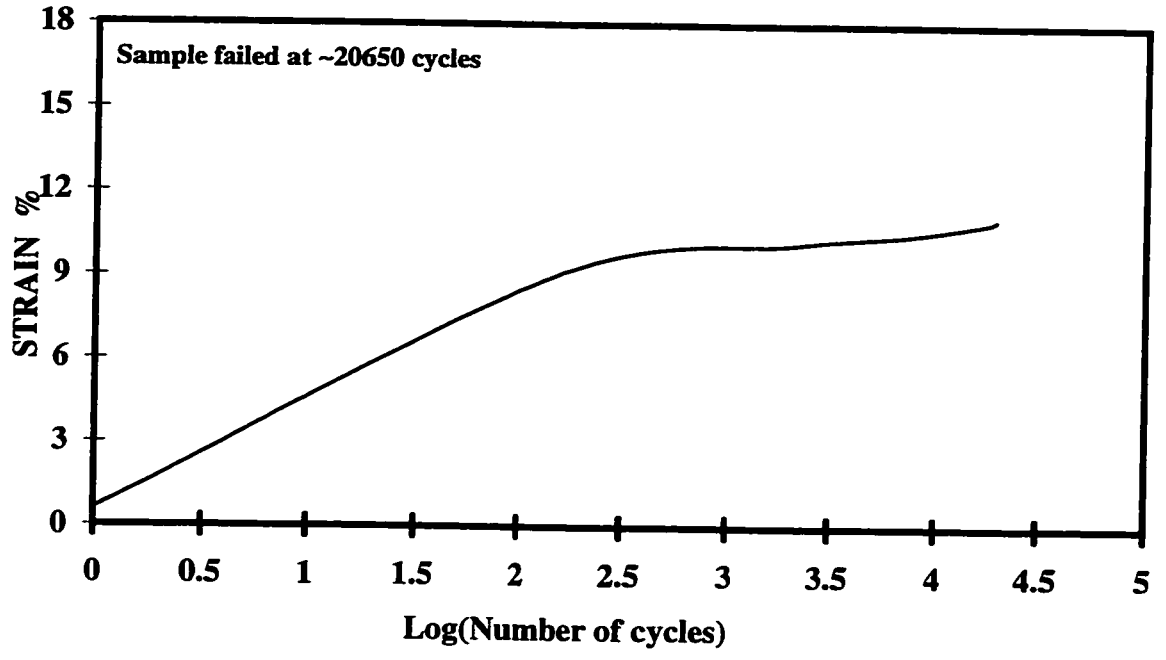

Fig.4.8 Variation in average maximum strain during fatigue at 1Hz and 70% of the ultimate strength

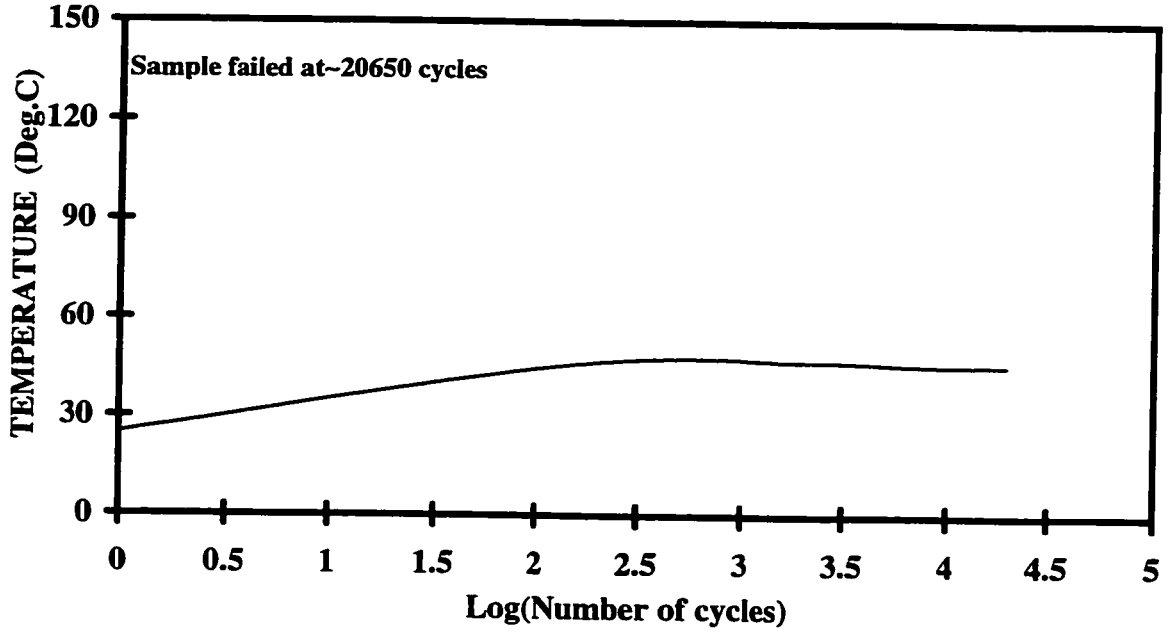

Fig.4.9 Temperature variation during fatigue at 1Hz and 70 % of the ultimate strength

the surface, and consisted of visible surface cracks along one of the fibers direction, with smaller cracks at perpendicular direction (-45), which probably did not develop completely because of the short fatigue life.

On the other hand, the stress-strain behavior at this loading condition (Fig.4.10) was similar to that at the two lower loading levels. At early stages, a considerable amount of hysteresis losses was developed, as well as great amount of strain deformation which rapidly started to decrease (Fig.4.11) and a significant increase in temperature (Fig.4.12). At later stages, some increase in strain rate and temperature to about constant values were noticed (which cannot be seen clearly because of the logarithmic scale), with some decrease in hysteresis losses as well. This indicates that the material was under a state of secondary creep and the accompanied cyclic hardening during the early stages of cycling which resulted later in stabilized strain rates most of the fatigue life until shortly before the final failure. This behavior can also be related to the fibers rotation due to cycling and consequently the increase in the material's stiffness. A third stage can be noticed where an increase in strain, temperature, and the size of hysteresis loops appeared for only a short period before the final failure.

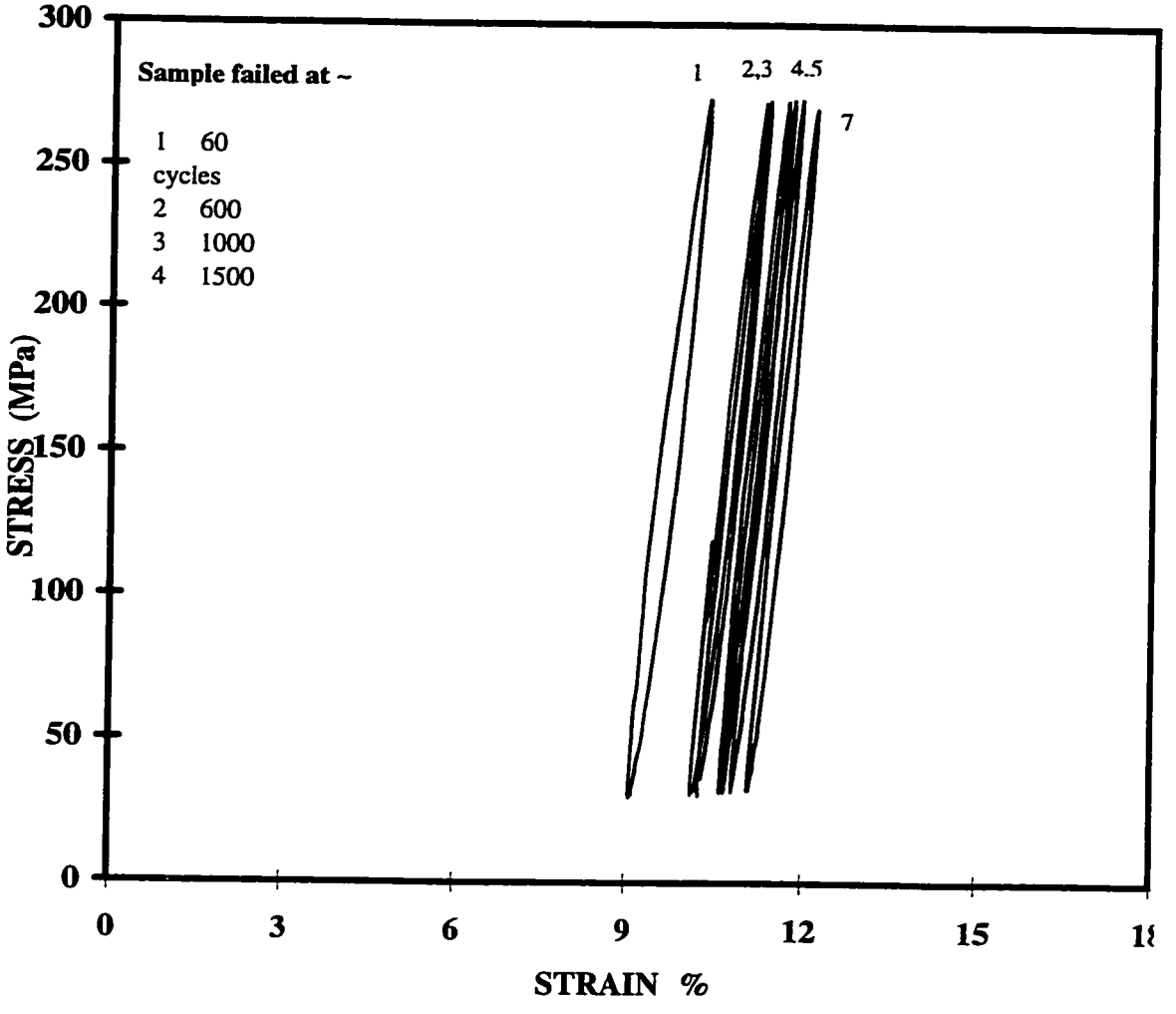

Fig.4.10 Variation in hysteresis loops during fatigue at 1Hz and 80% of the ultimate strength

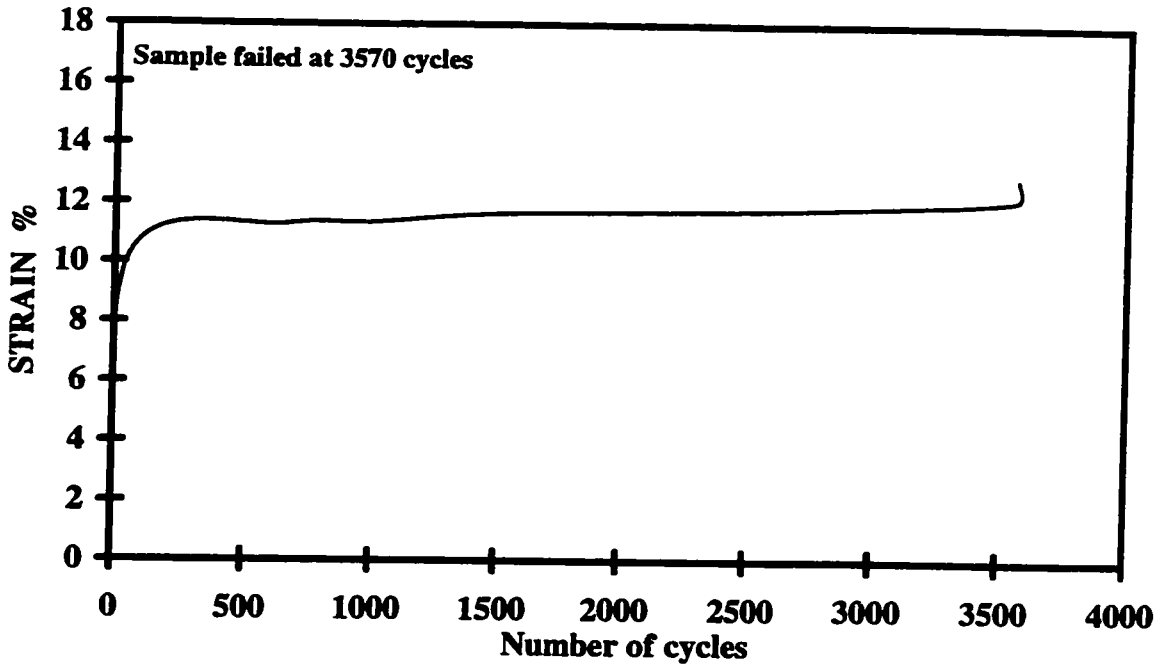

Fig.4.11 Strain variation during fatigue at 1Hz and 80% of the ultimate strength

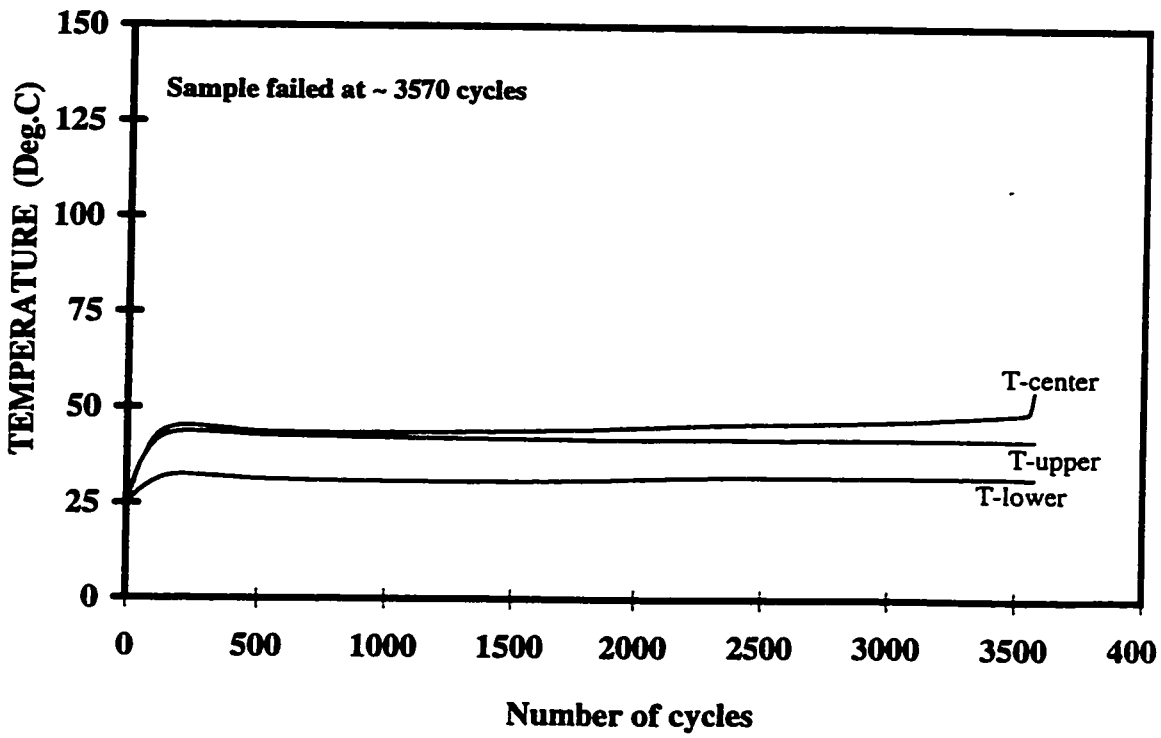

Fig.4.12 Temperature variation during fatigue at 1Hz and 80% of the ultimate strength

4.4.2 Fatigue tests at 5Hz

4.4.2.1 60%$\sigma_{ult.}$

More damage was observed at earlier stages as compared to the same loading level at 1HZ. The observed damage consisted of small surface cracks increasing in density continuously along the surface. Surface splittings were also observed at an early stage (at ~ 5% of fatigue life), increasing at a slow rate and at different locations along the sample. As fatigue progressed, more damage was observed throughout the surface, with more surface splitting along the fiber direction in the surface layer, and surface cracks intersecting at right angles. Through-the thickness damage was also observed at about 80% of fatigue life and increased until the final failure. Fig.4.13(top) shows a sample failed at this loading condition; the final failure occurred along the fibers direction and a significant reduction in the sample's cross section can be noticed. This may indicate that the final failure occurred due to continuous matrix deformation which resulted in weakening the interface strength due to accumulation of damage, and in turn fibers breaking due to continuous loading.

The variation in hysteresis losses is shown in Fig 4.14 for a sample cycled at this loading condition, while Fig 4.15 shows the strain variation behavior for the same sample. Significant hysteresis losses and strain deformation can be noticed at early stages

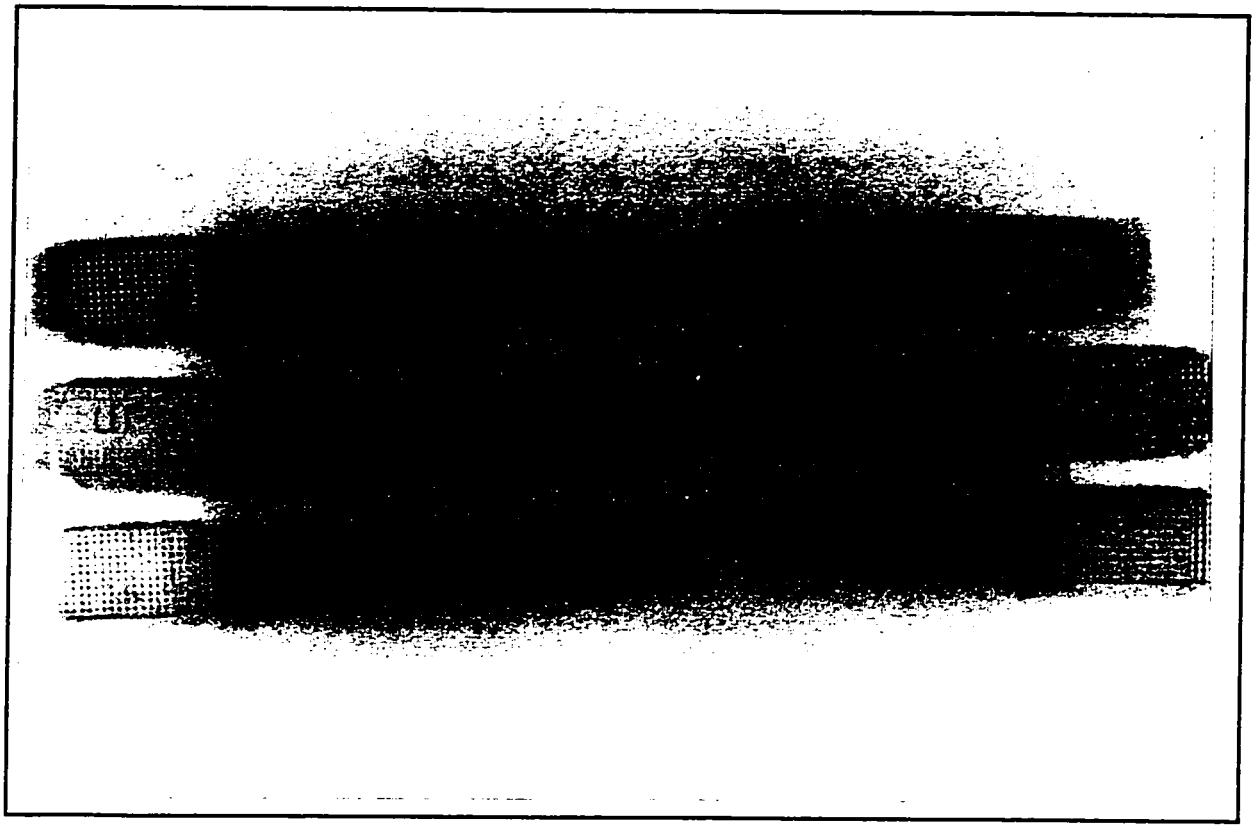

Fig. 4.13 Typical fatigue samples cycled at 5Hz and the three loading levels where; (top) at $60\%\sigma_{ult.}$, (center) at $70\%\sigma_{ult}$, and (bottom) at $80\%\sigma_{ult}$.

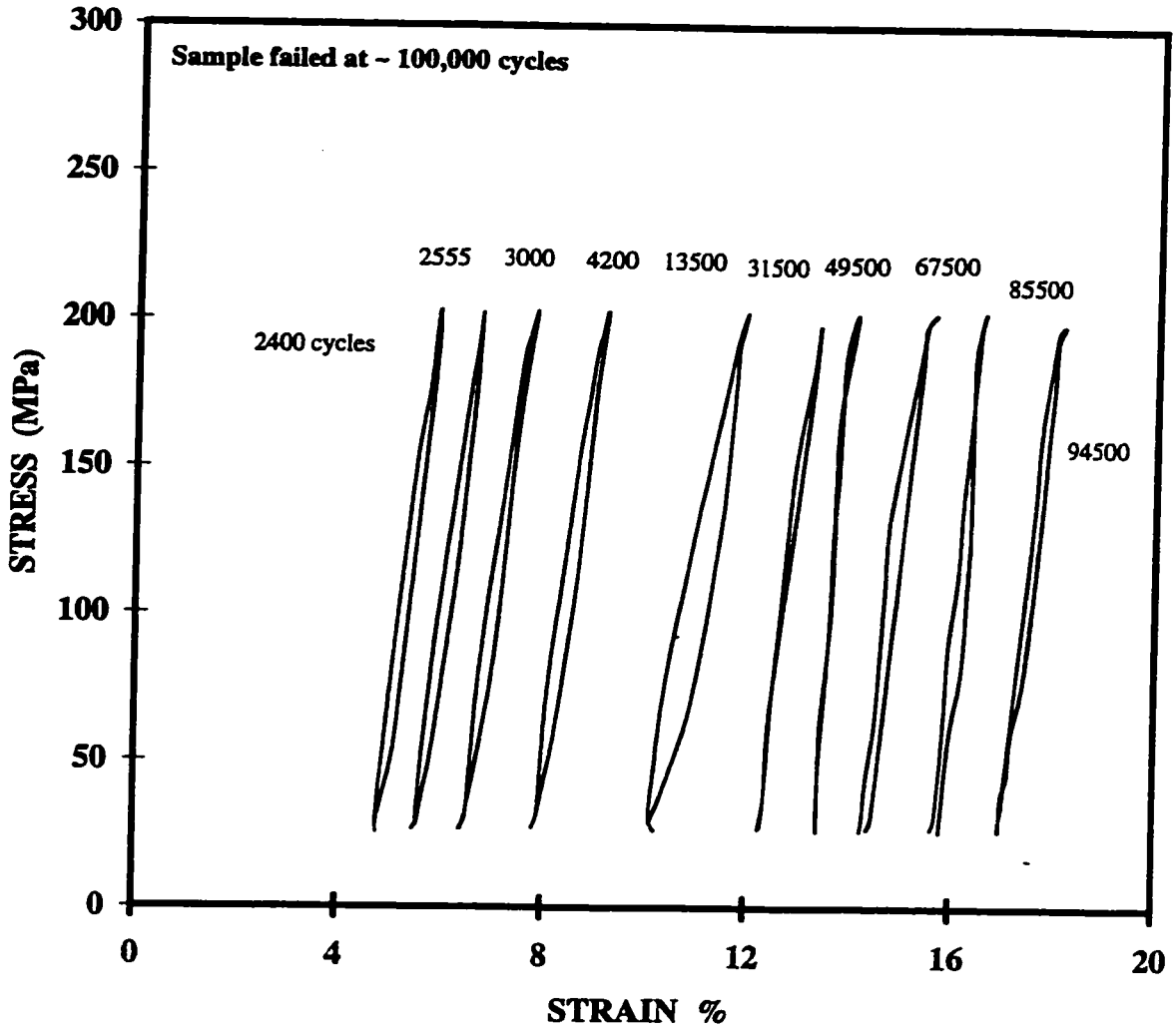

Fig.4.14 Variation in hysteresis loops during fatigue at 5Hz and 60% of the ultimate strength

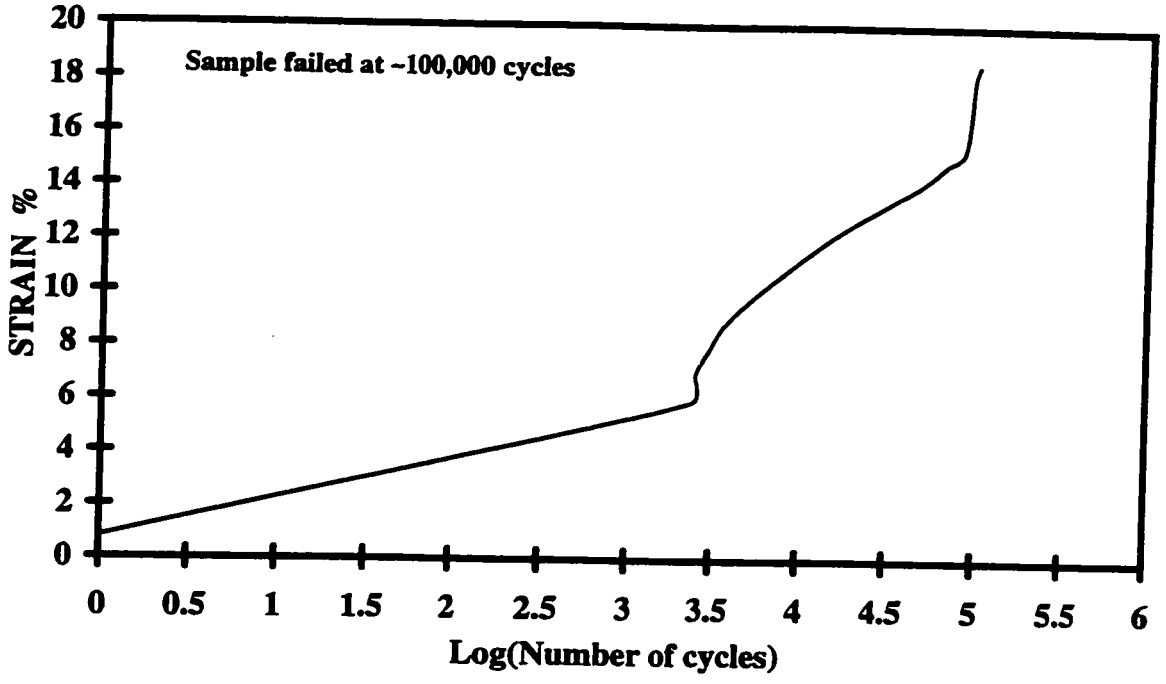

Fig.4.15 Strain variation during fatigue at 5Hz and 60% of the ultimate strength

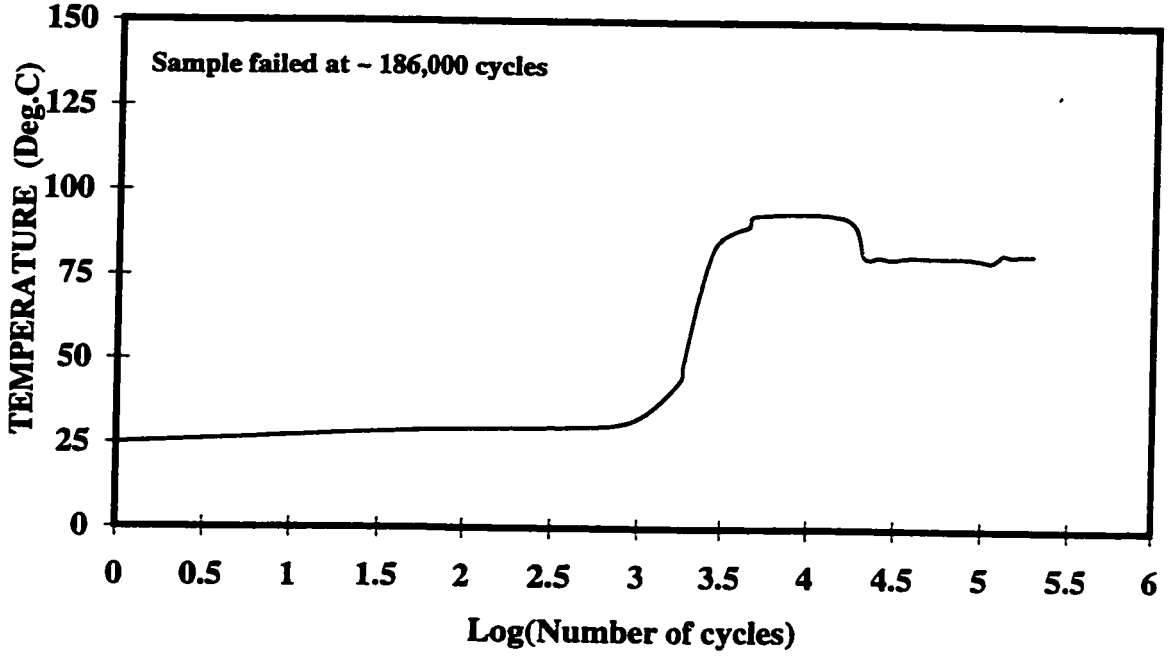

Fig.4.16 Temperature variation during fatigue at 5Hz and 60% of the ultimate strength

of fatigue life. However, because of the high loading frequency, it seems that the temperature was not able to develop during that early stages of fatigue life (Fig 4.16).

During further stages, more matrix damage and deformation occur which result in changing the heat transfer paths within the sample, and hence a rapid temperature increase can be observed.

Some features similar to those at 1Hz and the same load level can be noticed here. It is clear that the sample was under a state of creep during the early stages which resulted in continuous (and almost constant) strain deformation and hysteresis losses. A secondary state of creep was followed during later stages, which is characterized by a nearly constant creep rate. During this stage, temperature increased rapidly which can be related (as mentioned before) to the significant damage levels during earlier stages and the resulting variation in heat transfer paths. As a result of this temperature increase, significant matrix softening may occurred, which gave rise to higher values of fibers rotation. Therefore, the strain behavior during this stage can be attributed to an increase in the material's stiffness due to fibers reorientation. A third stage can be observed during which more hysteresis losses and strain deformation occurred until the final failure. However, the appearance of these stages was much faster at 5HZ and the damage was more severe. Also, because of the high levels of temperature rise at this loading condition, it can be said that the samples experienced a state of accelerated creep which resulted in shorter fatigue lives.

4.4.2.2 70%σ_{ult}:

A drastic decrease in fatigue life was obtained at this loading condition as a result of the high levels of fatigue damage and temperature increase. Fatigue damage developed very early in the form of surface cracks and splitting throughout the surface, and increased rapidly in size and density as fatigue progressed. Also, more damage was developed through the samples thickness, as observed on fractured samples.

In general, due to the shorter fatigue lives at this loading condition, it was difficult to follow the damage development and propagation. At failure, the samples were severely damaged throughout the surface (Fig. 4.13 center) and within the thickness where delamination could be observed . A significant decrease in the sample's cross section were also noticed as well as fibers reorientation.

Fig 4.17 and Fig 4.18 show the variation in hysteresis losses and strain behavior, respectively, for a sample fatigued at this loading condition. High levels of strain deformation and energy losses were resulted early in the fatigue life as a result of the high applied load and frequency. This was accompanied by a rapid increase in temperature due to the material's high damping and the associated energy dissipation (Fig 4.19).

The thermal effect was an important feature in samples fatigued at this loading condition. The temperature increased rapidly and continuously to high values near the material's softening temperature (~ 120°C) or even higher in some cases, which resulted in high rates of plastic deformation. As a result, the material failed mainly due to softening, and high energy dissipation rates can be noticed throughout most of the fatigue life. Also, as temperature reached high values, the shape of hysteresis loops changed and increased rapidly due to high damage rates and plastic deformation after softening.

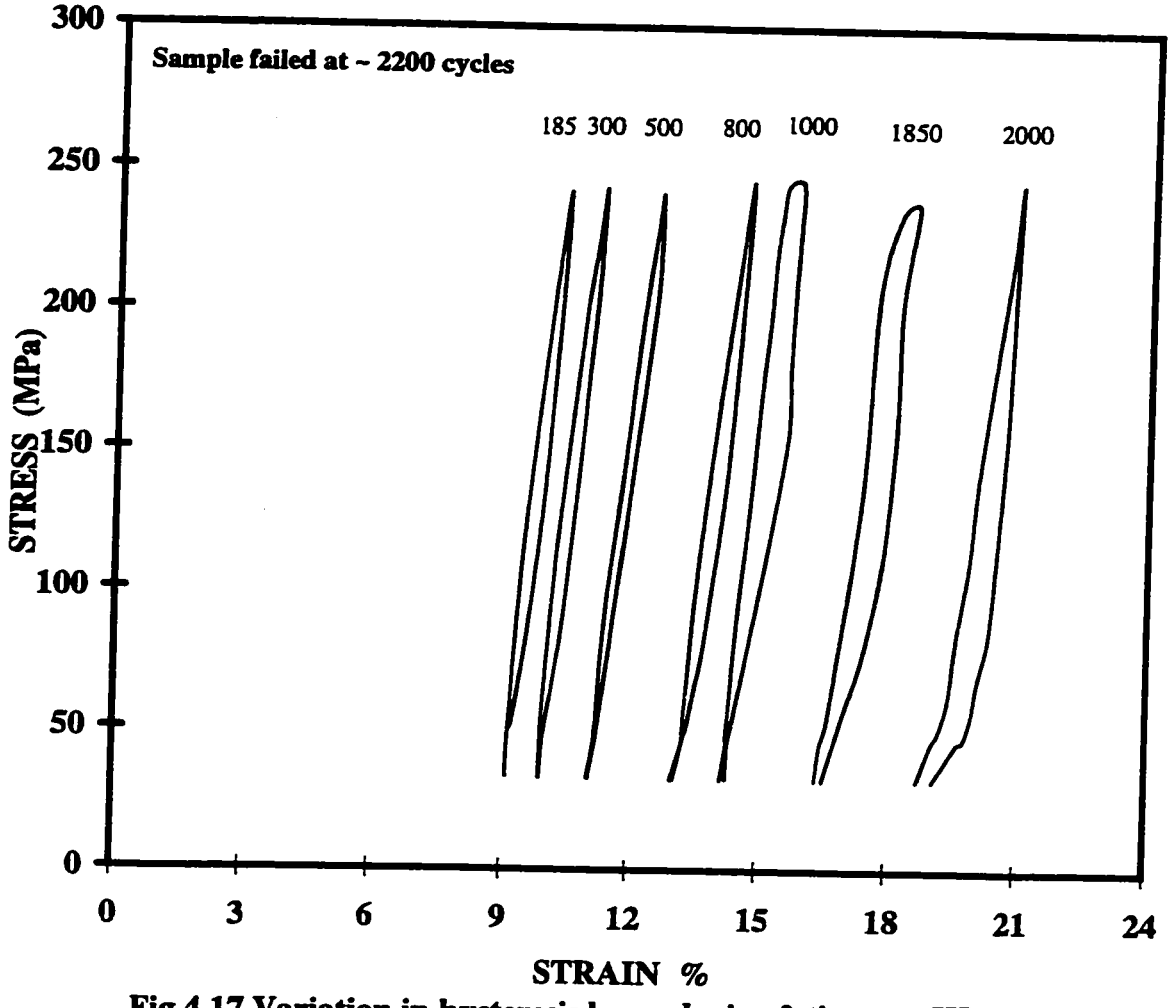

Fig.4.17 Variation in hysteresis loops during fatigue at 5Hz and 70% of the ultimate strength

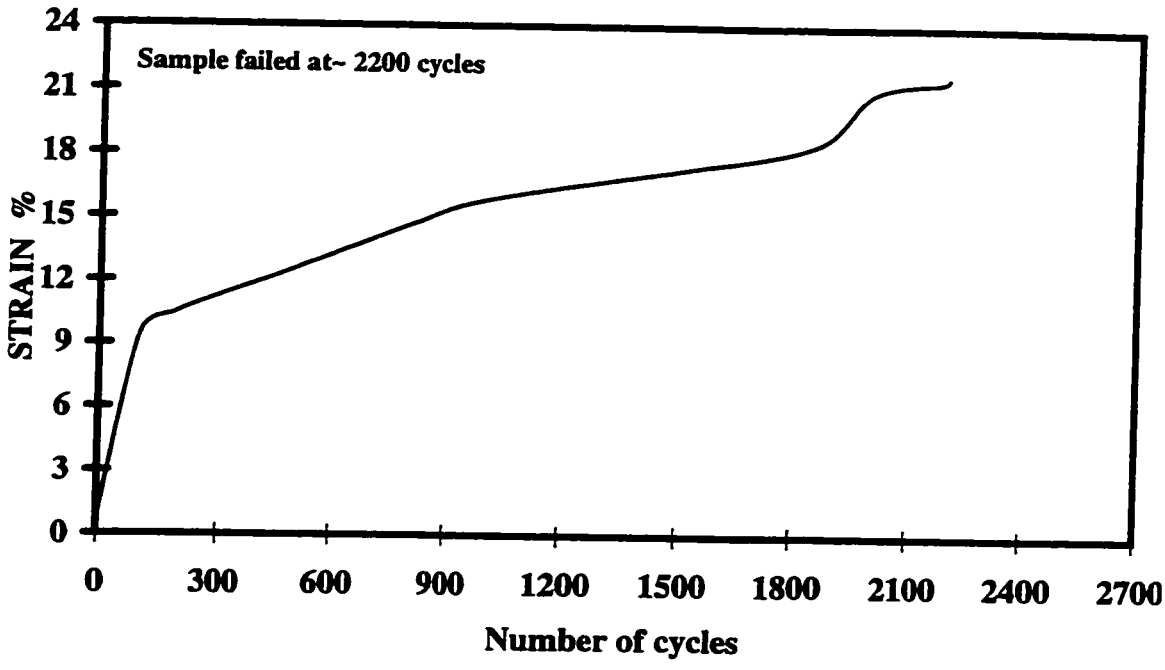

Fig.4.18 Strain variation during fatigue at5Hz and 70% of the ultimate strength

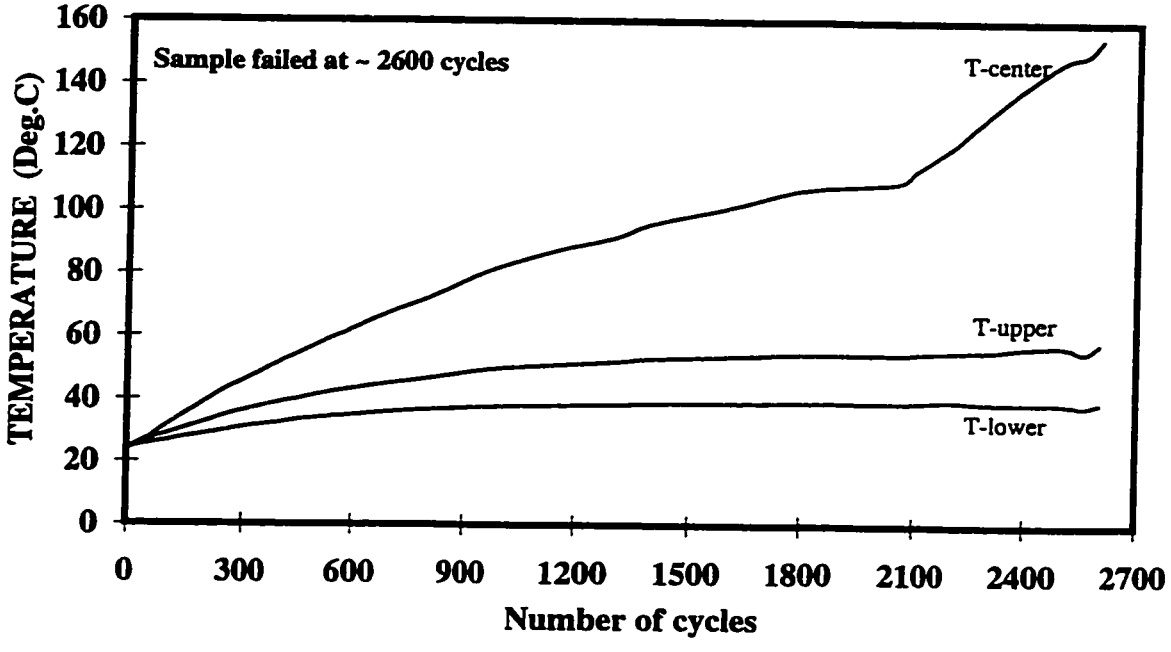

Fig.4.19 Temperature variation during fatigue at 5Hz and 70% of the ultimate strength

4.4.2.3 80%σ_{ult}

Further drastic reductions in fatigue lives were obtained, which is believed to be mainly due to thermal effect that resulted in high material's damage and plastic deformation. Fig 4.13 (bottom) shows a sample failed after fatigue at this loading condition; it's clear that the material experienced significant levels of damage consisted mainly of matrix deformation and softening, fiber-matrix debonding and matrix cracking. The thermal effect can be noticed clearly in terms of the significant reduction in the sample's cross section. This clearly indicates that the final failure occurred due to consecutive softening and plastic flow, which resulted consequently in loss of the material properties and its structural integrity. Significant fiber reorientation was also noticed in the failed specimens at this loading condition.

The hysteresis losses were huge at this loading conditions shown from the size of the hysteresis loops (Fig.4.20). The nonuniform shape and the significant size of these loops is an indication of the thermal effect the material experienced during the early stages of fatigue and up to failure. In addition, the rapid increase in strain (Fig.4.21) is another indication of the thermal effect which comes as a result of the high applied load and high loading frequency. This effect resulted in a rapid increase in temperature (Fig.4.22) due to the increase in the material's damping and the accompanied high energy dissipation rates.

However, due to the short fatigue lives at this loading condition and because of lack in the material's thermal conductivity , we believe that there was no enough time for temperature to develop completely. In some cases where one of the thermocouples survived sticking to its position on the sample's surface, higher temperatures were recorded after the sample's failure, which indicates that the actual temperature levels were much higher than the ones recorded before the sample's failure.

4.4.3 Fatigue tests at 10Hz

Very short fatigue lives and high temperatures were common features at this frequency. It was not possible to follow the damage development during fatigue because of the short lives, but in general, several damages were observed after failure. Fig.4.23 shows samples fatigued at this frequency. At 60% σ_{ult} (Fig. 4.23a), several types of damage can be observed like matrix cracking mostly along the fibers directions, delamination (not seen in the figure), and most commonly matrix softening which is reflected by the significant decrease in the sample's cross section. The same features can be observed at 70% σ_{ult} (Fig. 4.23b) and 80%σ_{ult} (Fig. 4.23c) but in an increasing rate. Therefore, it is clear that as the load level increased, the damage evolution (after failure) increased in size and density, especially in terms of matrix softening. Another common feature at this frequency is the brush-like pattern at the failed zone in all samples, which is more apparent at the higher load levels. This feature is a another indication of how severe the damage was at this loading frequency.

The fatigue failure at this frequency is believed to be mainly due to thermal effects, as evidenced by the extremely high temperature increases. This was associated with high rates of energy dissipation, and of course, other types of damages such as friction at the damaged sites which significantly contributed in increasing the temperature. At 60%σ_{ult}, areas of hysteresis loops increased continuously (Fig.4.24) and changed in shape from uniform slim elliptic ones at early stages to non-uniform ones (or almost collapsed ones in other samples) as fatigue life progressed. High strain deformation rates were recorded (Fig. 4.25) even at early stages, with a continuous increase throughout the fatigue life. Also can be seen is the failure strain at this loading condition which exceeds the static strain values. This can be attributed to the high temperature levels reached (Fig 4.26) which caused extensive matrix softening and loss of the materials integrity as a rigid body.

Higher values of energy dissipation and temperature rises were obtained as load level increased, as well as high strain deformation rates. The variation in hysteresis loops, strain, and temperature at 10HZ 70%σ_{ult} and 10HZ 80% σ_{ult} are shown in Figs.4.27-4.32.

An interesting feature can be recognized from the strain behavior at this frequency; that is, even with the very short lives obtained at all load levels and the resulted high temperature rises, the strain variation can be divided into three zones. In the first zone, the strain increases rapidly during the early stages of fatigue, followed by a slower and steady increase in the second zones which takes place in most of the fatigue

life. In the third zone, another rapid increase in strain can be observed shortly before the final failure. In this last stage, the values of failure strain exceeded that of static failure strains which may indicate that the material reaches high softening levels due to the high temperatures during the last stages of the sample's fatigue life. The three zones comprising the strain variation behavior are similar to those obtained at the 1HZ test, and also can be obtained in a creep test for such material. This behavior, however, may indicate that the material was experiencing a state of creep throughout its fatigue life, with the high temperatures increasing the creep rate.

4.5 DMA tests

The results of the DMA tests revealed that at the low amplitude load conditions of the tests, the material shows no significant variation in its viscoelastic properties (loss factor, compliance, and modulus) for the range of temperatures (25°C to around 120°C). At around 120°C and over, the viscoelastic properties start to change significantly and in high rates. This indicates that the matrix material starts to soften at around this temperature, which is less than its glass transition temperature (~143°C).

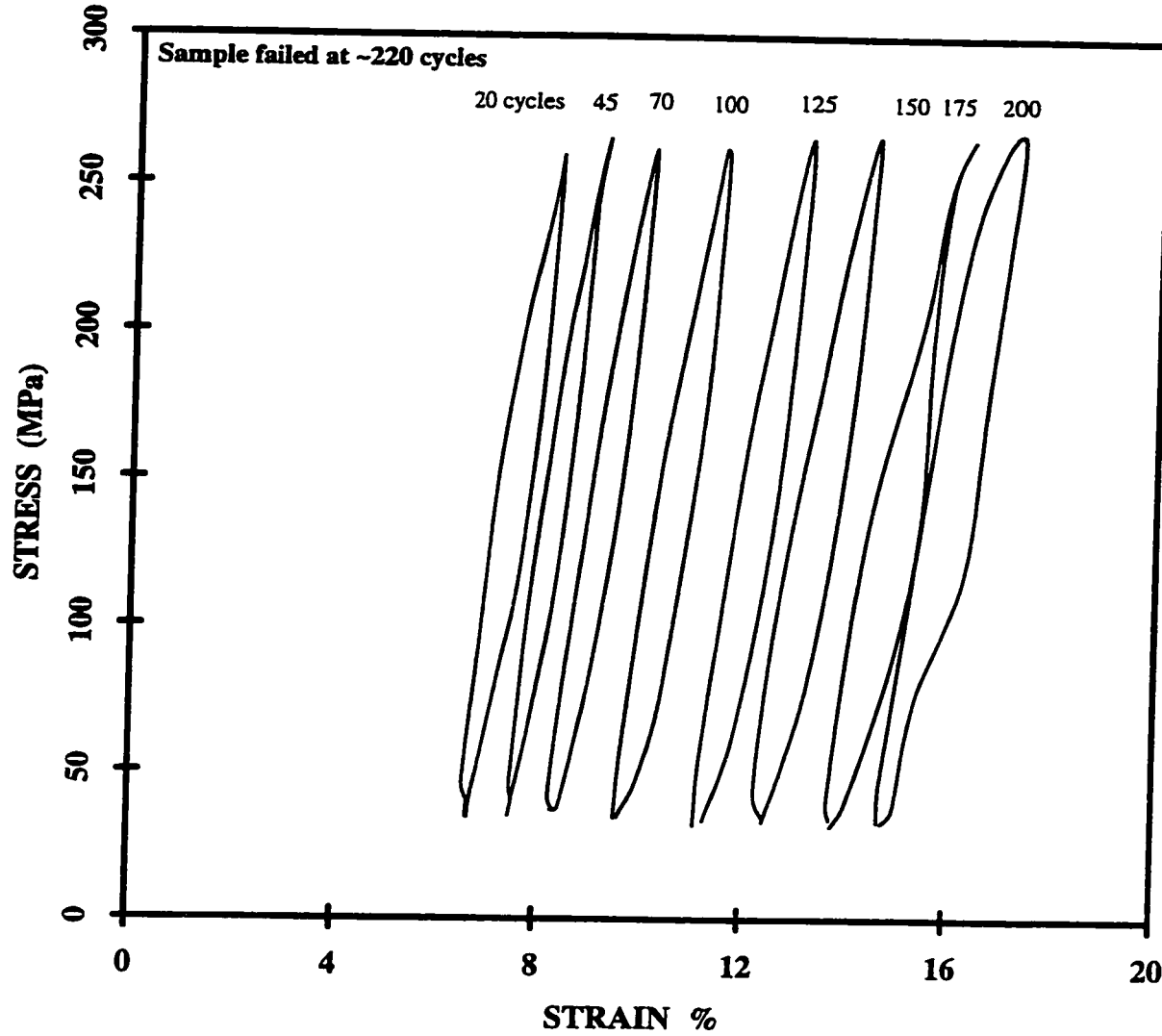

Fig.4.20 Variation in hysteresis loops during fatigue at 5Hz and 80% of the ultimate strength

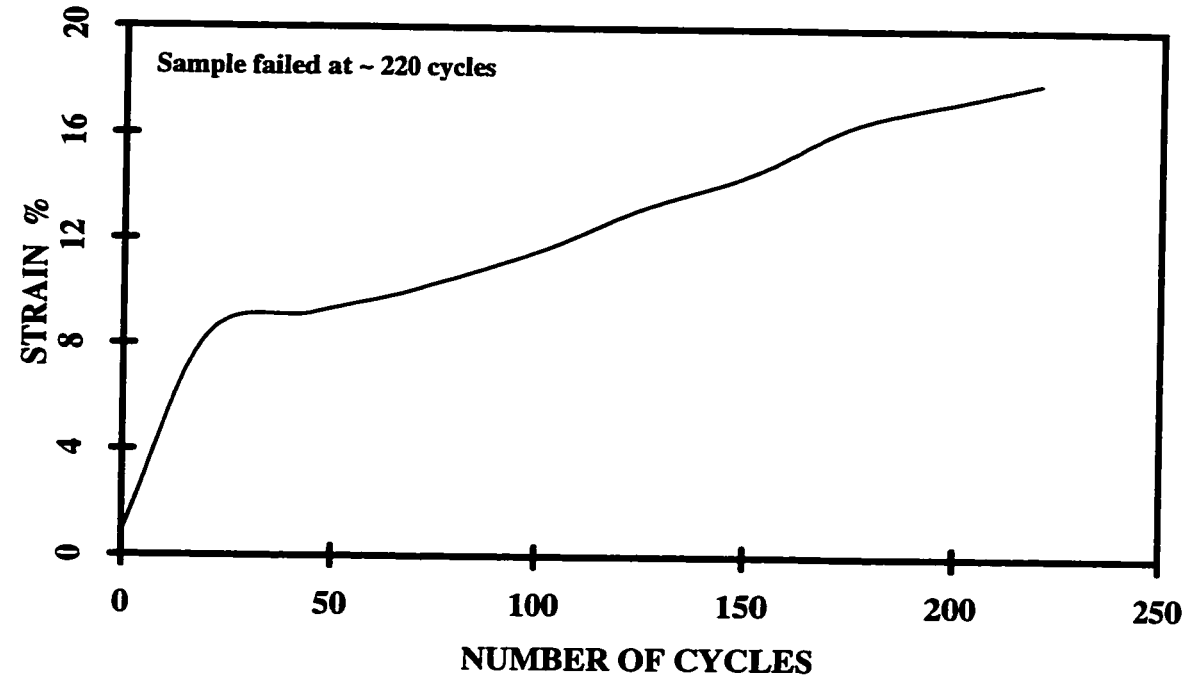

Fig.4.21 Strain variation during fatigue at 5Hz and 80% of the ultimate strength

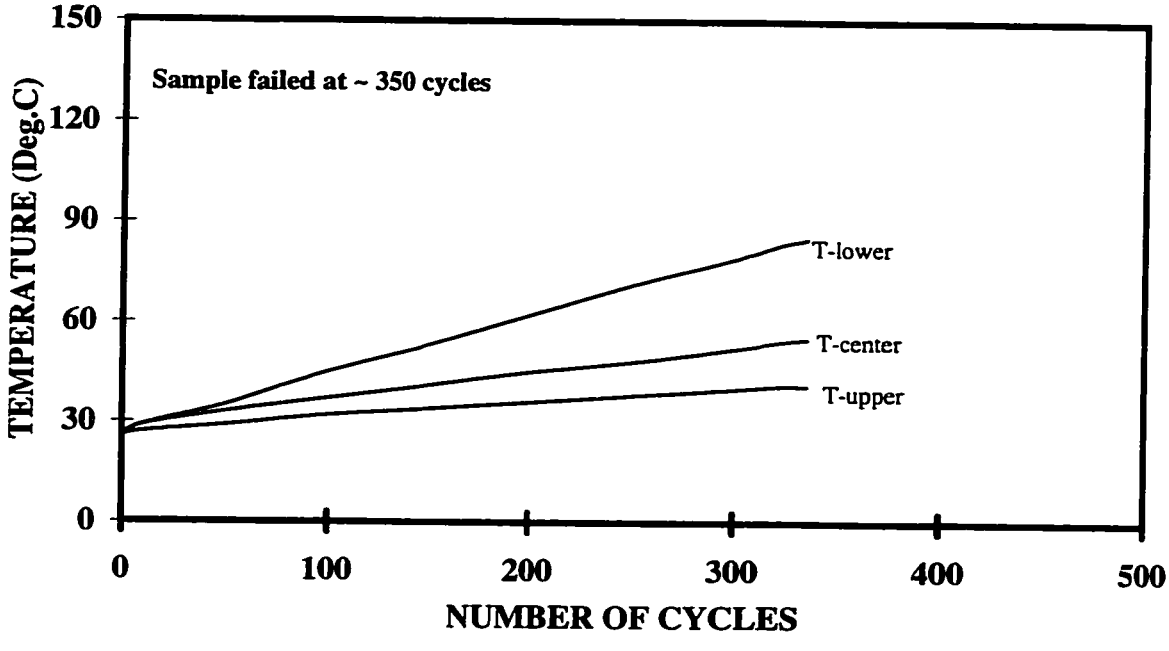

Fig.4.22 Temperature variation during fatigue at 5Hz and 80% of the ultimate strength

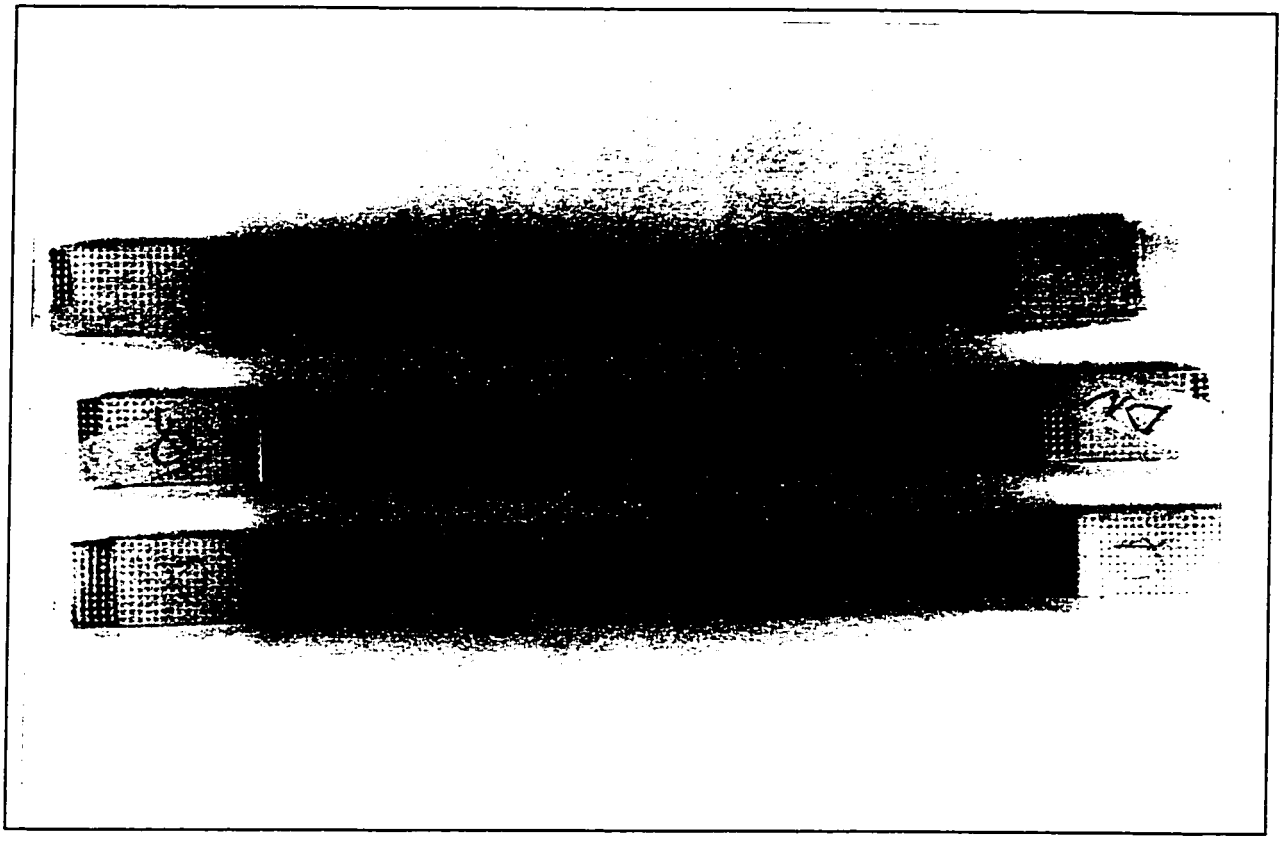

Fig. 4.23 Typical fatigue samples cycled at 10Hz and the three loading levels, where: (top) at 60%$\sigma_{ult.}$,(center) at 70%σ_{ult} , and (bottom) at 80%σ_{ult} .

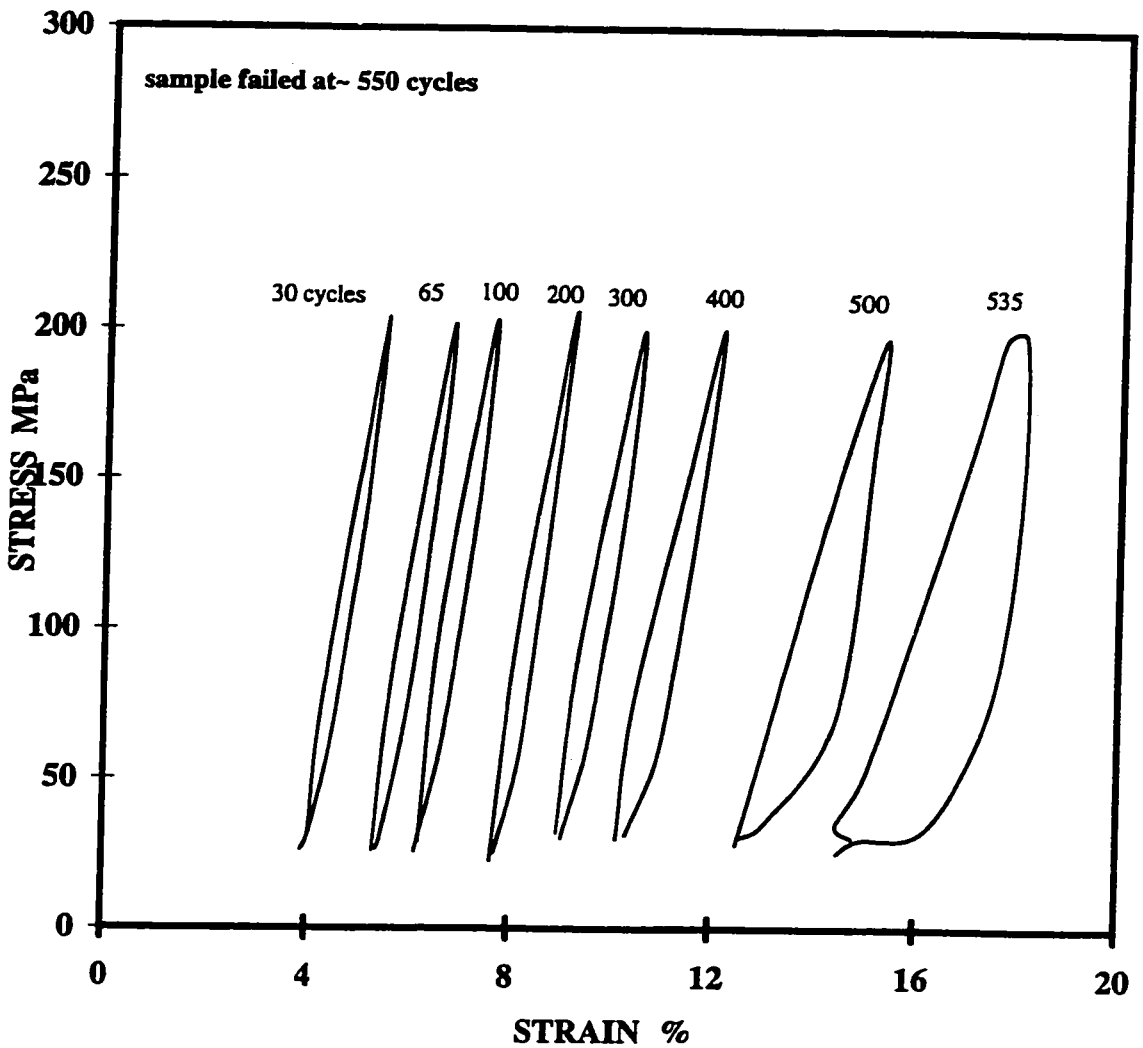

Fig.4.24Variation in hysteresis loops during fatigue at 10Hz and 60% of the ultimate strength

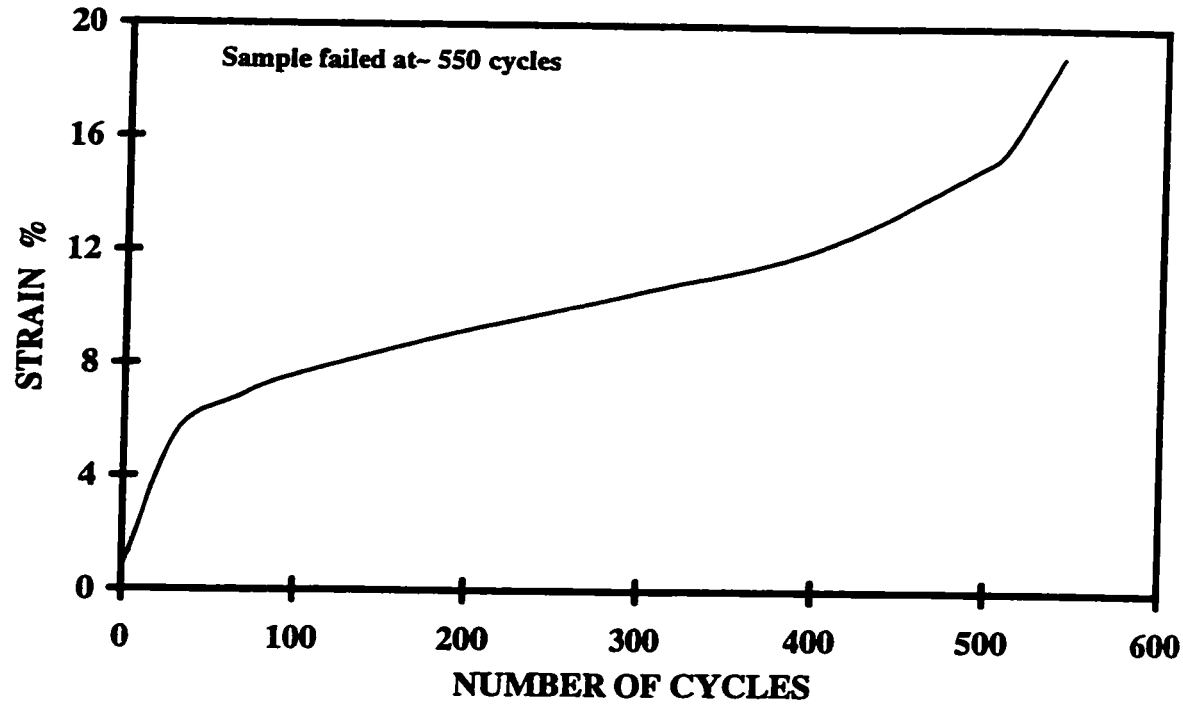

Fig.4.25 Strain variation during fatigue at 10Hz and 60% of the ultimate strength

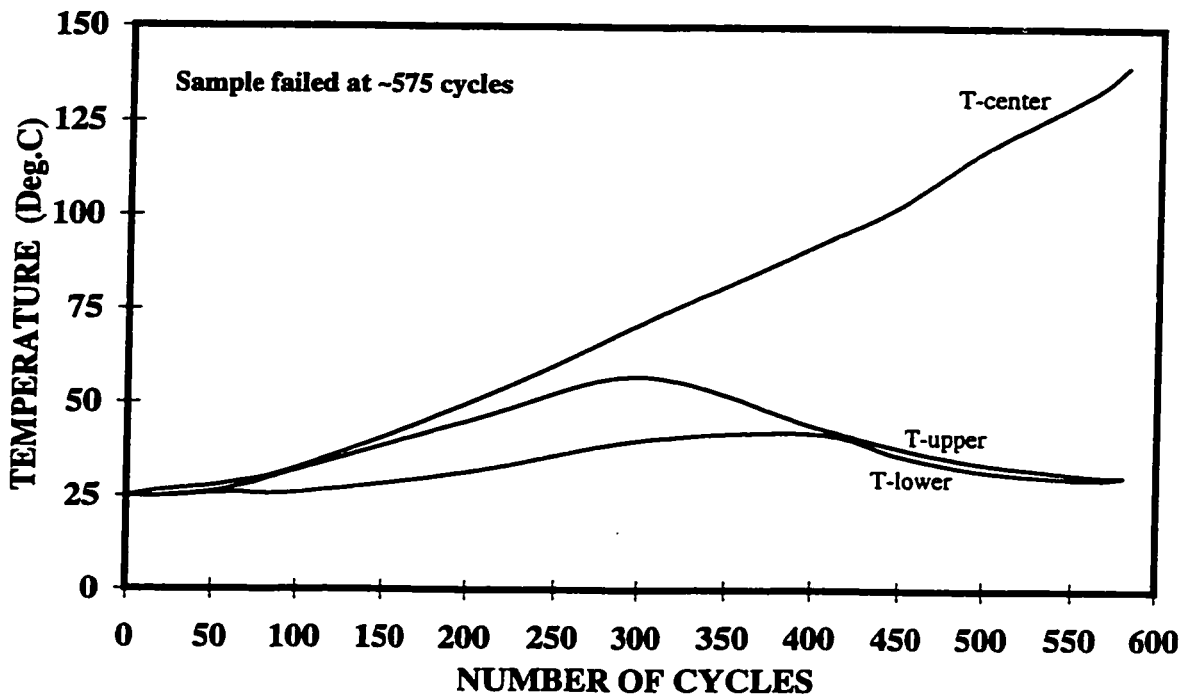

Fig.4.26 Temperature variation during fatigue at 10Hz and 60% of the ultimate strength

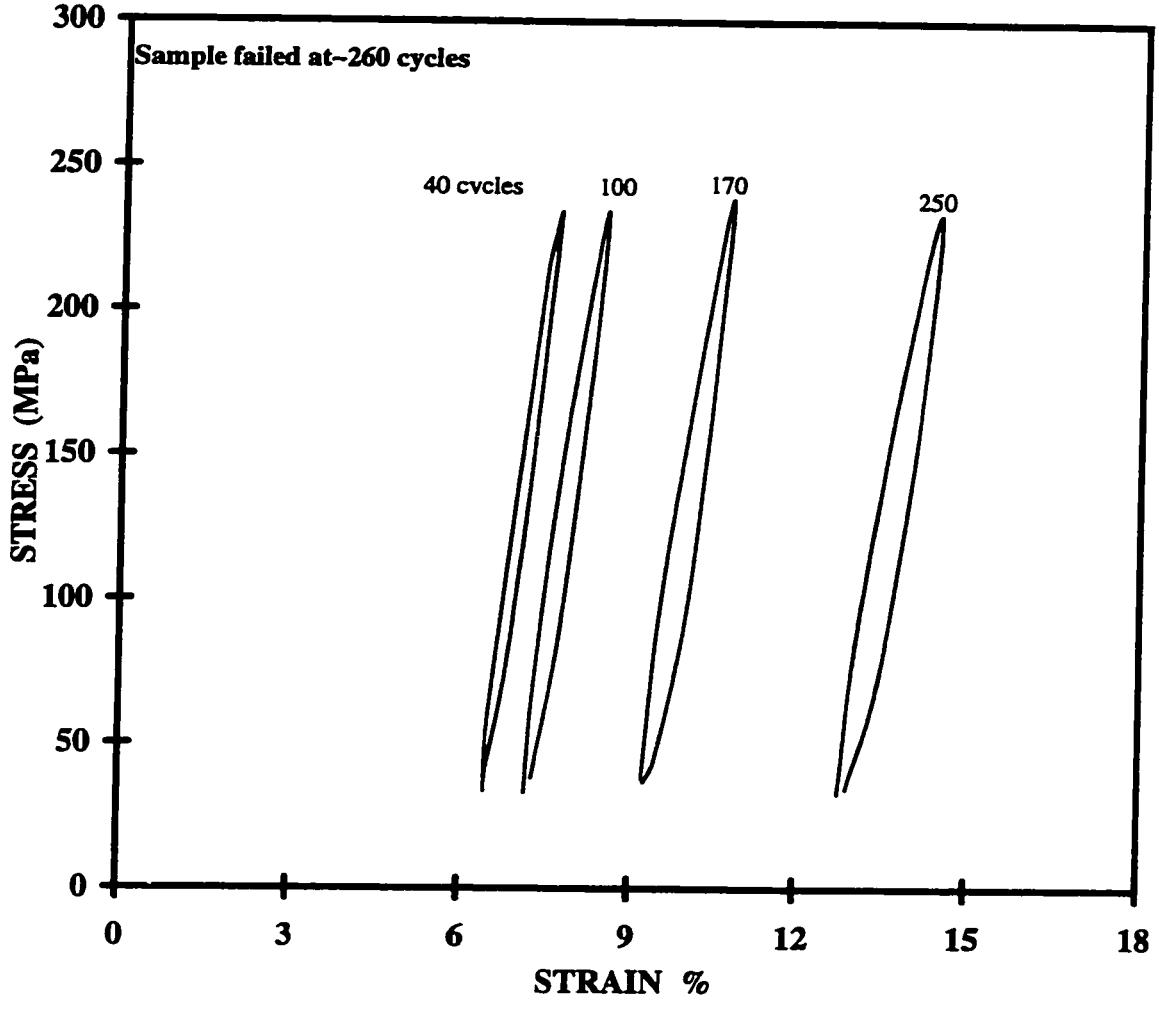

Fig.4.27 Variation in hysteresis loops during fatigue at 10Hz and 70% of the ultimate strength

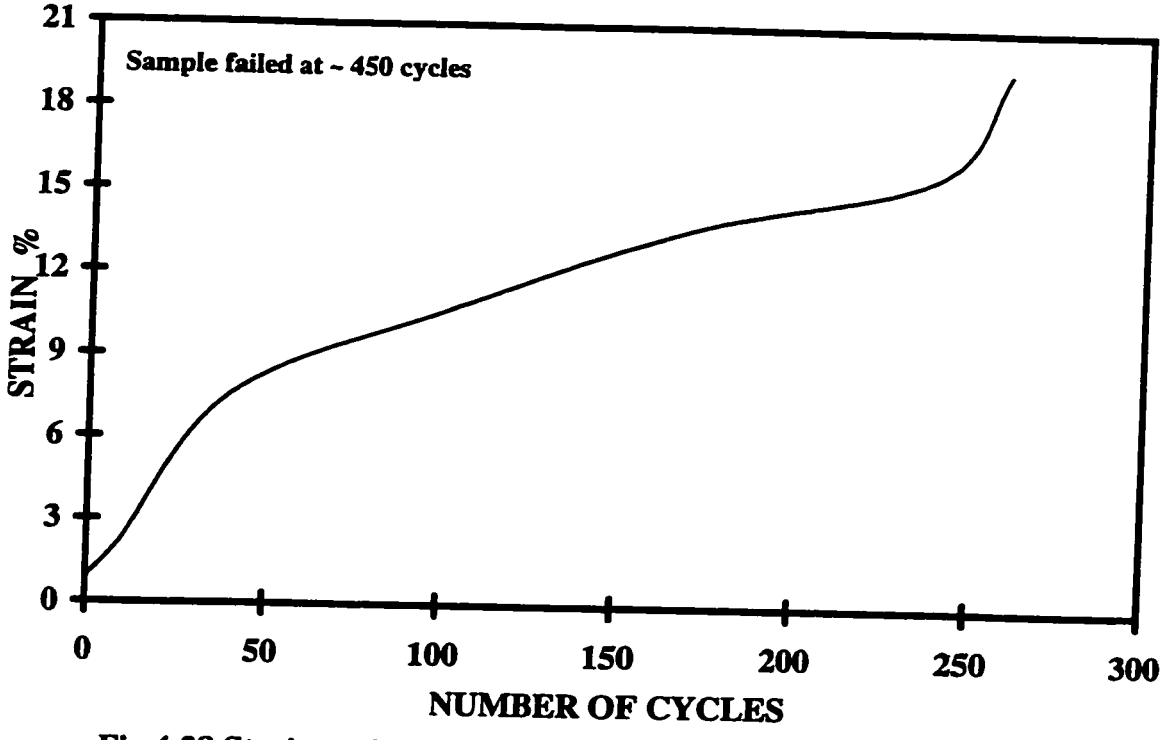

Fig.4.28 Strain variation during fatigue at 10Hz and 70% of the ultimate strength

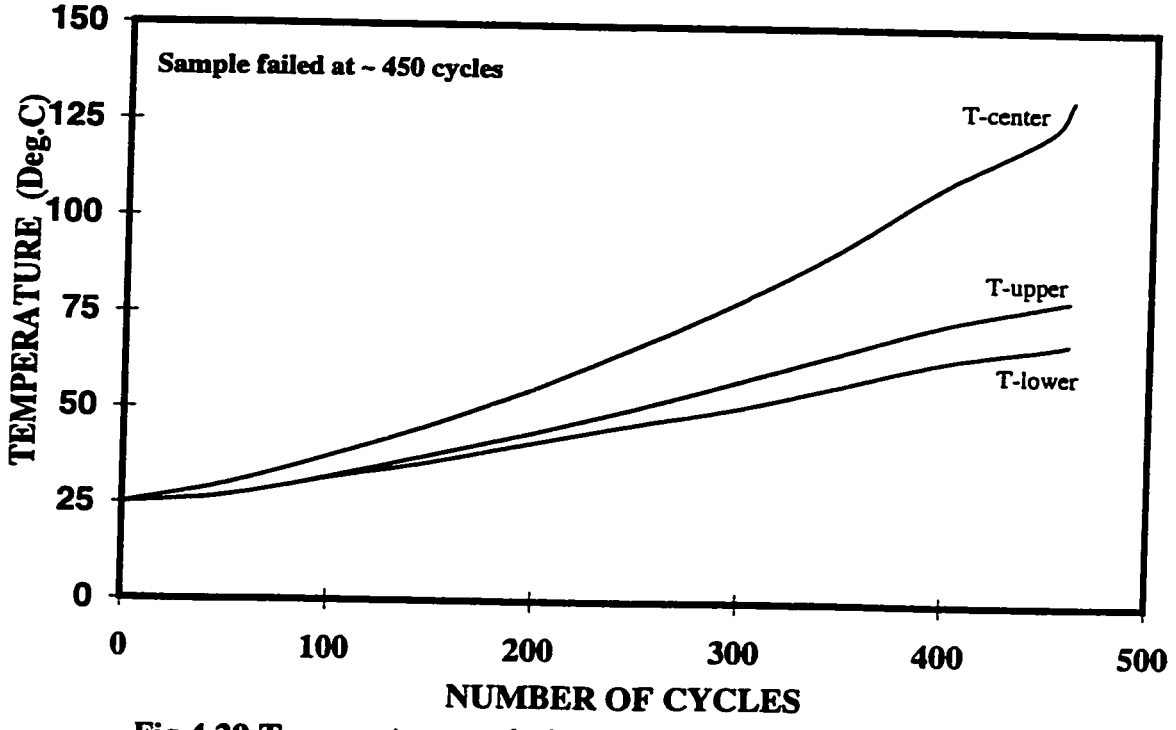

Fig.4.29 Temperature variation during fatigue at 10Hz and 70% of the ultimate strength

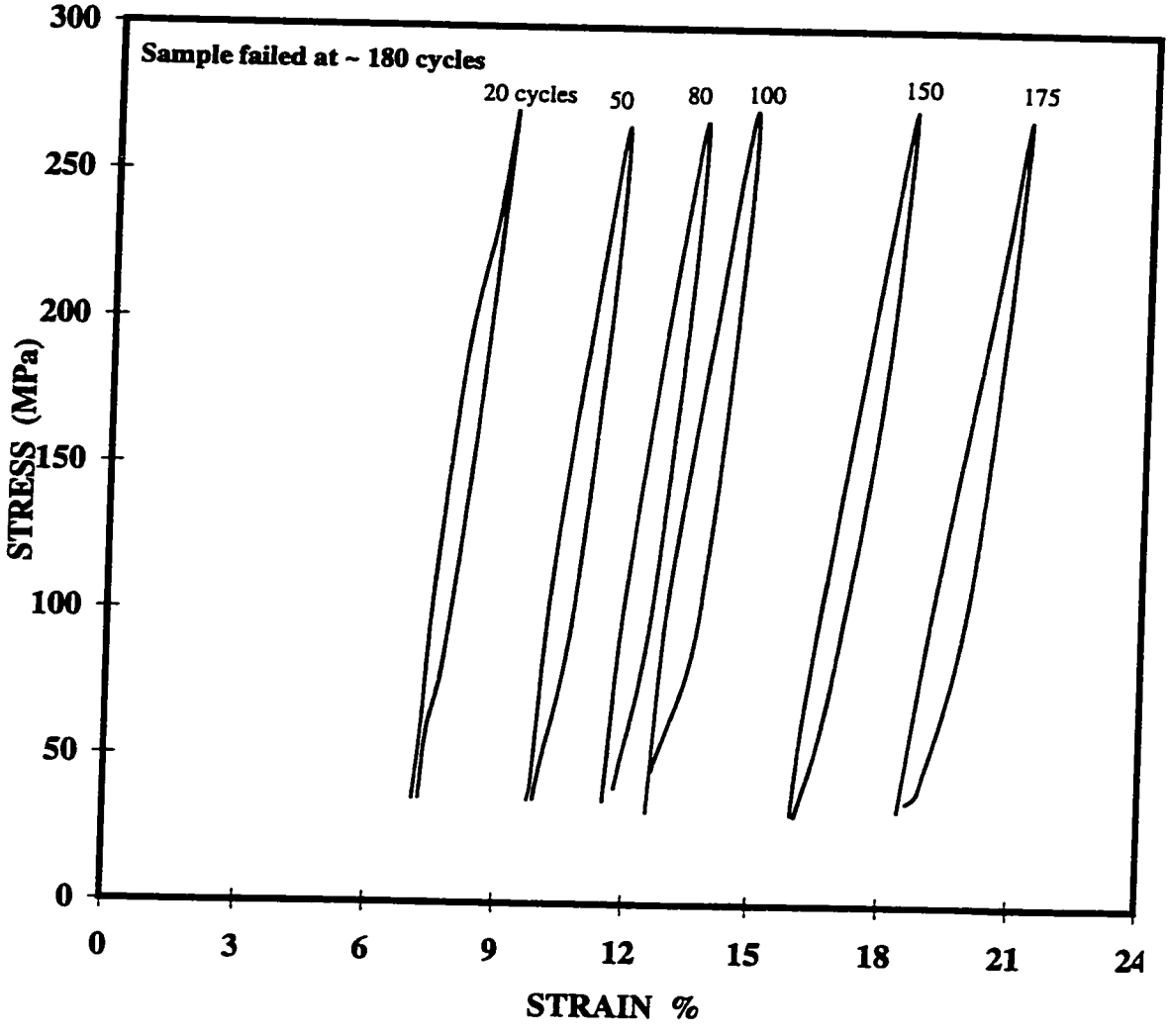

Fig.4.30 Variation in hysteresis loops during fatigue at 10Hz and 80% of the ultimate strength

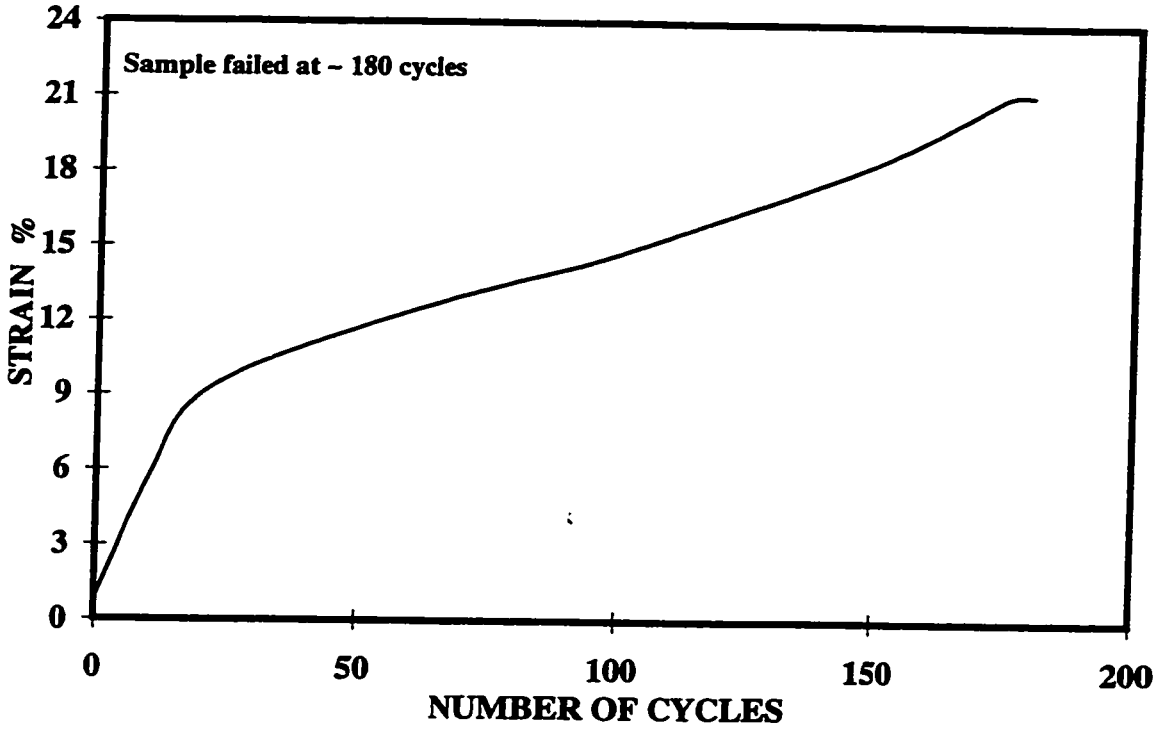

Fig.4.31Strain variation during fatigue at 10Hz and 80% of the ultimate strength

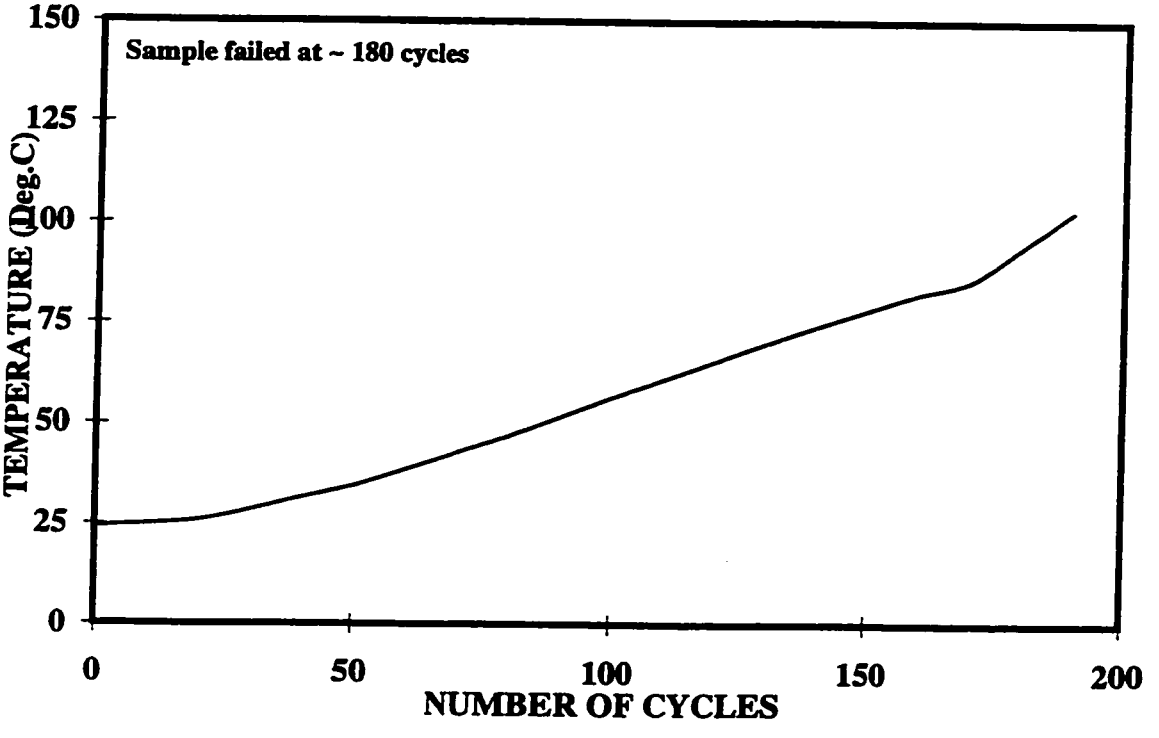

Fig.4.32 Temperature variation during fatigue at 10Hz and 80% of the ultimate strength

CHAPTER 5

ANALYSIS

5.1 Hysteretic energy dissipation

For linear viscoelastic materials, the rate of hysteretic heating is determined by the hysteretic energy dissipated under fatigue loading [7,13] and is given by:

$$q=\pi f D''(f, T)\sigma^2 \qquad (5.1)$$

where;

q is the energy dissipation rate per unit volume

f is the loading frequency

D'' is the loss compliance

σ is the stress amplitude

The hysteretic energy can also be measured directly from the area of the hysteresis loops. The area in this case indicates the total energy dissipation during each fatigue cycle. The heat dissipation rate (q) can then be calculated according to the relation:

$$q = w.f \qquad (5.2)$$

where (w) is the hysteresis loop area, and (f) is the loading frequency.

The areas of the hysteresis loops were measured at the different loading conditions. Fig 5.1 shows the variation in the hysteresis loop area at the three loading frequencies as a function of the normalized fatigue life (N/N_f) where N_f is the fatigue life. At 1Hz (Fig.5.1a), the area of the hysteresis loop decreased as the number of cycles increased at the lower load level ($60\%\sigma_{ult.}$). At $70\%\sigma_{ult}$ the loop area decreased but in lower rates, while at $80\%\sigma_{ult}$ the loop area started to increase slightly. Opposite trend was obtained at 5Hz and 10Hz, where the hysteresis loop area always increased significantly and this trend became stronger as the load level increased.

5.2 Thermal Analysis

In the present work, the heat generation is assumed to be uniform throughout the sample, since every point in the material is under the same tension load all the time. The heat generation during fatigue can be considered as a one-dimensional heat transfer problem, where the generated heat is dissipated from the sample's interior to the surface by conduction. Due to the hysteresis heat generation only, the temperature is expected to be maximum at the center (midplane) of the sample as shown by Dally and Broutman [1].

If adiabatic heating conditions are assumed, a case in which all the heat generated is manifested as temperature increase and none is lost to the surrounding, the temperature rise associated with hysteresic heating is given by:

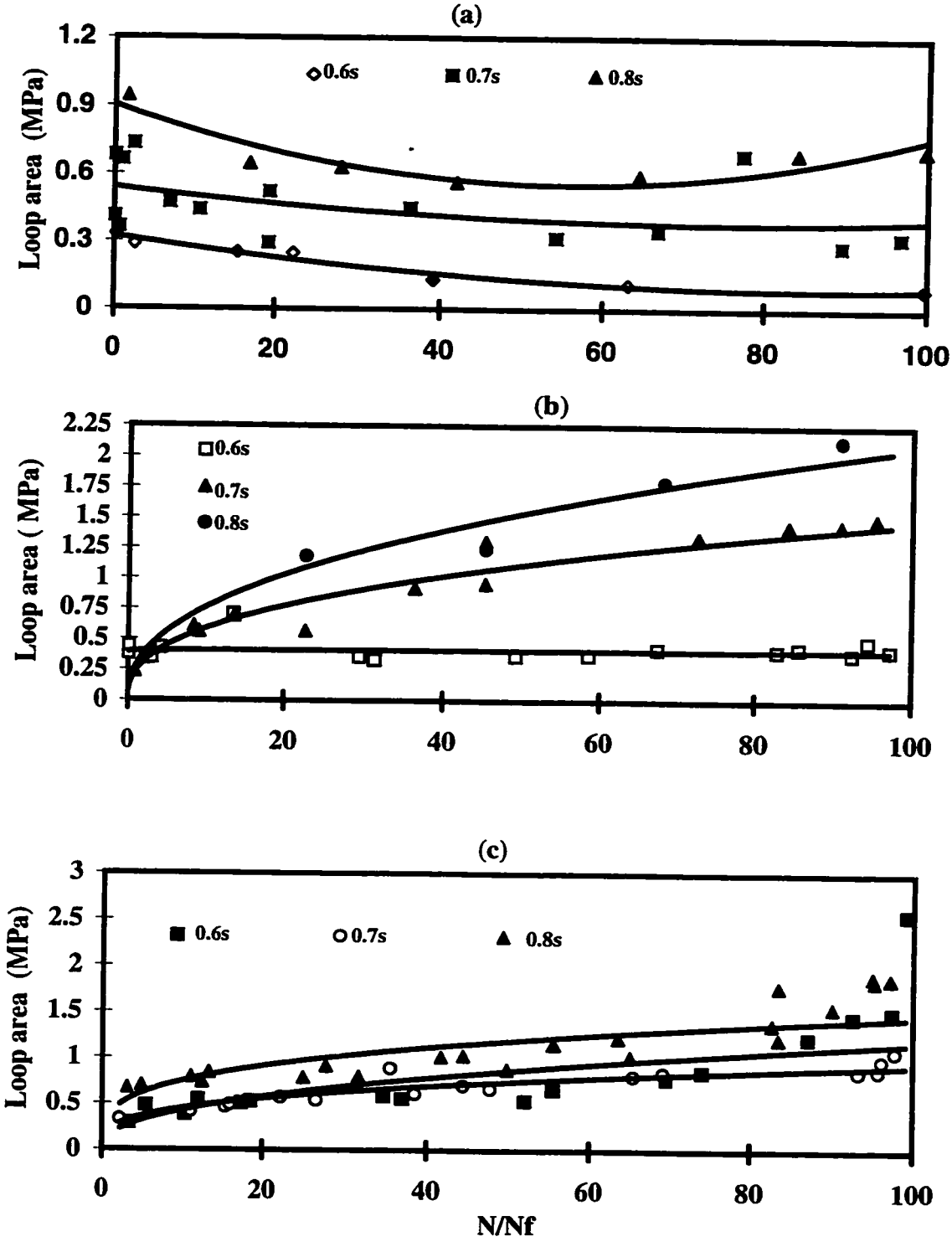

Fig. 5.1 Hysteresis loop area vs. normalized fatigue life.
(a) 1Hz, (b) 5Hz, and 10Hz

$$dT/dt=q/\rho C_p \quad (5.3)$$

where;

T is the temperature

t is the time

q is the heat generation rate

ρ is the material's mass density in gr/cm^3

C_p is the specific heat for the material in J/gr.°C .

Since a part of the generated heat will be lost to the surrounding, it is difficult to assume adiabatic conditions, and the heat loss should be considered. Taking into account the amount of heat loss, the temperature variation can be given by [32]:

$$dT/dt=q/\rho C_p - HA/\rho C_p V (T-T_0) \quad (5.4)$$

where;

H is the convection heat transfer coefficient in $J/(m^2.sec.°C)$

T_0 is the room temperature (taken as $25C^0$).

A is the surface area of the sample.

V is the sample's volume.

The heat generation rate (q) can also be estimated from the area of the hysteresis loops according to Eq. 5.2

The convection heat transfer coefficient can be estimated by assuming that equilibrium conditions of the heat transferred from the sample to the surrounding will prevail. At equilibrium, Eq.5.4 can be written as:

$$1/\rho C_p \ (q- HA/V \ (T_e-T_0))=0 \qquad (5.5)$$

where T_e is the equilibrium temperature. In our work, temperature equilibrium was reached only in fatigue tests conducted at 1HZ. Therefore, the value of heat transfer coefficient H can be estimated from these data, using q values from the area of the hysteresis loops collected at early stages of fatigue at the three load levels of the 1HZ data. Fig. 5.2 shows q values versus (T_e-T_0). From the slope of the straight line in this plot, HA/V is found to be about 40,000 $N/m^2.sec.C^0$ and in turn H is about 80 $J/m^2.sec.°C$.

Having determined the values of W and H, the transient temperature T at any time during fatigue can be estimated from Eq.5.4 by incremental method :

$$\Delta T_i =[(wf/\rho C_p)-(HA/\rho C_p V \ (T_i-T_0))]\Delta t \qquad (5.6)$$

$$T_{i+1}=T_i+\Delta T_i$$

$$t_{i+1}=t_i+ \Delta t$$

The experimental and predicted values of the transient temperature at the three loading frequencies are shown in Figs. 5.3-5.5 respectively.

At 1Hz, the predicted temperature tends to stabilize to a certain value after a certain number of cycles. The predicted equilibrium temperatures at this frequency are very near to the experimental ones, as well as the time elapsed before reaching equilibrium. It is also clear that the equilibrium temperature increases as the load level increases. The small differences between the experimental and predicted values of temperature indicate the amount of temperature rise due to the heat generated from sources other than the hysteretic losses. These sources include mainly the friction between damaged sites and the heat accumulation due to the poor thermal conductivity of the material. The relatively small differences in temperature indicate that only small and slow rates of these damages occurred during fatigue at this frequency.

The predicted temperatures at 5Hz and 10Hz indicate that the temperature will reach an equilibrium value after a certain number of cycles, and that this equilibrium temperature increases as the load level and loading frequency increases. The experimental values, on the other hand, show that the material fails under fatigue long time before reaching this equilibrium temperature. It can be noticed that the material's failure occurs when the material's temperature during fatigue reaches its softening temperature (~120°C). In some cases at high frequencies and load levels, the failure temperature exceeded this value before failure.

A comparison between the predicted temperature behavior and the actual (experimental) one gives an indication about the role of the different types of damage that occur during fatigue. The poor thermal diffusivity of the material results in accumulation of the thermal energy within the material instead of being dissipated to the surrounding. As a result, the thermal energy accumulates significantly inside the material, especially at high frequencies and load levels. Since fibers are less sensitive to this level of temperatures, the temperature rise will affect the thermoplastic matrix by imposing it to near or over its softening point. The matrix softening results not only in loss of the matrix integrity as a rigid body, which give a rise to fibers reorientation, but also in acceleration of the creep deformation.

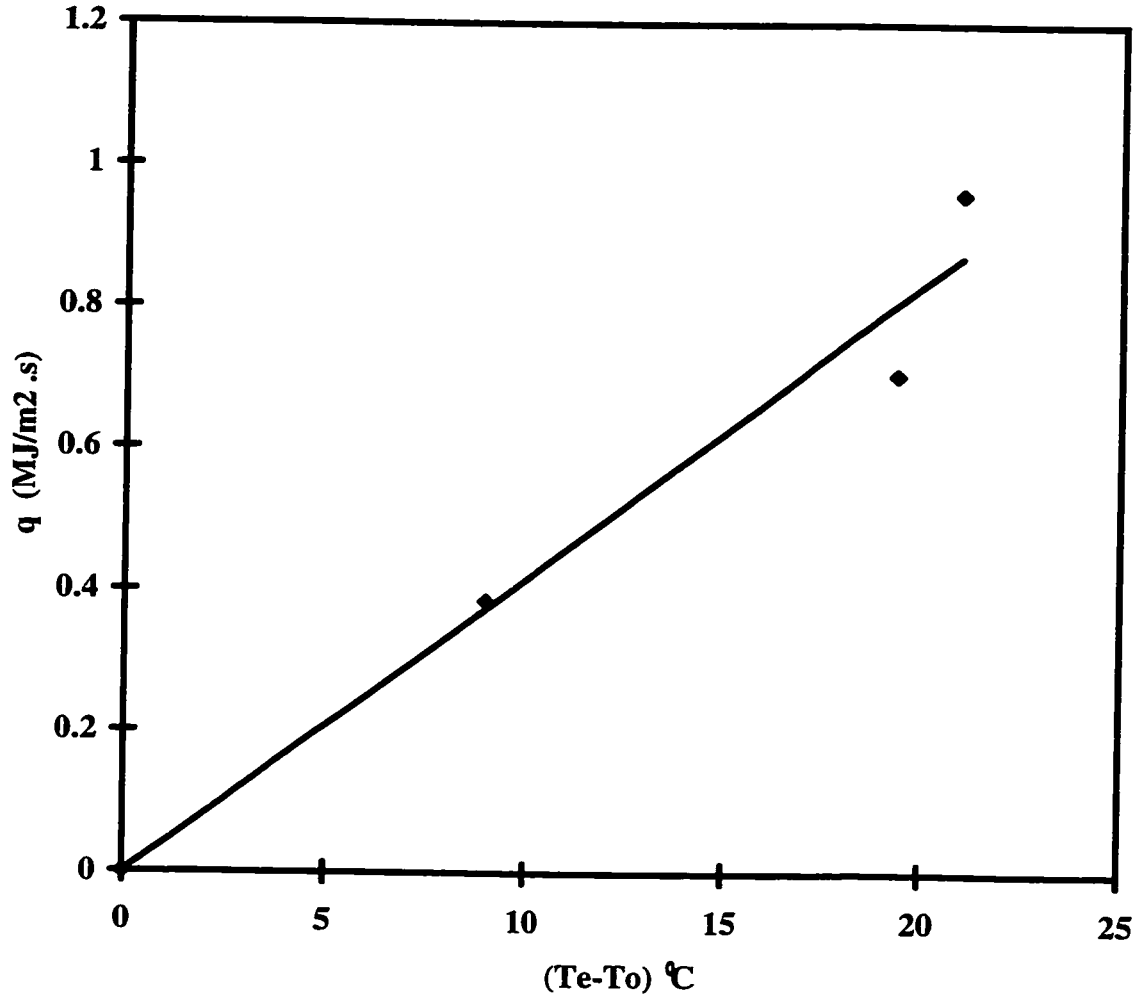

Fig. 5.2 Estimation of the heat transfer coefficient from the loop area vs. equilibrium temperature at 1Hz.

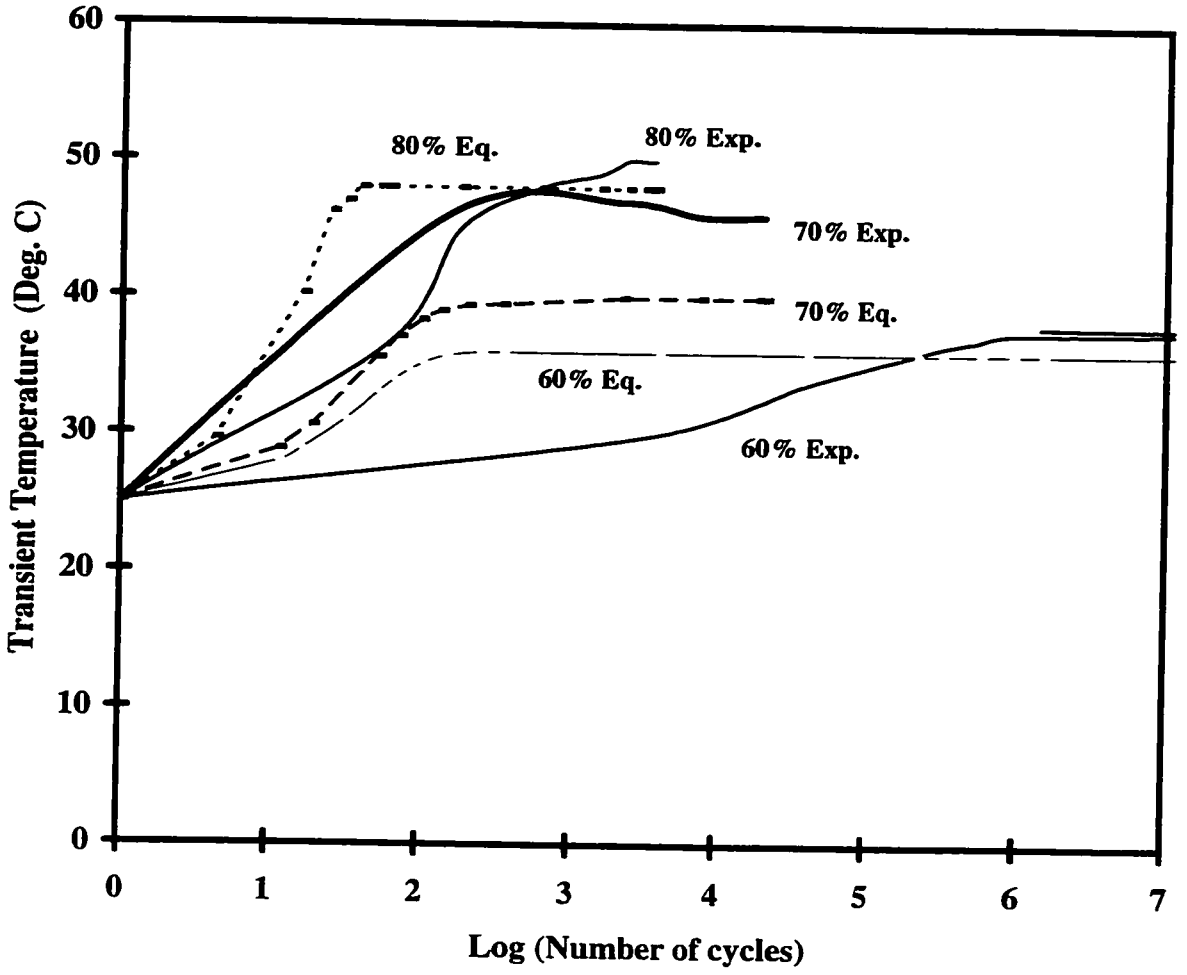

Fig. 5.3 Temperature variation during fatigue at 1Hz.
Solid lines represent experimental data, while dashed lines represent data predicted from Eq. 5.6.

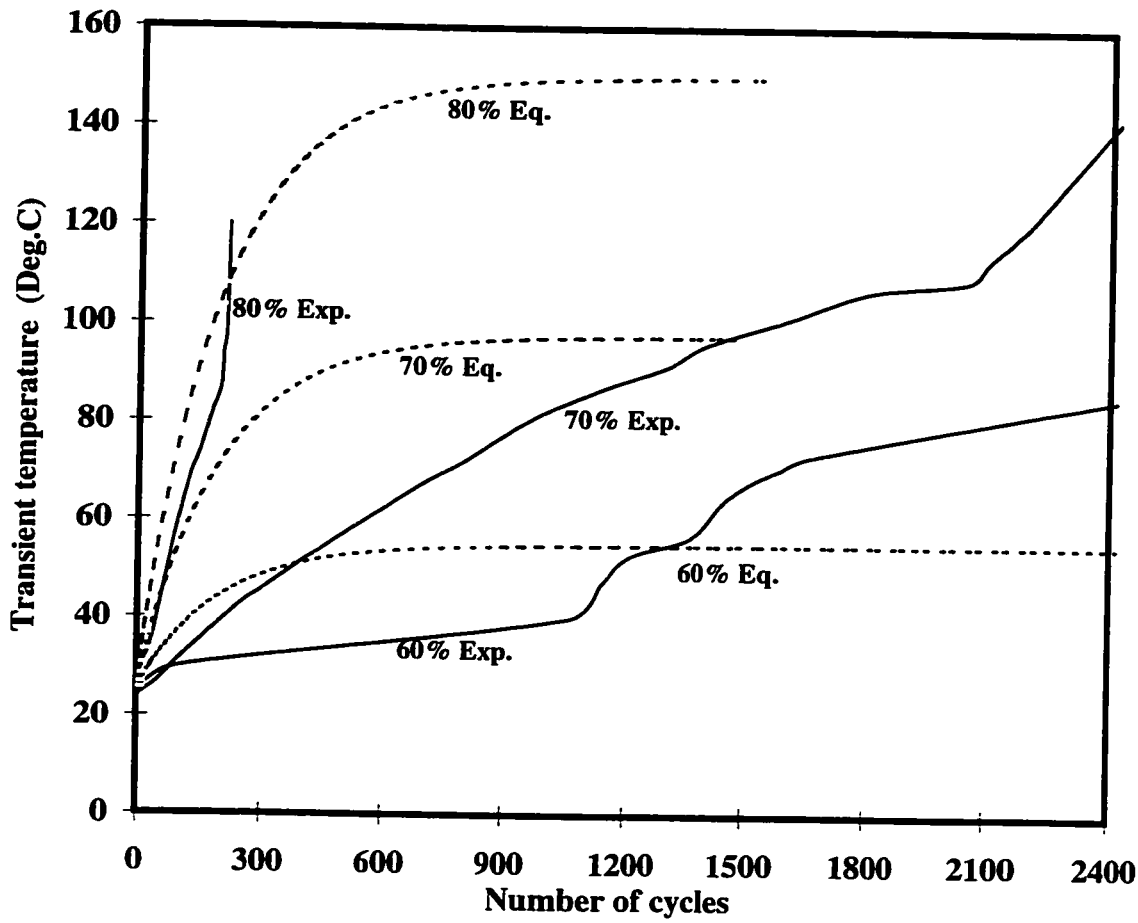

Fig. 5.4 Temperature variation during fatigue at 5Hz. Solid lines represent experimental data, while dashed lines represent predicted data from Eq. 5.6.

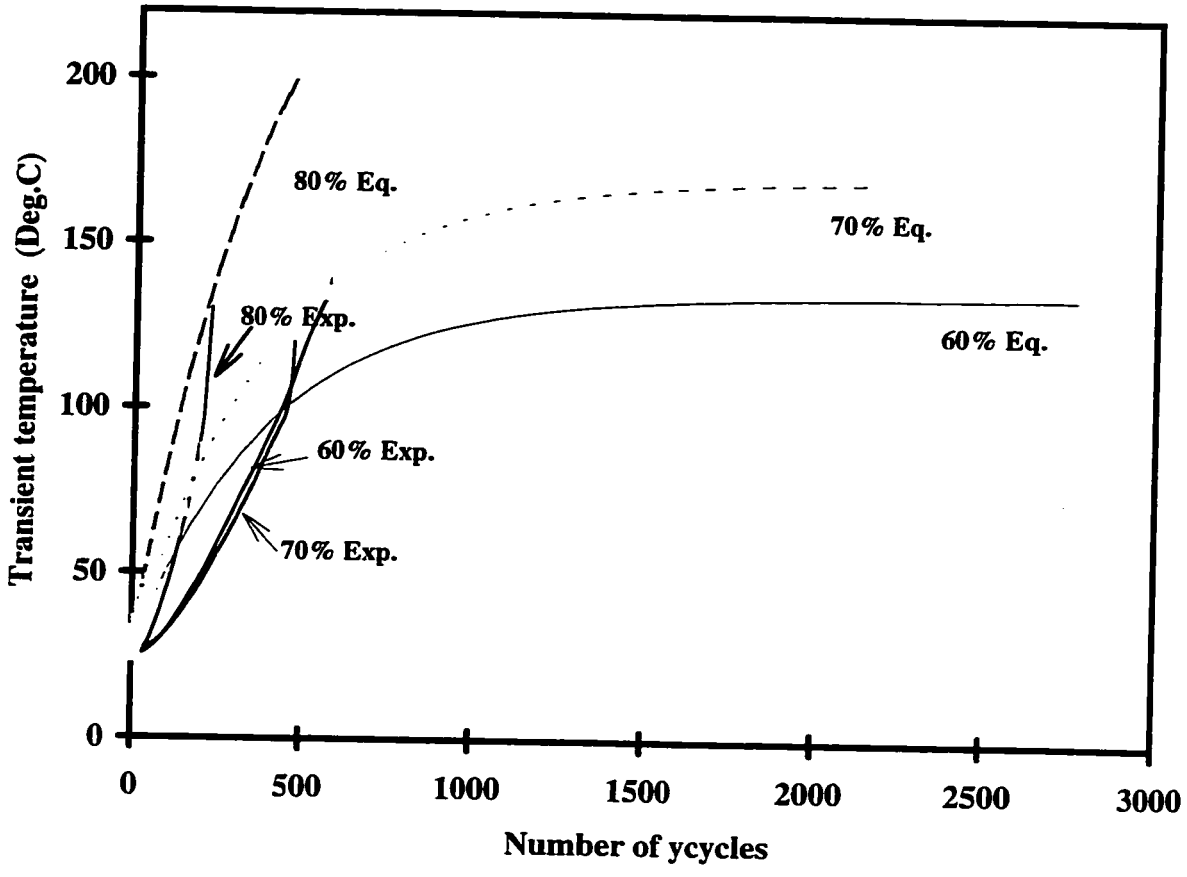

Fig. 5.5 Temperature variation during fatigue at 10Hz. Solid lines represent experimental data, while dashed lines represent predicted data from Eq. 5.6.

5.3 Modeling the frequency effect on fatigue life:

Literature data and our experimental results have shown that thermal degradation associated with hysteresis heating is the dominant frequency effect on fatigue life of the thermoplastic composite AS4/PEEK. This effect increases significantly as the role of the thermoplastic matrix becomes more dominant as in the case of angle-ply lay-ups.

The hysteresis heating can also be measured directly from the area of the hysteresis loops. Hahn and Kim[33] have shown that the hysteresis energy can be approximated by :

$$w = C(1-R^2)\sigma(\sigma-\sigma_t) \qquad (5.7)$$

where;

C is a parameter related to the mid-width of the hysteresis loop and its relation to the maximum fatigue strength.

R is the stress ratio of the fatigue test ($R=\sigma_{min}/\sigma_{max}$)

σ_t is the threshold stress below which no hysteresis heating is measured.

The hysteresic heating rate is given by:

$$q = C(1-R^2)\sigma(\sigma-\sigma_t)f \qquad (5.8)$$

This hysteresic heating is manifested as temperature increase during fatigue. However, an observation of the variation in hysteresis loops and temperature at the different load levels and frequencies indicates that hysteresis heating contributes to a certain limit in the thermal effect, while the evolution of other kinds of damage contribute to the rest. The main type of damage observed on fatigue failed specimens was matrix cracking. It was clear from the experimental results that the intensity of matrix cracking increased with increasing load frequency and stress level. The additional energy dissipated as reflected by the expanded hysteresis loops is likely to be due to friction at the different internal and external damaged sites.

Taking this point into consideration, the experimental results as well as the heat transfer analysis indicate that the temperature increase during fatigue is proportional to the hysteretic heating rate (q) and hence may be predicted by;

$$T=T_0+\eta'[(1-R)^2\sigma(\sigma-\sigma_t)f]^{\beta} \qquad (5.9)$$

where;

η' and β are parameters

T_0 is the ambient temperature at the experiment environment.

An observation of the S.N curves suggests that these curves may be described by the following function:

$$Log(N)(\sigma-\sigma'_0)= C \qquad (5.10)$$

where σ_0 is the fatigue limit without thermal effect, and C is a parameter

The strength of viscoelastic materials is sensitive to temperature, and so is the fatigue limit. Assuming that the effect of temperature on fatigue limit (σ'_0) follows an exponential function

$$\sigma'_0=\sigma_0\exp[-\eta'(T-T_0)] \qquad (5.11)$$

After substituting for $(T-T_0)$ from Eq.5.9, Eq.5.11 becomes;

$$\sigma'_0=\sigma_0\exp\{-\eta[(1-R)^2\sigma(\sigma-\sigma_t)f]^{\beta}\} \qquad (5.12)$$

Substituting Eq.5.12 into Eq.5.10, and introducing the following stress parameters:

$P=\sigma/\sigma_{ult.}$ $P_0=\sigma_0/\sigma_{ult.}$ and $P_t=\sigma_t/\sigma_{ult.}$

We obtain the mathematical model for the thermal effect on the fatigue life of such a viscoelastic material :

$$\text{Log}(N)\{P-P_0\exp[-\eta((1-R)^2P(P-P_t)f)^{\beta}]\}=C \qquad (5.13)$$

Eq.5.13 is actually a variation of the model presented by Dan-Jumbo et al. [2] but, instead of employing the temperature rise data, here the thermal effect is directly related to the stress level and loading frequency. Those quantities can be easily pre-investigated

as design parameters instead of the temperature rise data which come as a result of fatigue loading. In addition, the model suggested in [2] is based on crack growth in viscoelastic media, whereas Eq.5.13 is based on the assumption of general strength degradation of the material, and hence is suitable for smooth (unnotched) composite samples.

By curve fitting the data given in Table 4.2 and with P_0=0.55 , P_t=0 and R=0.13 , the values of the parameters in Eq.5.13 were determined as follows : C=1.7 , η=1 and β=0.5

Fig 5.6 is a reproduction of the experimental S-N data (Fig. 4.2) along with the curves predicted by Eq.5.8 which are shown in solid or dashed lines. In general, it can be seen that the model predicted the trend of the load frequency effect. At low frequency tests, the model prediction fits the experimental data better than it does at high frequencies. The reason for this is that this model does not account for the other types of damages that occur extensively at high frequencies and contribute in thermal effects other than those resulting from the viscoelastic behavior of the material during fatigue. However, it can be said that this model gives a good indication about the effect of frequency on the fatigue life, and can be improved if the damage factors are taken into account.

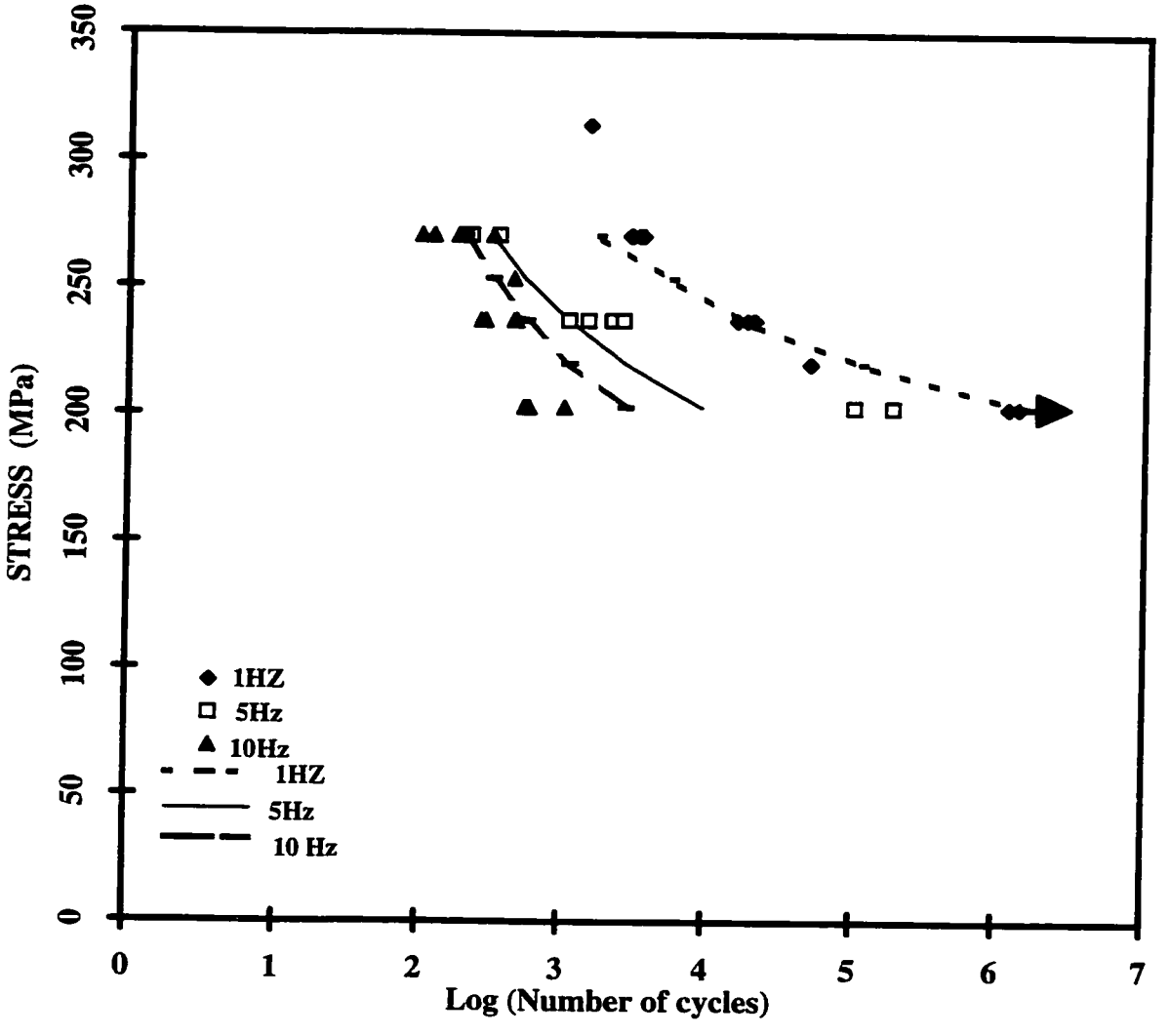

Fig. 5.6 S-N curves for AS4/PEEK angle-ply laminates. The symbols are the experimental data, while dashed and solid lines are the predicted data by Eq.5.8

5.4 Viscoelastic properties

When a linear viscoelastic material is subjected to a sinusoidal cyclic load, there exists a phase lag(δ) between the applied stress (σ) and the resulting strain (ε) response. The stress and strain at any time (t) is given by:

$$\varepsilon(t) = \varepsilon_o \sin(\omega t) \tag{5.14}$$

$$\sigma(t) = \sigma_o \sin(\omega t + \delta) \tag{5.15}$$

where;

$\omega = (2\pi f)$ is the angular frequency.

ε_o and σ_o are the strain amplitude and stress amplitude respectively.

δ is the phase angle between the stress and strain.

The damping capacity of viscoelastic materials is measured in terms of the loss factor (or damping factor) which is a function of the phase lag between the stress and strain according to the relation:

$$d = \tan\delta = E'/E'' \tag{5.16}$$

where;

d is the loss factor.

E' is the storage modulus.

E" is the loss modulus.

The storage modulus denotes the ratio of strain in phase with the stress to the strain and is given by:

$$E' = (\sigma_o / \varepsilon_o) \cos(\delta) \qquad (5.17)$$

The loss modulus denotes the ratio of the stress which is 90° out of phase with the strain to the strain and is given by:

$$E'' = (\sigma_o / \varepsilon_o) \sin(\delta) \qquad (5.18)$$

Figure 5.7 shows a typical recording of stress and strain signals during fatigue loading. The phase angle at different number of cycles was measured. The variation in dynamic properties during fatigue is obtained using the measured values of phase angles and substituting in the above equations.

Figure 5.8 shows the variation in dynamic viscoelastic properties during fatigue at 1Hz. At $60\%\sigma_{ult.}$, the loss factor decreased in small amounts during most of the fatigue life. At $70\%\sigma_{ult}$ and $80\%\sigma_{ult.}$, the loss modulus showed no significant variation except before the final failure where it increased in a relatively gradual manner. Similar behavior can be noticed in the variation of the loss modulus. On the other hand, the storage modulus increased relatively at low stress levels, while no variation can be seen at $80\%\sigma_{ult}$. The variations in the viscoelastic dynamic properties at 1Hz can be (in general)

attributed to the effect of creep deformation and the associated state of orientation hardening at the different stages of fatigue life.

Fig. 5.9 and fig. 5.10 show the variation in dynamic viscoelastic properties at 5Hz and 10Hz respectively. A significant difference can be noticed in the values of the loss modulus and loss factor as compared to their values at 1Hz. Even though the figures show a nonuniform variation in the properties throughout the fatigue life, a general behavior can be noticed; an increase in both the loss factor and loss modulus as load level increases, and a consequent decrease in the storage modulus. The local variations in these properties during the fatigue life can be attributed to the different states of deformation that takes place during fatigue such as creep deformation.

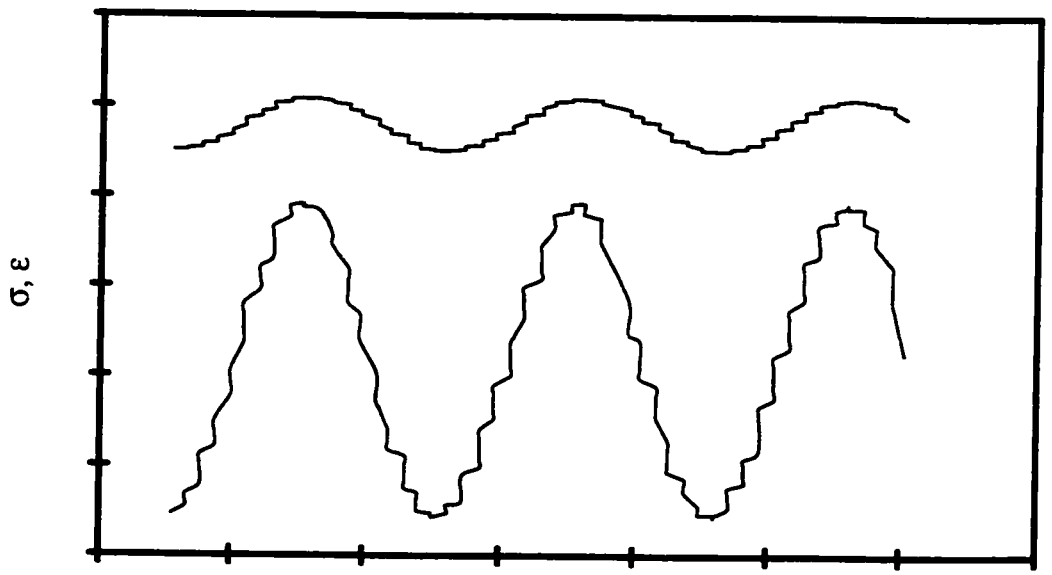

Fig. 5.7 Typical sinusoidal stress (lower) and strain (upper) signals during fatigue loading.

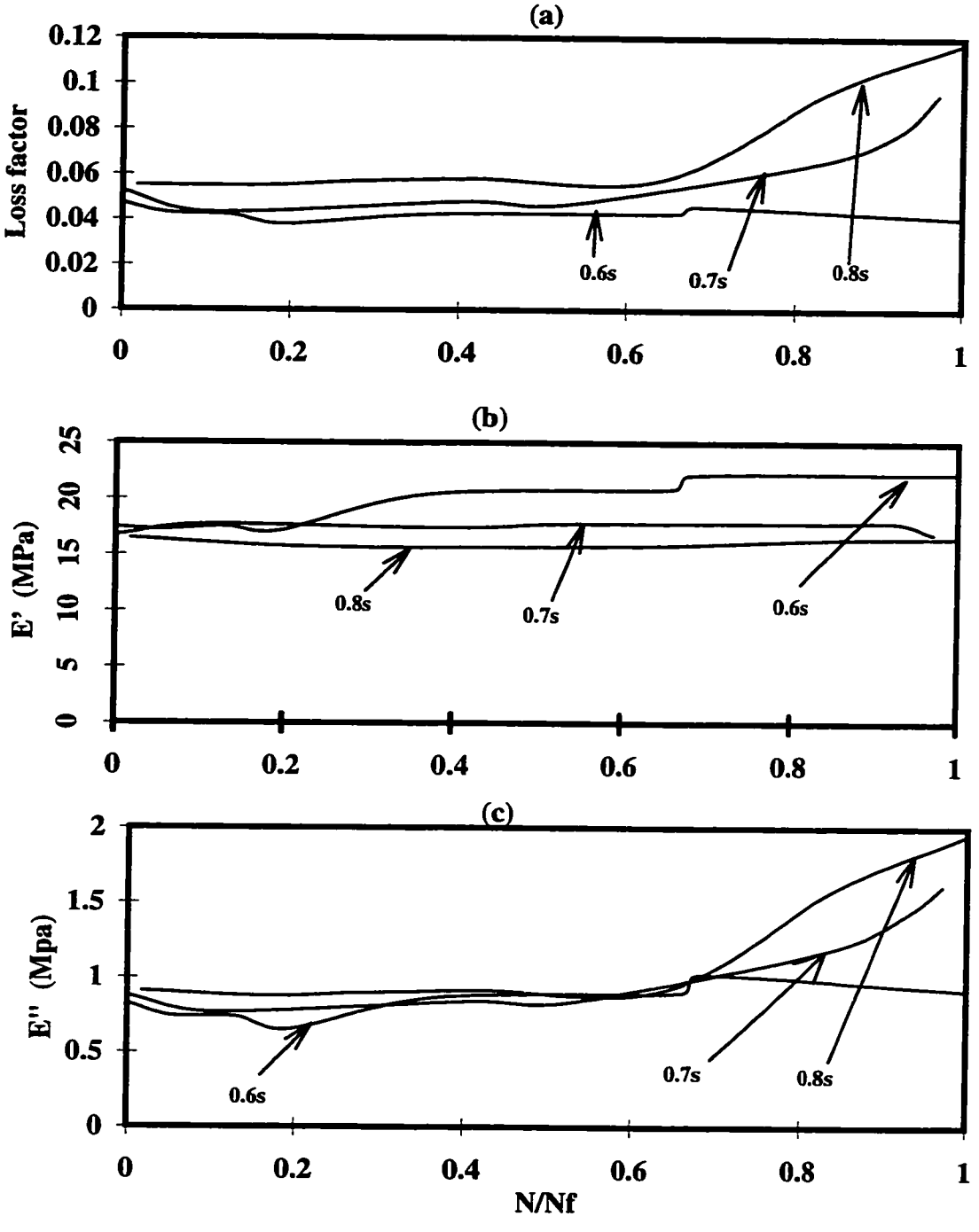

Fig. 5.8 Variation in dynamic viscoelastic properties during fatigue at 1Hz and the three loading levels: (a) loss factor, (b) storage modulus, and (c) loss modulus.

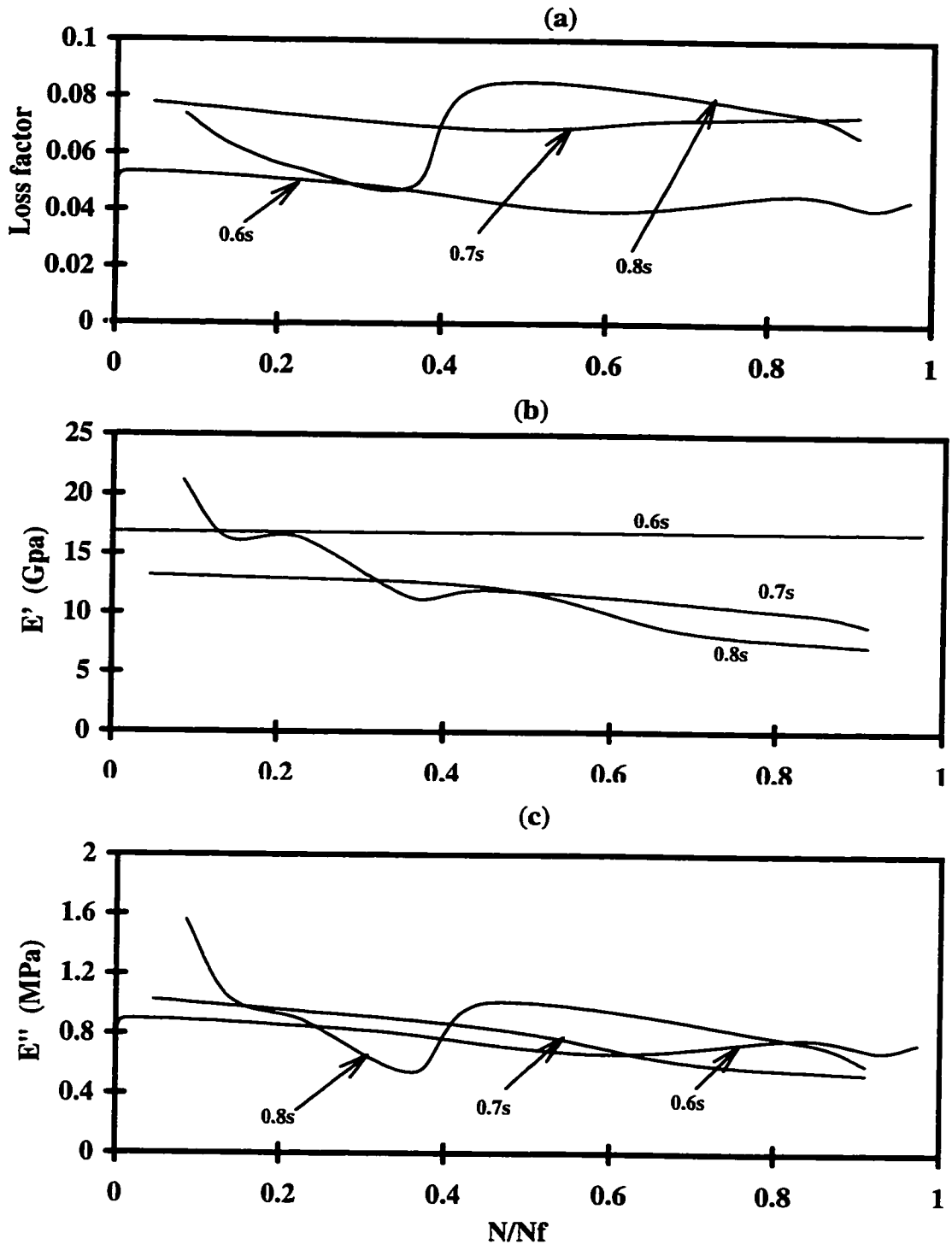

Fig 5.9 Variation in dynamic viscoelastic properties during fatigue a 5Hz an the three loading conditions:
(a) Loss factor, (b) Storage modulus, and (c) Loss modulus.

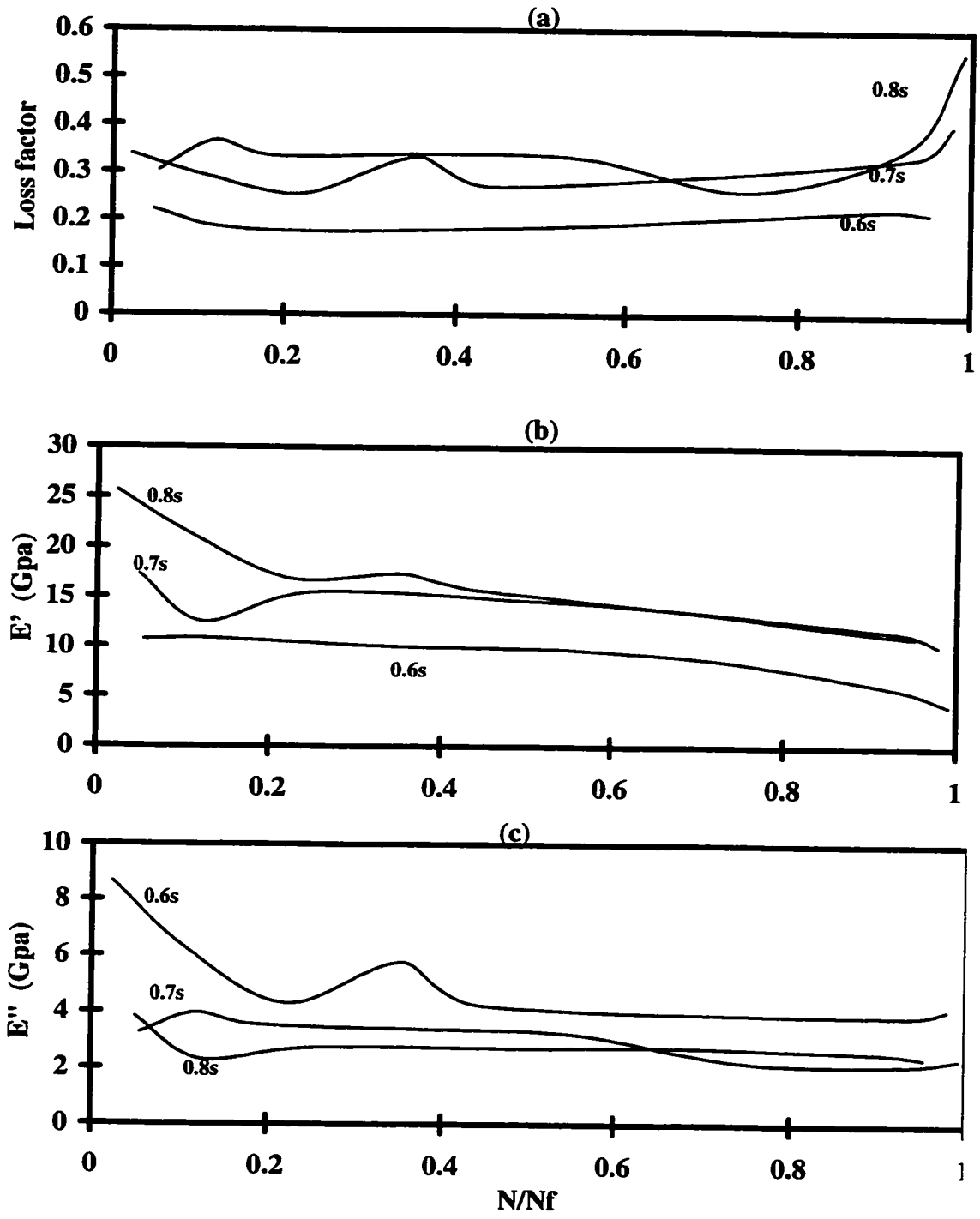

Fig. 5.10 Variation in dynamic viscoelastic properties during fatigue at 10Hz and the three loading levels:
(a) loss factor, (b) storage modulus, and (c) loss modulus.

CHAPTER 6

DISCUSSION

6.1 General fatigue behavior

The results of the fatigue tests conducted in this study suggest that the fatigue life of carbon/PEEK angle ply composites decreases as the loading frequency increases. At the same loading frequency, the fatigue life also decreases as the load level increases, with more decline at high loading frequencies. This behavior is related to a number of failure mechanisms that evolve according to the loading conditions (loading level and frequency) applied. These failure mechanisms include the damage propagation, the creep deformation, and the thermal effect.

6.2 Fatigue damage mechanism

At low frequencies, low levels of fatigue damage generally result because of the material's ductility and high fracture toughness. The damage evolution increases as the load level increases at the same loading frequency. Most of the damage at low frequencies consists of matrix cracking that increases in size and densities as the load level increases, leading to other types of damage to start such as delamination and fiber-matrix debonding. The accumulation of these damages leads to the weakness of the interface

strength and to the loss of the material's properties.

The damage propagation and accumulation behavior at high frequencies is similar to that at low frequencies, except that the higher frequencies accelerate the process of damage propagation and lead to more types of damages to occur at higher densities. This explains the effect of loading frequency on the rate of damage propagation and accumulation, and in turn, the importance of taking this factor into account in the characterization of the fatigue behavior of such thermoplastic composite.

6.3 Thermal effect

The investigation of temperature variation during fatigue indicated the significant effect of loading frequency and loading level on the fatigue life of this material. It is also possible to notice the interaction between the thermal effect and other factors that affect the fatigue life such as creep deformation and mechanical damage. The higher temperature levels lead to further matrix softening and give rise to other types of damage to occur and to the interaction between the damaged sites. This interaction will, in turn, lead to further temperature rise and energy dissipation which is not due to the damping behavior of the material but rather a direct result of it.

The results of this study and other studies as well indicate that the thermal degradation associated with hysteretic heating is the dominant frequency effect on the fatigue life of this material. The thermal analysis performed in this study was based on this assumption. The deviation between the results predicted from this analysis and the experimental ones is due to the thermal effect resulting from the mechanical damage mechanisms and the interaction between these mechanisms and the actual thermal effect. This part which is not accounted for in our analysis plays an important role in characterizing the fatigue behavior of all composite materials. However, the thermal analysis and the fatigue modeling suggested in this study give a reasonable approximation and a general overview for the thermal effect associated with loading frequency.

Another feature that occurs as a result of the thermal effect and the consequent matrix softening is the possibility of fibers reorientation especially at high temperature levels. The variation in the fibers orientation in the load's direction will result in an increase in the composite's stiffness, and in turn, an increase in fatigue life. Since high temperatures occurred only at high frequencies and load levels, it can be said that the fibers reorientation at these conditions did not contribute significantly in increasing the fatigue life due to the high damage levels and thermal degradation. Rather, at moderate temperature levels, fibers reorientation may contributed in increasing the fatigue life or delaying the final failure.

6.4 Creep and viscoelastic effects

Creep deformation occurred throughout the fatigue tests at all frequencies and load levels. Those deformation can be clearly distinguished at low frequencies, which is a common feature in thermoplastic polymers and their composites. Three zones were observed in the strain variation behavior (see for example Fig. 4.25) and the associated shifting in hysteresis loops.

The first zone was characterized by a decrease in the strain rates. At loading conditions where the temperature increase was insignificant, this behavior can be related to two possible factors. The first is the possibility of fiber reorientation due to the continuous loading and unloading, and the consequent increase in the material's stiffness. The second factor, which is the more possible factor, is the cyclic hardening that takes place due to molecular reorientation in the material. This phenomenon has been reported for a number of thermoplastic polymers and thermoplastic matrix composites[20, 31, 32, 34, 37-39] including PEEK composites. The molecular reorientation in the material's microstructure results in recrystallization, and hence an increase in the material's strength. This behavior becomes less significant as the load level increases at the same frequency, and much less significant at high frequencies and load levels.

The second zone was usually characterized by constant strain rates and a decrease in hysteresis loop shifting as a consequence of the reorientation occurring in the earlier stages. In the third zone, high levels of deformation can be observed shortly before the final failure.

The creep deformation can also be recognized at high frequencies. The high temperatures at such frequencies accelerate the creep deformation. An investigation of the strain variation behavior may indicate similar results to the those at low frequencies, but for shorter duration. Also, an investigation of the dynamic viscoelastic properties indicates some local variations at these loading conditions, which may be related to the different stages of creep deformation occurring at accelerated rates.

The viscoelastic behavior of the material shows great amounts of nonuniformity, especially at high frequencies. This behavior indicates that the material's viscoelastic response is highly nonlinear. Even though the use of the theory of linear viscoelasticity in the analysis gave an overview about the general variation in the dynamic properties as a function of loading conditions, a more detailed investigation is required to account for the nonlinearity in the creep and viscoelastic behavior of this material.

CHAPTER 7

CONCLUSION

- The fatigue life of $[\pm 45]_{ns}$ carbon/PEEK composites was investigated at three stress levels (60%, 70%, and 80%$\sigma_{ult.}$) and three loading frequencies (1Hz, 5Hz, and10Hz). It was found that the fatigue life of this composite decreases as the loading frequency increases.
- Temperature rise during fatigue was recorded. It was found that the temperature rise increases as stress level and loading frequency increase. At 1Hz, the temperature reached an equilibrium value with a maximum temperature recorded at 80%σ_{ult} of about 42°C. At 5Hz and 10Hz, continuous temperature rises were recorded with a maximum of around 150°C.
- Hysteretis loops during fatigue were recorded. At 1Hz, it was noticed that the size of the hysteresis loops decreases during most of the fatigue life except shortly before the final failure where they increase rapidly. Continuous increase in the size of hysteresis loops was noticed at 5Hz and 10Hz.
- Mechanical damages contribute to the decline of fatigue life by increasing the thermal degradation as a result of the heat generated at the damaged sites.
- The material shows significant creep deformation at all frequencies. Fiber reorientation was also measured at all frequencies. At 1Hz, small fiber reorientation was measured, with a maximum of ±4 degrees. Higher values of fiber reorientation

were measured at 5Hz and 10Hz, with a maximum of around ±34 degrees. The accumulation of creep strain shows three stages which is similar to that obtained in a classical creep test.

- A fatigue model based on the general degradation of strength was proposed, which accounts for the effect of the stress level and loading frequency. The model predicted the fatigue life at 1Hz very well, while some deviations from the experimental values were obtained at 5Hz and 10Hz.

References:

[1]-Dally, J.W. and Broutman, L.J. "Frequency effect on the fatigue of glass reinforced plastics" J.composite materials, Vol.1(1967)pp.424-442.

[2]-Jumbo, E. Dan, Zhou, S.G., and Sun, C.T. "Load-frequency effect on fatigue life of IMP6/APC-2 thermoplastic composite laminates" Advances in thermoplastic matrix composite materials, ASTM STP 1044(1989)pp.113-132.

[3]-Reifsnider, K.L., Stinchomb, W.W., and O'Brien, T.K. "Frequency effect on a stiffness-based fatigue failure criterion in flawed composite specimens" Fatigue of filamentary composite materials, ASTM STP 636(1977)pp.171-184.

[4]-Curtis, D.C., Moore, D.R., Slatter, B., and Zahlan, N. "Fatigue testing of multi angle laminates of CF/PEEK" Composites, Vol.19, No.6(1988)pp.446-452.

[5]-Sun, C.T. and Chan, W.S. "Frequency effect on the fatigue life of a laminated composite" Composite materials; testing and design, ASTM STP 674(1976) pp.418-430 .

[6]-Kujawski, D. And Ellyin, F. "Rate/frequency-dependent behavior of fiberglass/epoxy laminates in tensile and cyclic loading" Composites, Vol.26, No.10(1995) pp.719-723.

[7]-Herzberg, R.W. and Manson, J.A. "Fatigue of engineering plastics" Academic press Inc. New York(1980).

[8]-Harris, W.J. "Metallic fatigue" Pergamon press(1961).

[9]-Forrest, P.G. "Fatigue of metals" Addison-wesley(1962).

[10]-Williams, R.S., Reifsnider, K.L., Stinchomb, W.W., and Turgay, H. "The effect of

frequency and strain amplitude on the fatigue damage of Boron-epoxy fiber reinforced composite materials" Airforce office of scientific research (AFOSR-TR-75-1387) October1974.

[11]-Williams, R.S., Reifsnider, K.L., Stinchomb,W.W., and Turgay, H. "The effect of frequency on the fatigue damage of Boron-Aluminum fiber reinforced composite materials" AFOSR-TR-75-1394, October1974.

[12]-Saff, C.R. "Effect of load frequency and lay-up on fatigue life of composites" Long-term behavior of composites, ASTM STP 813(1983)pp.78-91.

[13]-Mandell,J.F. and Meier, U. "Effect of stress ratio, frequency, and loading time on the tensile fatigue of glass-reinforced epoxy" Long-term behavior of composites, ASTM STP 813(1983)pp.55-77.

[14]-Stinchomb, W.W., Reifsnider, K.L., Marcus, L.A. and Williams, R.S. "Effect of frequency on the mechanical response of two composite materials to fatigue loading" Fatigue of composite materials, ASTM STP 569(1975)pp.115-129.

[15]-Ma, C.C.M....et. al. "Fatigue behavior of carbon fiber reinforced thermoplastic and thermoset polymeric composites.." Proc. of the ICCM-10(1995)Vol.1, pp.569-576.

[16]-Talreja, R. "Fatigue of composite materials" Springer-Verlag (1976).

[17]-James, T.L., Appl, F.J. and Bert, C.W. "Low-cycle fatigue of a glass-fabric reinforced laminate" Experimental mechanics, July 1988, pp.327-330.

[18]-Miner, L.H., Wolffe, R.A. and Zweben, C.H. "Fatigue, creep, and impact resistance of aramid fiber reinforced composites" Composite reliability, ASTM STP 580(1975) pp549-559.

[19]-Xiao, X.R. "Studies of the viscoelastic behavior of thermoplastic resin composites" Composites science and technology, Vol.134(1989) pp.163-182.

[20]-Rui, Y. and Sun, C.T. "Cyclic plasticity in AS4/PEEK composite laminates" J. Thermoplastic composite materials, Vol.6-October 1993, pp.312-322.

[21]-O'Brien, T.K. and Reifsnider, K.L. " " J. composite materials, Vol.15 (1981).

[22]-O'Brien, T.K. "fatigue delamination behavior of PEEK thermoplastic composite laminates" J. reinforced plastics and composites, Vol.7-July1988, PP>341-359.

[23]-Hennaff, G.C and Lafarie, M.C. "Fatigue behavior of thermoset and thermoplastic cross-ply laminates" Composites, Vol.23 No.2(1992) pp.109-116.

[24]-Simonds, R.A. and Stinchomb, W.W. "Response of notched AS4/PEEK laminates to tensile-compression loading" Advances in thermoplastic matrix composite materials, ASTM STP 1044(1989) pp.133-145.

[25]-Bilaut, F. and McGarry, F.J. "Damage and residual properties of notched $[0/\pm45/90]_s$ and $[0/90]_{2s}$ Graphite/PEEK Woven laminates under reversed fatigue" J. Thermoplastic composite materials, Vol.7-July1994, pp. 230-242.

[26]- ICI data sheet No. 2, 3, 4. (1991).

[27]- Annual book of ASTM standards, Designation: D 3039/3039M-93, Vol. 14.02, pp. 115-124. (1993).

[28]- Annual book of ASTM standards, Designation: D 3479-76, vol. 03.01, pp. 142-144. (1993).

[29]- Hennaff-Cardin, and Lafarie, M.C. "fatigue behavior of thermoset and thermoplastic cross-ply laminates" Composites, Vol. 23, No.2 (1992) pp. 109-116.

[30]- Tai, N. H., Ma, C.C., and Wu, S.H. "Fatigue behavior of carbon fiber/PEEK laminate composites" Composites, Vol. 26, No.5 (1995) pp. 335-370.

[31]- Richard, W. Hertzberg " Deformation and fracture of engineering materials" 4th. Edition, Jhon Wiley & Sons Inc. (1992).

[32]- S. Surish "Fatigue of materials" 2nd Edition, Cambridge University Press, New Yorrk. (1991).

[33]- Hahn, H.T., and Kim, R.Y. "Fatigue behavior of composite laminates" J. Composite materials, Vol. 10 (1976) pp. 156-180.

[34]-Selvie, Beland "High performance thermoplastic resins and their composites" Noyes Data Corp., New Jersey (1990).

[35]- Cogswell, F.N. "Thermoplastic aromatic polymer composites" Butterworth-Heinmann Ltd. (1992).

[36]-Kausch, Hans-Henning (Editor) "Advanced thermoplastic composites" Hanser Publishers (1993).

[37]- Lesser, J. Alan "Effective volume changes during fatigue and fracture of polymers" Polymer Engineering and Science. Vol. 36, No.18 (1996).

[38]-Narisawa, Ikou "Fatigue behavior of reinforced thermoplastics" Joint Canada-Japan Workshop on Composites (1196) pp. 57-62.

[39]- Johnson, T.A. "Cyclic deformation and failure of polymers" Cyclic stress-strain behavior-analysis, experimental, prediction, and failure, ASTM STP 519 (1973) pp.70-79.

[40]- Sims, G.D. and Bascomb, D. " Continuous monitoring of fatigue degradation in

composites by dynamic mechanical analysis" ICCM 9 (1995) pp. 4.161-171.

[41]- Flugge, Wihelm "Viscoelasticity" 2nd Edition, Springer-Verlag (1975).

[42]- Read, B E and Dean G D " The determination of dynamic properties of polymers and composites" Adam Hilger Ltd. (1978).

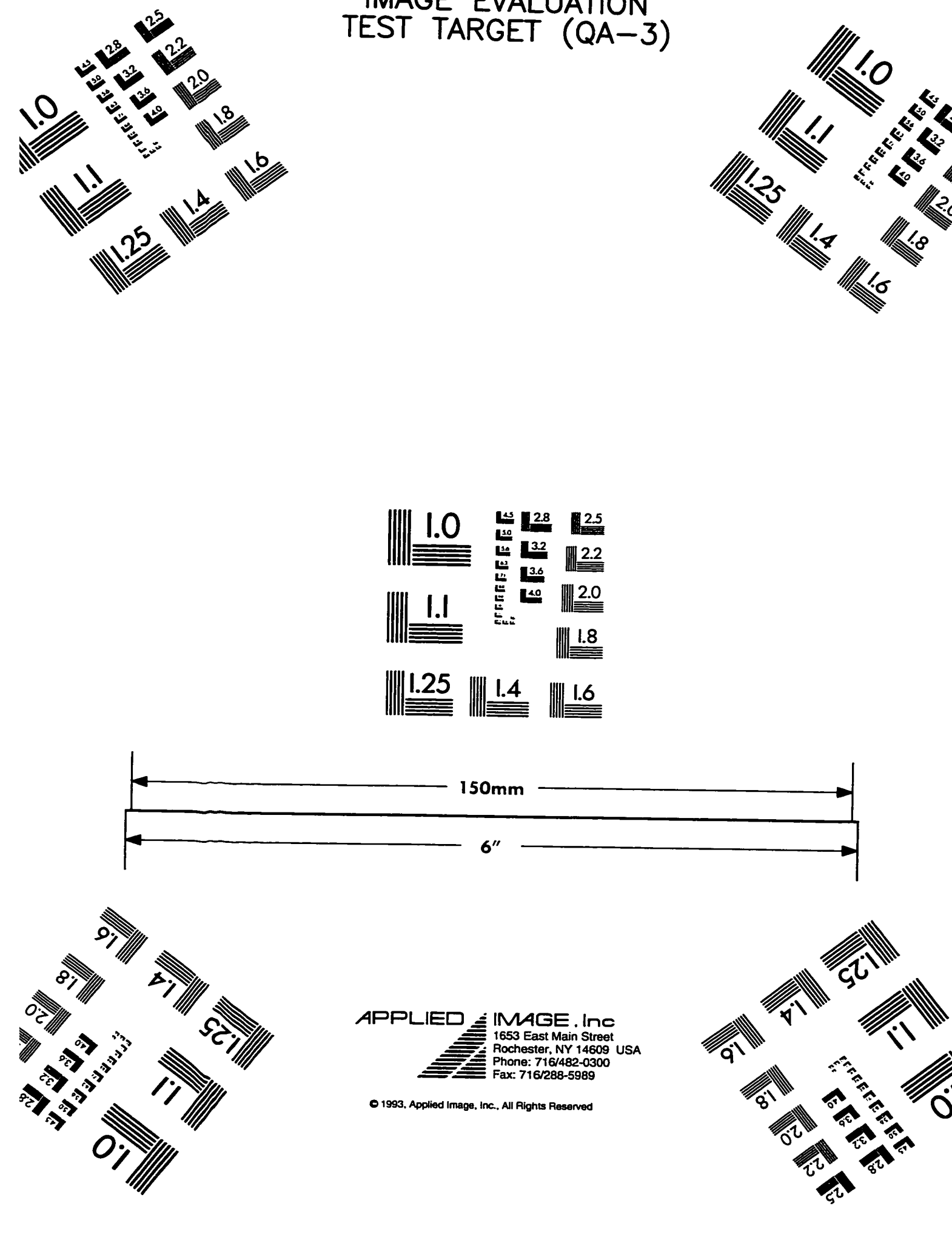
IMAGE EVALUATION
TEST TARGET (QA-3)
150mm
6"
APPLIED IMAGE, Inc
1653 East Main Street
Rochester, NY 14609 USA
Phone: 716/482-0300
Fax: 716/288-5989
© 1993, Applied Image, Inc., All Rights Reserved